1986

Determination Of The Sequence Distribution And Ionization Constant Of Poly(Acrylic Acid), Poly(Vinylamine) And Poly(Acrylic Acid - Co-Vinylamine) By Nmr Spectroscopy (Carbon-13 Two-Dimensional, Nitrogen-15 Nmr, Titration).

Chen Chang
University of Alabama at Birmingham

Chang, Chen

DETERMINATION OF THE SEQUENCE DISTRIBUTION AND IONIZATION CONSTANT OF POLY (ACRYLIC ACID), POLY(VINYLAMINE) AND POLY(ACRYLIC ACID-CO-VINYLAMINE) BY NMR SPECTROSCOPY

The University of Alabama in Birmingham PH.D. 1986

PLEASE NOTE:

In all cases this material has been filmed in the best possible way from the available copy. Problems encountered with this document have been identified here with a check mark __✓__.

1. Glossy photographs or pages _____
2. Colored illustrations, paper or print _____
3. Photographs with dark background _____
4. Illustrations are poor copy _____
5. Pages with black marks, not original copy _____
6. Print shows through as there is text on both sides of page _____
7. Indistinct, broken or small print on several pages ✓
8. Print exceeds margin requirements _____
9. Tightly bound copy with print lost in spine _____
10. Computer printout pages with indistinct print _____
11. Page(s) _____ lacking when material received, and not available from school or author.
12. Page(s) _____ seem to be missing in numbering only as text follows.
13. Two pages numbered _____. Text follows.
14. Curling and wrinkled pages _____
15. Dissertation contains pages with print at a slant, filmed as received ✓
16. Other _____

_____

_____

University
Microfilms
International

DETERMINATION OF THE SEQUENCE DISTRIBUTION AND IONIZATON CONSTANT OF POLY(ACRYLIC ACID), POLY(VINYLAMINE) AND POLY(ACRYLIC ACID-CO-VINYLAMINE) BY NMR SPECTROSCOPY

by

CHEN CHANG

A DISSERTATION

Submitted in partial fulfillment of the requirements for the degree of Doctor of Philosophy in the Department of Chemistry in the Graduate School, University of Alabama at Birmingham

BIRMINGHAM, ALABAMA

1986

ABSTRACT OF DISSERTATION
GRADUATE SCHOOL, UNIVERSITY OF ALABAMA AT BIRMINGHAM

Degree Ph.D. Major Subject Chemistry

Name of Candidate Chen Chang

Title DETERMINATION OF THE SEQUENCE DISTRIBUTION AND IONIZATION CONSTANT OF POLY(ACRYLIC ACID), POLY(VINYLAMINE) AND POLY-(ACRYLIC ACID-CO-VINYLAMINE) BY NMR SPECTROSCOPY

^{1}H NMR analysis of the methylene protons of poly(acrylic acid) (PAA) resulted in a 48 and 52% distribution of the meso (m) and racemic (r) dyad, respectively. Curve deconvolution of the ^{13}C NMR spectrum of PAA for the methine carbon resonances gave relative areas of 27, 50, and 23% for the rr, mm and mm triad sequence, from downfield to upfield, respectively. Using Bernoullian statistics, the corresponding probabilities of the m and r configuration for the methylene carbon are 48 and 52%, respectively. The acid dissociation constant for each methine triad of PAA is slightly different. The most acidic tacticity corresponds to the mm sequence.

The methylene carbon dyad assignment of poly(vinylamine) (PVAm) was determined by ^{13}C-^{1}H heteronuclear correlated two-dimensional (2-D) NMR experiments with and without broadband decoupling in the ^{1}H domain. The upfield carbon resonances were assigned to the m dyad and the downfield carbon resonances, assigned to the r dyad. According to these m and r assignments, the dyad distribution was found to be 44.2 m and 55.8% r. The triad analysis was obtained from the relative area of the three

distinct methine carbon regions and was found to be 29% rr, 54% mr and 17% mm from upfield to downfield, respectively. This analysis is supported by ^{1}H and ^{15}N NMR. The ^{13}C NMR pH titration of the methylene carbons were examined and there is no significant difference in the pKa of the m and r dyad. A bell-like ^{13}C NMR titration curve for each methine triad sequence of PVAm was observed and due to its complex nature could not be used to determine pK_a. Therefore, ^{15}N NMR pH titration was employed to analyze the acid-base behavior of the three PVAm triads. There is a sudden change in the middle of the titration curves but the data could be used to determine the pK_a's and the mm sequence is a stronger acid than the rr sequence.

Three copolymers, (poly acrylic acid-co-vinylamine) (SP) were analyzed by ^{13}C NMR and the results were compared to the previously analyzed homopolymers. The various comonomer sequence distributions were identified and by means of peak areas. It was determined that (1) the reactivity was not significantly influenced by the triad tacticity of the parent PAA, (2) SP52 is characterized by an essentially alternating sequence and (3) there is extensive lactam formation between neighboring carboxyl and amino groups. A ^{13}C NMR pH titration of SP12 showed that the carboxyl group with a neighboring amino group is more acidic than a carboxyl group flanked by two carboxyl groups.

Abstract Approved by: Committee Chairman Thomas H. Pinnavaia

Program Director L. J. Pinnavaia

Date 12/11/85 Dean of Graduate School Kenneth J. Rosen

ACKNOWLEDGEMENT

I would like to thank the members of my graduate committee, Drs. L. Hall, N. R. Krishna and G. S. Vigee for their guidance and suggestions. I wish to especially express my sincere gratitude to Dr. D. D. Muccio for providing me with a most valuable training experience of NMR and assistance in conducting this research and in the preparation of this dissertation. I would like to express my sincerest thanks to my advisor, Dr. T. St. Pierre for his excellent guidance, continuous encouragement, endless patient, daily involvement in research work throughout my graduate studies and allowing me to merge my interests in polymers and NMR.

Finally, I want to thank my wife Tai Chang for her encouragement and understanding.

TABLE OF CONTENTS

		Page
ABSTRACT		ii
ACKNOWLEGEMENTS		iv
LIST OF TABLES		vii
LIST OF FIGURES		viii
LIST OF ABBREVIATIONS		xiv
CHAPTERS		
I.	INTRODUCTION	1
	REFERENCES	7
II.	DETERMINATION OF THE TACTICITY AND ANALYSIS OF THE pH TITRATION OF POLY(ACRYLIC ACID) by ^{1}H and ^{13}C NMR	9
	REFERENCES	33
III.	HETERONUCLEAR CORRELATED TWO-DIMENSIONAL NMR SPECTROSCOPY APPLIED TO THE DYAD ASSIGNMENT OF VINYL POLYMERS	35
	REFERENCES	56
IV.	A CONFIGURATIONAL STUDY OF POLY(VINYLAMINE) BY MULTINUCLEAR NMR	57
	REFERENCES	77
V.	^{13}C AND ^{15}N NMR pH TITRATION STUDY OF POLY(VINYLAMINE)	78
	REFERENCES	97
VI.	DETERMINATION OF THE SEQUENCE DISTRIBUTION AND IONIZATION CONSTANT OF POLY(ACRYLIC ACID-CO-VINYLLAMINE) BY ^{13}C NMR	98
	REFERENCES	125
VII.	CONCLUSION	127

Page

VIII. APPENDICES

APPENDIX A ^{13}C NMR of concentration study..... 131

APPENDIX B ^{13}C NMR study of polymers with different molecular weight..... 136

APPENDIX C Temperature study..... 141

APPENDIX D ^{1}H NMR model study..... 146

APPENDIX E Nuclear Overhauser effect (NOE) study..... 159

APPENDIX F ^{13}C and ^{15}N NMR spin lattice relaxation time (T_1) study..... 186

APPENDIX G ^{13}C NMR pH titration study of model compounds, m and r (DAP)..... 209

APPENDIX H NMR pH titration study of polymers..... 214

APPENDIX I Two-dimensional heteronuclear NMR study of PVAm and its model compounds, m and r DAP..... 231

LIST OF TABLES

Chapter II

Page

Table 1. Peak Assignments, T_1, NOE, and Peak Areas for PAA..... 21

Table 2. Simulated Methine Carbon Resonance for Pentad Sensitivity..... 23

Table 3. Acid Dissociation Constants of PAA..... 30

Chapter IV

Table 1. C-13 NMR ANALYSIS OF POLY(VINYLAMINE)..... 69

Chapter V

Table 1. ACID DISSOCIATION CONSTANTS FOR PVAm..... 90

Chapter VI

Table 1. Triad Sequence Distribution for the Conversion of PAA Carboxyl Groups to Amino Groups via the Schmidt Reaction..... 118

Table 2. Acid Dissociation Constants for Copolymer SP12 and Homopolymer PAA 123

LIST OF FIGURES

Chapter II		Page
Figure 1.	^{13}C NMR Spectrum of CH for Poly(acrylic acid).....	14
Figure 2.	^{13}C NMR Spectrum of CH_2 for Poly(acrylic acid).....	16
Figure 3.	Curve Deconvolution of ^{13}C NMR Spectrum of CH for Poly(acrylic acid).....	19
Figure 4.	^{1}H NMR Spectra of CH_2 of Poly(acrylic acid) and a mixture of m and r 2,4-Dimethylglutaric acid.....	25
Figure 5.	^{13}C NMR pH Titration Curves for CH and CO of Poly(acrylic acid).....	27
Chapter III		
Figure 1.	^{1}H NMR Spectra of 2,4-Diaminopentane and Poly(vinylamine).....	42
Figure 2.	^{13}C NMR Spectra of 2,4-Diaminopentane and Poly(vinylamine).....	44
Figure 3.	Contour Plot for 2,4-Diaminopentane.....	47
Figure 4.	Cross Sections parallel to the ^{1}H axis for CH_2 of 2,4-Diaminopentane and Poly(vinylamine).....	49
Figure 5.	Contour Plot for Poly(vinylamine).....	52
Chapter IV		
Figure 1.	^{13}C NMR Spectra of Poly(vinylamine).....	62
Figure 2.	Curve Deconvolution of ^{13}C NMR Spectrum of CH and CH_2 of Poly(vinylamine).....	65
Figure 3.	Curve Deconvolution of ^{15}N NMR Spectrum of Poly(vinylamine).....	71
Figure 4.	^{1}H NMR Spectra of Poly(N-vinylacetamide).....	74
Chapter V		
Figure 1.	Coupled ^{13}C NMR Spectra of m 2,4-Diaminopentane.....	83
Figure 2.	Attached Proton Test Spectra of Poly(vinylamine).....	86

Page

Figure 3. ^{13}C NMR Titration Curves of CH and CH_2 of Poly(vinylamine)..... 88

Figure 4. ^{15}N NMR Titration Curves of Poly(vinylamine)..... 94

Chapter VI

Figure 1. Curve Deconvolution of ^{13}C NMR Spectrum of SP12..... 105

Figure 2. ^{13}C NMR Spectra of Poly(acrylic acid), Poly(acrylic acid-co-vinylamine) and Poly(vinylamine)..... 108

Figure 3. Attached Proton Test Spectra for CH and CH_2 of Copolymers..... 114

Figure 4. ^{13}C NMR spectra for CO of Copolymers..... 116

Figure 5. ^{13}C NMR Titration Curves for CH and CO of Coplymers..... 120

Appendix A

Figure 1. ^{13}C NMR of Concentration Study of Poly(acrylic acid) at pH = 12..... 132

Figure 2 ^{13}C NMR of Concentration Study of Poly(acrylic acid) at Low pH..... 134

Appendix B

Figure 1. ^{13}C NMR of Molecular Weight Study of Poly(acrylic acid) at pH = 2..... 137

Figure 2. ^{13}C NMR of Molecular Weight Study of Poly(acrylic acid) at pH = 12..... 139

Appendix C

Figure 1. ^{1}H NMR of Temperature Study of Poly(acrylic acid) at pH = 12..... 142

Figure 2. ^{13}C NMR of Temperature Study of Poly(acrylic acid) at pH = 12..... 144

Appendix D

Figure 1. ^{1}H NMR Spectrum of a Mixture of m and r isomers of 2,4-Dimethylglutaric Acid at 25°C..... 147

Page

Figure 2. ^1H NMR Spectrum of a Mixture of m and r isomers of 2,4-Dimethylglutaric Acid at 80°C..... 149

Figure 3. ^1H NMR Spectrum of r-2,4-Diaminopentane at pH = 1.8..... 151

Figure 4. ^1H NMR Spectrum of r-2,4-Diaminopentane at pH=11.8..... 153

Figure 5. ^1H NMR Spectrum of m-2,4-Diaminopentane at pH=1.8..... 155

Figure 6. ^1H NMR Spectrum of m-2,4-Diaminopentane at pH=11.8..... 157

Appendix E

Figure 1. Nuclear Overhauser Effect as a Function of Correlation Time..... 160

Figure 2. Nuclear Overhauser Effect Study of Poly(acrylic acid) (Molecular Weight=4,500) at pH=12..... 162

Figure 3. Nuclear Overhauser Effect Study of Poly(acrylic acid) (Molecular Weight=15,000) at pH=12..... 164

Figure 4. Nuclear Overhauser Effect Study of Poly(acrylic acid) (Molecular Weight=15,000) at pH=2..... 166

Figure 5. Nuclear Overhauser Effect Study of Poly(acrylic acid-co-vinylamine)(SP12) at pH=2..... 168

Figure 6. Nuclear Overhauser Effect Study of Poly(acrylic acid-co-vinylamine)(SP30) at pH=2..... 170

Figure 7. Nuclear Overhauser Effect Study of Poly(acrylic acid-co-vinylamine)(SP52) at pH=2..... 172

Figure 8. Nuclear Overhauser Effect Study of Poly(vinylamine) at pH=2..... 174

Figure 9. Nuclear Overhauser Effect Study of Poly(vinylamine) in D_2O at pH=7..... 176

Figure 10. Nuclear Overhauser Effect Study of Poly(vinylamine) in 10% D_2O at pH=7..... 178

Figure 11. Nuclear Overhauser Effect Study of Poly(vinylamine) at pH = 8.56..... 180

Page

Figure 12. Nuclear Overhauser Effect Study of Poly(vinylamine) at pH = 8.68..... 182

Figure 13. Nuclear Overhauser Effect Study of Poly(vinylamine) at pH = 10.5..... 184

Appendix F

Figure 1. Spin-Lattice and Spin-Spin Relaxation Time as a Function of Correlation Time..... 187

Figure 2. Spin-Lattice Relaxation Time Study of Poly(vinylamine) (Molecular Weight = 1,000) at pH = 12..... 189

Figure 3. Spin-Lattice Relaxation Time Study of Poly(vinylamine) at pH = 12, 75°C..... 191

Figure 4. Spin-Lattice Relaxation Time Study of Poly(acrylic acid) at pH = 2..... 193

Figure 5. Spin-Lattice Relaxation Time Study of Poly(acrylicacid-co-vinylamine) (SP12) at pH = 2..... 195

Figure 6. Spin-Lattice Relaxation Time Study of Poly(acrylic acid-co-vinylamine) (SP30) at pH = 2..... 197

Figure 7. Spin-Lattice Relaxation Time Study of Poly(acrylic acid-co-vinylamine) (SP52) at pH = 2..... 199

Figure 8. Spin-Lattice Relaxation Time Study of Poly(vinylamine) at pH = 2..... 201

Figure 9. Spin-lattice Relaxation Time Study of Poly(vinylamine) at pH = 7..... 203

Figure 10. Spin-lattice Relaxation Time Study of Poly(vinylamine) at pH = 8.68..... 205

Figure 11. Spin-lattice Relaxation Time Study of Poly(vinylamine) at pH = 10.5..... 207

Appendix G

Figure 1. Titration Study of m-2,4-Diaminopentane..... 210

Figure 2. Titration Study of r-2,4-Diaminopentane..... 212

Appendix H Page

Figure 1. Titration Study of Poly(acrylic acid) (Molecular Weight = 4,500)..... 215

Figure 2. Titration Study of Poly(acrylic acid) (Moleculat Weight = 15,000)..... 217

Figure 3. Titration Study of Poly(acrylic acid-co-vinylamine) (SP12)..... 219

Figure 4. Titration Study of Poly(acrylic acid-co-vinylamine) (SP30)..... 221

Figure 5. Titration Study of Poly(acrylic acid-co-vinylamine) (SP52)..... 223

Figure 6. Titration Study of Poly(vinylamine) at pH = 2.0-9.8..... 225

Figure 7. Titration Study of Poly(vinylamine) at pH = 9.8-13.5..... 227

Figure 8. Titration Study of Poly(vinylamine)..... 229

Appendix I

Figure 1. Contour Plot of a 1:2 Molar Mixture of m and r Isomers of 2,4-Diaminopentane from a CSCM Experiment at pH = 1.5..... 232

Figure 2. Contour Plot of a 1:2 Molar Mixture of m and r Isomers of 2,4-Diaminopentane from a CSCMBB Experiment at pH = 1.5..... 234

Figure 3. Slices for the Methylene Protons of a 1:2 Molar Mixture of m and r Isomers of 2,4-Diaminopentane from CSCM and CSCMBB Experiments at pH = 1.5..... 236

Figure 4. Contour Plot of Methine Carbon of Poly(vinylamine) at pH = 6.5 from a CSCMBB Experiment at pH = 6.5..... 238

Figure 5. Slices for the Methine Protons of Poly(vinylamine) from a CSCMBB Experiment at pH = 6.5..... 240

Figure 6. Contour Plot of Methylene Carbon of Poly(vinylamine) at pH = 6.5..... 242

Page

Figure 7. Slices for the Methylene Protons of Poly(vinylamine) from a CSCMBB Experiment at pH = 6.5..... 244

Figure 8. Contour Plot of a 1:2 Molar Mixture of m and r Isomers of 2,4-Diaminopentane from a CSCM Experiment at pH = 8.8..... 246

Figure 9. Contour Plot of Poly(vinylamine) from a CSCM at pH = 8.8..... 248

Figure 10. Slices for Methylene Protons of Poly(vinylamine) from a CSCM Experiment at pH = 8.8..... 250

Figure 11. Contour Plot of 1:2 Molar Mixture of m and r Isomers of 2,4-Diaminopentane from a CSCMBB Experiment at pH = 8.8..... 252

Figure 12. Contour Plot of Poly(vinylamine) from a CSCMBB Experiment at pH = 8.8..... 254

Figure 13. Slices for Methylene Protons of a 1:2 Molar Mixture of m and r Isomers of 2,4-Diaminopentane from a CSCMBB Experiment at pH = 8.8. 256

LIST OF ABBREVIATIONS

α	Mole Fraction of Charged Sites
APT	Attached Proton Test
CSCM	Heteronuclear Shift-Correlated Two-Dimensional NMR
CSCMBB	Broadband Homonuclear Decoupling Heteronuclear Shift-Correlated Two-Dimensional NMR
DAP	2,4-Diaminopentane
HH	Henderson-Hasselbalch
m	Meso
mm	Isotactic
mr	Heterotactic
MW	Molecular Weight
NGI	Neighboring Group Interactions
NMR	Nuclear Magnetic Resonance
NOE	Nuclear Overhauser Effect
PAA	Poly(acrylic acid)
pKa	Acid Dissociation Constant
$pK_{1/2}$	Acid Dissociation Constant at Half Neutralization
pKi	Intrinsic Dissociation Constant
PVAm	Poly(vinylamine)
PVAc	Poly(N-vinylacetamide)
r	Racemic
rr	Sydiotactic
SP	Poly(acrylic acid-co-vinylamine)

CHAPTER I

INTRODUCTION

In past years a considerable effort has been devoted to the study of the properties of polyelectrolytes in aqueous solution and several review articles have appeared on this subject[1-5]. A polyelectrolyte is simply a polymer containing ionizable groups on the polymer chain. Polyelectrolytes include synthetic polymers and biopolymers. Polyelectrolytes can be divided into three families; polyacid, polybase and polyampholyte, depending on whether the ionizable centers are anionic, cationic or a mixture of acidic and basic groups. Most polyelectrolytes dissolve in water and dissociate into polyions which produce a strong electric field. The most distinctive feature of polyelectrolytes is that their acid dissociation constants (pKa) are dependent on the degree of neutralization. Because a charged polymer will interact with hydrogen ions, protons will be removed with increasing difficulty from the polyanion with increasing charge density. On the other hand, the hydrogen ions will be repelled by the polycation, and the acid strength will increase with increasing charge density. In addition to this typical polyelectrolyte effect, the pKa also depends on the configurational or structural details of these ion-containing polymers. Due to these two features, the understanding of polyelectrolyte behavior in aqueous solution becomes a complicated problem.

Since Overbeek first reported the polyelectrolyte effect in 1948[6], many publications have appeared in the literature based on a theoretical

treatment of model calculations for the relationship between pKa and α (mole fraction of charged sites) ranging from the Lifson-Katchalsky's rod-like model[7] to the counterion condensation theory of Mannning[8]. These theoretical approaches appear to work well for polyelectrolytes like poly(acrylic acid) (PAA)[1], where the neighboring group interactions (NGI) are relatively weak. But, for polyelectrolytes with stronger NGI, these theories are in poor agreement with experimental data[9,10].

Experimentally, potentiometric titration of polyelectrolytes is frequently employed to study acid dissociation reactions. The data are usually treated with empirical equations such as the extended Henderson-Hasselbalch (HH) equation, originally proposed by Katchalsky and Spitnik[11] (equation 1),

$$pH = pKa + n \log \left(\frac{\alpha}{1 - \alpha}\right) \qquad (1)$$

where n is the slope of the plot of pH vs $\log \frac{\alpha}{1 - \alpha}$ and α is the mole fraction of charge sites. However, the extended HH equation is not always valid over the entire titration curve. It is most applicable for a limited range of α values centered near $\alpha = 0.5$. Alternatively, Mandel has established a simple, polynomial relationship (equation 2) to describe the dependence of pKa on for studying the titration of PAA[12],

$$pKa = pKi + a\alpha + b\alpha^2 \qquad (2)$$

where pKi is the intrinsic dissociation constant and a and b are the experimental coefficients for the α terms. The advantage of the Mandel

equation appears to be its validity over the entire range of the titration.

Unfortunately, potentiometric experiments can only relate pKa or ΔG^{o} (free energy change) and α. The solution properties of polyelectrolytes and their acid-base behavior are not only described by pKa or ΔG^{o} but also by other thermodynamical parameters (ΔH^{o}, enthalpy change and T ΔS^{o}, entropy change) as well. Calorimetric measurements can provide ΔH which, combined with ΔG^{o}, will allow the calculation of T ΔS^{o} for the proton ionizaton reaction. Relatively little calorimetric work has been performed on proton ionization reactions of polymeric solutions[9,10,13-15]. St. Pierre and co-workers[9,10] developed a system for simultaneously studying the potentiometric and calorimetric titration of poly(vinylamine) (PVAm). Their studies indicated that ΔH^{o} and $T\Delta S^{o}$ were more sensitive measures of polyelectrolyte effects than either pKa or ΔG^{o}.

Carbon (^{13}C) NMR has been used extensively for studying aqueous solutions of natural biopolymers[16,17] with ionizable groups as well as low molecular weight amino acids and mono- or di-acids and/or amines[18,19,]. The application of ^{13}C NMR to these compounds is based on the characteristic behavior of nuclei near ionizable groups influenced by a change in charge density resulting from a change in pH. Therefore, the titration of polyelectrolytes may be determined by plotting chemical shifts versus pH. In this manner, α can be established from pH versus chemical shift and then be fitted to the empirical titration curves, such as the extended HH or Mandel equation to yield ionization constants.

It may be important to know the configurational or other structural details of polyelectrolytes in order to understand their ionization behavior during the course of titration. In the past few years, high resolution NMR has proved to be a most powerful tool in providing the significant features of homopolymer configuration and of copolymer sequence distribution. Traditionally, only proton (^1H) NMR was used to characterize the microstructure of the polymers until Fourier Transform (FT) instruments became available. FT NMR can detect the low natural abundant nuclei such as carbon and nitrogen by multiple accumulations. This development makes polymer chemistry more exciting because the ^{13}C nucleus exhibits both a greater chemical shift range and a sensitivity than that of the ^1H nucleus. Potentially, ^{13}C NMR can provide the fine features of polymer structure which were not available before. More recently, modern pulse experiments have been extensively developed ranging from J-modulation spin echo[20] to two-dimensional NMR spectroscopy[21]. In addition to resolving the question of overlapping peaks and increasing sensitivity, pulse techniques can provide quantitative and dynamic information for these polymers.

Since Bovey pioneered the use of NMR as a tool to study the stereochemical features of vinyl polymers, an extensive effort has been devoted to this field[22,23]. The general structural features of vinyl polymers is $-(CH_2CHR)-_n$, where R can be OH, CN, Cl, CO_2H, $OCOCH_3$, etc.. The polymer may have stereochemical differences depending on the relative stereochemistry of adjacent repeating units throughout the polymer chain. The configuration can be recognized through the Fischer projection of the extended polymer chain:

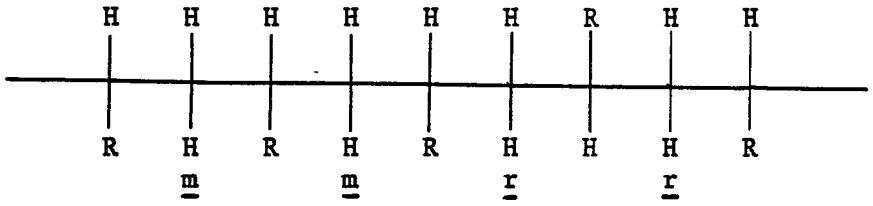

The distribution of meso (m) and racimic (r) configurations is called tacticity. Quantitative tactyicity measurements are made on the basis of successive units in vinyl homopolymers such as dyads, triads, tetrads, etc.. The isotactic polymer contains configurations of the predominately m type and the syndiotactic polymer contains configurations of the predominately r type. If the two configurations are approximately equal, the polymer is defined as heterotactic and the peak intensity of mm, mr or rm[24] and rr triads will be present in the ratio of 1:2:1, respectively.

The general structural features of vinyl copolymers is $(CH_2CHA)_x(CH_2CHB)_{1-x}$, where A and B define two different monomer units. The sequence distribution of vinyl copolymers can arise from different placements of the comonomers, here symbolized simply as A and B. The three resulting sequences for the methylene carbon or protons are AA, AB and BB, whereas the methine carbons or protons result in six triads, three A centered triads, AAA, AAB, and BAB, and three B centered triads, ABA, ABB and BBB. The sequence distributions of the copolymers may also be complicated by tacticity effects. For example, twenty possible sequence distributions can be obtained for the methine triad.

From Kawaguchi and Nagasawa's potentiometric study of PAA[25], they concluded that syndiotactic PAA is a stronger acid than isotactic PAA. Kitajima-Yamashita studied the ionization behavior of isotactic and heterotactic poly(2-vinylpyridine) by means of potentiometric titration[26]. They indicated that the heterotactic polymer is a stronger base than the isotactic polymer. However, it is possible by means of the NMR pH titration experiment to analyze the configurational effect on pKa during the course of titration for all three triad sequences in the same heterotactic polymer. At present, there is no such information available in the literature regarding this point.

In this study, three different kinds of synthetic vinyl polyelectrolytes were used to systematically investigate the relationship between their structures and ionization reactions in aqueous solution. The sequence distribution of the homopolymers, PAA and PVAm, and their SP copolymers, were determined by ^{1}H, ^{13}C and ^{15}N NMR. The pKa of each of these three polymers were determined by NMR pH titration experiments and application of the extended Henderson-Hasselbach or the Mandel equation. PAA was obtained from Celanese Water Soluble Polymers, and PVAm was prepared from N-vinyl-t-butylcarbamate (PVAmI) or from N-vinylacetamide (PVAmII). Three SP coppolymers containing 12%, 30% and 52% amino groups were synthesized from PAA by means of the Schmidt reaction for this study.

REFERENCES

1. "Chemical Physics of Ionic Solution"; Conway, B. E.; Barvades, F. G. (Editors), John Wiley: New York, 1966.

2. "Polyelectrolytes"; Oosawa, F. (Editor), Marcel Dekker, Inc.: New York, 1971.

3. "Polyelectrolytes"; Selegny, E.; Mandel, M.; Strauss, U. (Editors), D. Reidel Publishing Company: Dordrecht, Holland 1973.

4. "Polyelectrolytes and their Applications"; Rembaum, A.; Selegny, E. (Editors), D. Reidel Publishing Company: Dordrecht, Holland 1975.

5. "Ions in Polymers"; Eisenberg, A. (Editor), American Chemical Society: Washington, D. C. 1980.

6. Overbeek, J. Th. Bull. Soc. Chim. Belges. 1948, 57, 252.

7. Lifson, S.; Katchalsky, A. J. Polymer Sci. 1954, 13,43.

8. Manning, G. S.; Holtzer, A. J. Phys. Chem. 1973, 77, 2206.

9. Lewis, E. A.; Barkley, J.; St.Pierre, T. Macromolecules 1981, 14, 546.

10. Lewis, E. A.; Barkley, J.; Renee Reams, R.; Hansen, L. D.; St.Pierre, T. Macromolecules 1984, 17, 2847.

11. Katchalsky, A.; Spitnik, P. J. Polym. Sci. 1947, 2, 432.

12. Mandel, M. Eur. Polym. J. 1970, 6, 807.

13. Quadrifoglio, F.; Cressenzi, V.; Dolar, D; Delbin, F. J. Phys. Chem. 1973, 77, 539.

14. Fenyo, J. C.; Delbin, F., Paoletti, S.; Crescenai, V. J. Phys. Chem. 1977, 81, 1900.

15. Martin,P.J.; Morss, L. R.; Strauss, U. P. J. Phys. Chem. 1980, 84, 577.

16. Saito, H.; Smith, I. C. P. Arch. Biochem. Biophys. 1973, 158, 154.

17. Saito, H.; Ohki, T.; Kodama, M.; Nagata, C. Biopolymers 1978, 17, 2587.

18. Rabenstein, D. C.; Sayer, T. L. J. J. Magn. Reson. 1976, 24, 27.

19. Surprenant, H. L.; Sarneski, J. E.; Key, R. R.; Byrd, J. T.; Reilley, C. N. J. Magn. Reson. 1980, 40, 231.

20. Patt, S. L.; Shoolery, J. N. J. Magn. Reson. 1982, 46, 535.

21. Bax, A. "Two-Dimentional Nuclear Magnetic Resonance in Liquids"; Reidel: Boston, 1982.

22. Bovey, F. A. "High Resolution NMR of Macromolecules"; Academic Press: New York, 1972.

23. Randall, J. C. "Polymer Sequence Determination ^{13}C NMR method": Academic Press: 1977.

24. The mr and rm triad are indistinguishable and will be represented collectively as mr.

25. Kawaguchi, Y.; Nagasawa, M. J. Phys. Chem. 1969, 73, 4382.

26. Kitajima-Yamashita, T. Polym. J. 1973, 4, 262.

CHAPTER II

DETERMINATION OF THE TACTICITY AND ANALYSIS OF THE pH TITRATION OF POLY(ACRYLIC ACID) by ^{1}H AND ^{13}C NMR.

Chen Chang
Donald D. Muccio
Thomas St. Pierre

Department of Chemistry
University of Alabama at Birmingham
Birmingham, Alabama 35294

ABSTRACT

The tacticity, to triad and partial pentad resolution, of a commercial sample of poly(acrylic acid) was determined by ^{1}H and ^{13}C NMR. Curve deconvolution of the ^{13}C NMR spectrum for the methine resonances gave relative areas of 27, 50 and 23% for the rr, mr and mm sequence respectively, based on Schaefer's peak assignments. The use of Bernoullian statistics gives the corresponding probabilities of the r and m configuration as 52% and 48%, respectively, suggesting that the polymer is atactic. This is confirmed by the ^{1}H NMR spectrum of the methylene protons. The simulated pentad spectrum was constructed on the basis of these probabilities and the experimental spectrum. The changes in chemical shift of the methine resonance for each tacticity and for the carbonyl resonance with changing pH were treated as typical polyelectrolyte titrations and analyzed by the extended Henderson-Hasselbalch and by Mandel's equation. We found a small tacticity effect on the acid dissociation behavior of poly(acrylic acid).

INTRODUCTION

^{13}C NMR has been extensively used for elucidating the stereochemical sequence of vinyl polymers, such as poly(methyl methacrylate),[1] poly-(vinyl acetate),[2] and polyacrylonitrile.[3] By comparison, there have been only a few studies[4-8] of poly(acrylic acid) (PAA) and these are incomplete. Schaefer[5] has reported on the triad sequence of the methine carbon for PAA by ^{13}C NMR. Comparing the spectrum of isotactic PAA, with that of the atactic polymer, he found that the upfield portion of both methine and methylene carbon resonances were attributed to the meso (m) configuration and, by default, the downfield region to the racemic (r) configuration. Furthermore, it was shown that the tacticity of the methine and methylene carbons was observed only at high pH. At low pH the resonance for each carbon nucleus was a single peak, shifted upfield. Interestingly, the carbonyl peak was insensitive to tacticity at both high and low pH. Watts,[7] in contrast, ascribed the downfield component of the methylene carbon resonances to the m configuration and the upfield component as a mixture of both m and r configurations. His assignments, however, were made on an unjustified extrapolation of ^{1}H NMR results. In the first part of this paper, we will provide a quantitative solution to the tacticity of PAA by ^{13}C NMR at the triad level and propose a pentad analysis as well.

The acid dissociation constant (pK_a) of a polyelectrolyte generally depends on the mole fraction of charged sites (α). The change of pK_a with respect to α is due primarily to an electrostatic effect.[9] The titration data can be treated in principle according to Manning's model.[10]

Alternatively, the data can be treated empirically either with the extended Henderson-Hasselbalch (HH) equation[11] or Mandel's equation.[12] Relatively little work has been done on NMR pH titration of polyelectrolytes. The titration behavior of PAA may be determined by ^{13}C NMR by plotting chemical shifts vs. pH. Schaefer[5] worked at three different pH's (2, 5, and 8) in order to maximize tacticity effects, but he made no attempt to titrate PAA. Prosser et al.,[8] however, did titrate this polymer using ^{13}C NMR to monitor the change in ionization state; and they used the HH equation to calculate $pK_{1/2}$ from at the change in chemical shift of the carbonyl carbon where, $pK_{1/2}$ is the value of pKA at $\alpha = 0.5$. In this paper, we will examine the titration behavior of PAA in more detail and analyze the influence of tacticity on pKA.

EXPERIMENTAL

PAA (Celanese Water Soluble Polymers) with a weight-average molecular weight of 10,000-20,000 was used as received. The ^{13}C NMR spectra were obtained using GE 300 WB spectrometer (NT series) equipped with an 1180e computer and 293c pulse programmer. The concentration of PAA was 5% by w/v. This concentration was sufficient to minimize any changes of chemical shifts with dilution of the polymer. The tacticity studies were performed on D_2O solutions at 75°C. The NMR titrations were done at 25°C with the polymer dissolved in H_2O at 25°C. Pulse angles of 62° (27 μs), repetition rates of 5.5 s, sweep widths of $\pm$ 7575 Hz and 16K data points were used to acquire the free induction decays. Dioxane was used as an internal chemical shift reference (66.5 ppm relative to tetramethylsilane). Nuclear Overhauser effects (NOE) were determined by

the ratio of the peak intensity of the fully proton-decoupled and gated-decoupled (decoupler off during delay time) spectra. The repetition rate for this measurement was at least 10 times the longest spin lattice relaxation time (T_1). The T_1 values were obtained from the inversion recovery pulse sequence[13] using a composite 180° pulse with delay values of 0.025, 0.08, 0.2, 1.0 and 3.0 sec. The T_1 values were calculated by using a nonlinear three-parameter fitting procedure.[14] Curve deconvolution was accomplished with the NMCCAP Program provided by the GE software using a completely Lorentzian line shape. ^1H NMR experiments were performed at 80°C on 0.5% (w/v) D_2O solutions. The pH's were adjusted with 5 µl additions of 9 N sodium hydroxide and recorded on an Orion research model 701 A pH meter with a microcapillary Ingold combination electrode and with no D_2O corrections.

RESULTS AND DISCUSSION

Determination of Tacticity of PAA . The ^{13}C NMR spectra of PAA were recorded in full through the pH, range of 1-13. There was no fine structure apparent in the spectra at low pH whereas at high pH there was good resolution for the methine carbon, poor resolution for the methylene carbon and a single peak for the carbonyl carbon. The methine carbon resonances obtained at 75°C showed some pentad sensitivity, whereas at 25°C only triad sensitivity was observed. The proton-decoupled ^{13}C spectrum of the methine carbon of PAA at 75°C (Fig. 1) appeared as six resolved peaks at 46.98, 46.75, 46.41, 45.99, 45.85 and 44.95 ppm, labeled A through F, respectively. The methylene region (Fig. 2) has three major peaks at 38.65, 37.06 and 36.15 ppm, G through I. Finally,

Figure 1: ^{13}C NMR spectrum of CH for PAA at 75°C in D_2O 5%, wt/vol) at pH = 12. Upper trace - spectrum for 10732 acquisitions, under the conditions described in the experimental section. Lower trace - the reconstructed spectrum from the deconvoluted peaks with a rms error of < 1%.

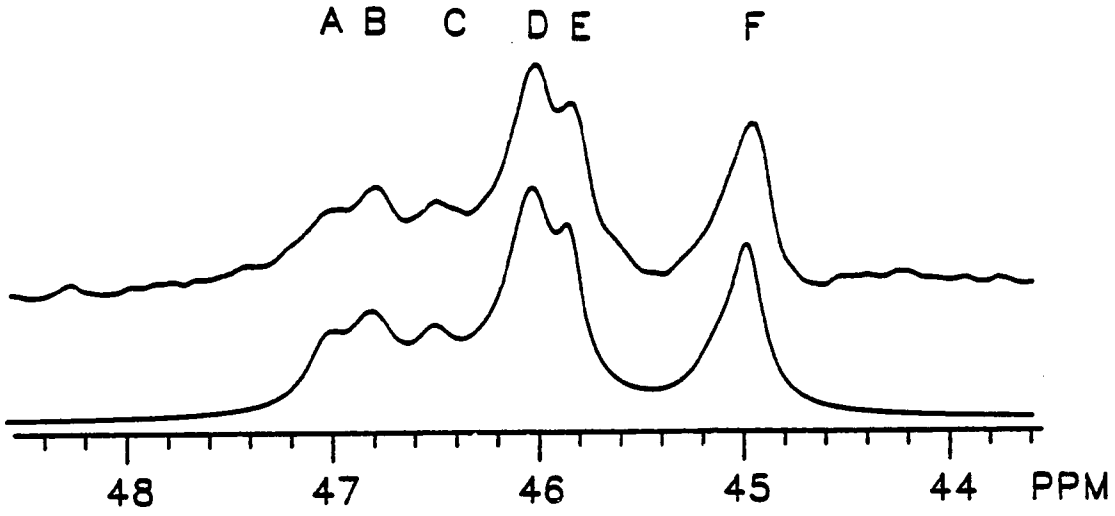
A B C D E F
48
47
46
45
44
PPM

Figure 2: ^{13}C NMR spectrum of CH_2 for PAA under the same experimental conditions described in the caption of Figure 1.

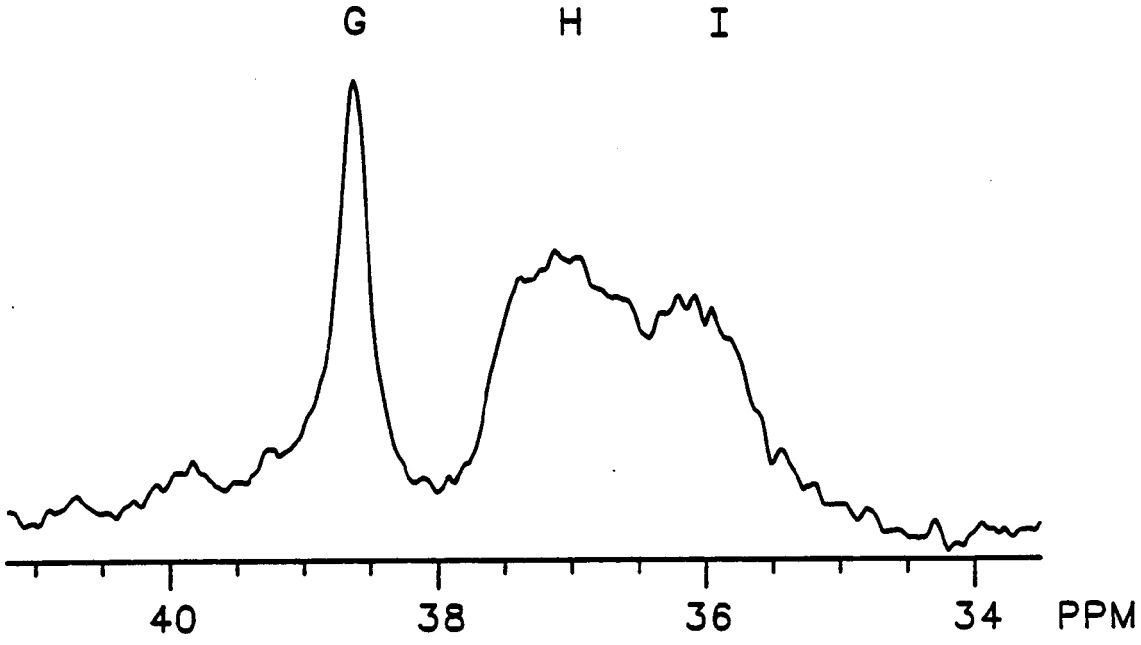
G
H
I
40
38
36
34
PPM

the carbonyl carbon, spectrum not shown, exhibited no apparent tacticity. Schaefer reports[5] three principal peaks for the methine carbon of atactic PAA and one principal peak for isotactic PAA that corresponds to the upfield peak of the atactic polymer. Consequently, we assign peaks A, B and C to the rr sequence, D and E to the mr or rm sequence and F to the mm sequence. The rr resonance has three components and represents pentad sensitivity. Schaefer shows one methylene peak for isotactic PAA, that corresponds to peak I which we assign to the m dyad.

Triad tacticity of the methine carbon is estimated from the combined peak areas which are 27, 50 and 23% for the rr, mr and mm sequences, respectively. The intensities of these peaks may be influenced by T_1 and NOE.[15] As shown in Table 1, the T_1 values for each methine resonance are nearly equal. Since the experiment utilized repetition rates of more than 10 times T_1, the areas in this respect require no correction. Furthermore, NOE measurements show only slightly different values for the three regions (Table I), and these differences are within the experimental error, estimated at $\pm$ 5%, therefore, no corrections for peak areas were necessary for the proton-decoupled spectrum.

The probability for the m configuration and r configuration, calculated from peak areas based on Bernoullian statistics[16-18], are 48 and 52%, respectively. With these values, a simulated spectrum to pentad resolution is constructed which is shown in Fig. 3; and the contribution to the area of each sequence is given in Table II. The simulated spectrum was generated by using the following assumptions: (1) the mm, mr and rr centered resonances do not overlap, (2) the pentad distribution follows Bernoullian statistics and (3) the line widths for

Figure 3: ^{13}C NMR spectrum of CH for PAA under the same experimental conditions described in the caption of Figure 1, compared to the reconstituted curve (middle trace) based on the pentad analysis (lower trace) with an rms error of < 1%.

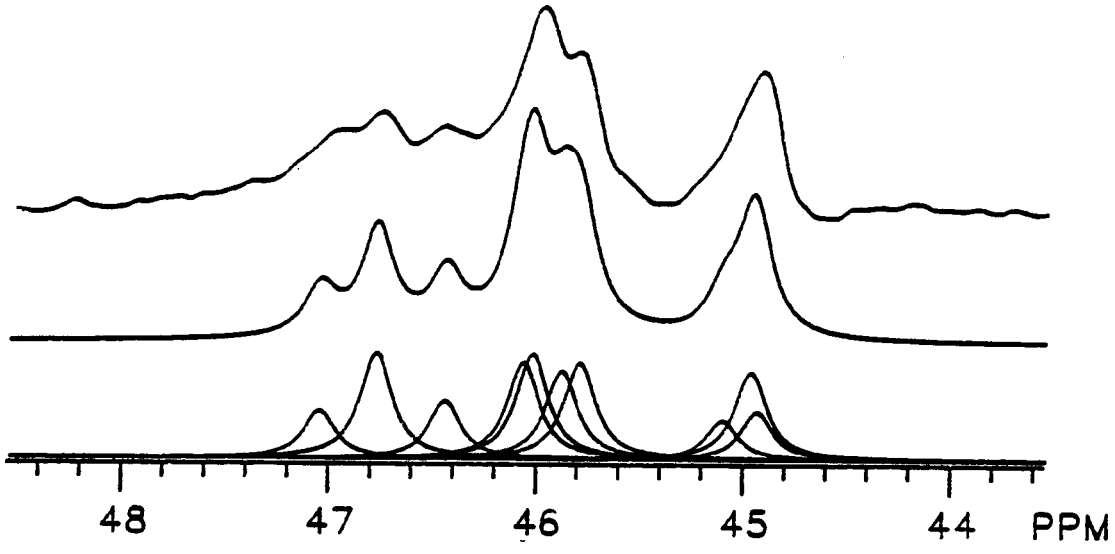
48
47
46
45
44
PPM

TABLE I

Peak Assignments, T_1, NOE, and Peak Areas for PAA[a]

Carbon	Configuration	Measured Region (ppm)	NOE (+0.1)	T_1 (+0.001)	Area%[b]
CH	rr	46.3 - 47.2	2.2	0.306	27
	mr(+rm)	45.4 - 46.3	2.2	0.290	50
	mm	44.7 - 45.4	2.3	0.293	23
CH_2	--	38.1 - 39.1	2.7	0.159	23
	--	35.5 - 38.0	2.5	0.158	77
CO_2	--	178.6	1.2	2.497	--

[a] 5% (w/v) in H_2O adjusted to pH = 12 and at 75°C.
[b] Estimated error ± 5%.

all tacticities are equal. The last assumption is based on the fact that T_1 is proportional to T_2 (spin-spin relaxation time) in the extreme narrowing region. Since the line width is inproportional to T_2, it follows that equal T_1 values predict equal line widths. Under these conditions only the position of each resonance was varied manually in a curve deconvolution program to yield the lowest root mean square error between the observed and calculated composite spectra, Fig. 3.

Since pentad sensitivity was displayed in the observed spectrum of the rr region, it was possible to predict the ordering of the rr centered pentads with some confidence. As shown in Table II these peaks are, left to right, mrrm, mrrr (and rrrm), and rrrr. Interchanging mrrm with rrrr results in a noticeably poorer fit. The ordering for the mm centered pentads is hampered by poor resolution and only the mmmr (and rmmm) can be assigned with confidence.

The fully decoupled spectrum of the methylene carbon, Fig. 2, despite the poor resolution, may be analyzed according to the m and r content established above. The spectrum was deconvoluted by the same procedure as used for the methine carbon resonances. The peak identified as G accounts for 23% of total CH_2 area. However this analysis is complicated by the presence of a spurious peak.[19] It is easily identified in acidic solutions as a separate peak upfield from the principal CH_2 resonances. It moves downfield with increasing pH and at pH=12 contributes 9.4% to the peak areas of H or I. Its presence is confirmed by the T_1 studies, appearing as an inverted peak when the rest of the CH_2 peaks are nulled. After correction for this

TABLE II

Simulated Methine Carbon Resonance for Pentad Sensitivity

Triad	Pentad	Chemical shift (ppm)
	mrrm	47.03
rr	mrrr	46.76
	rrrr	46.44
	rmrm	46.07
mr	rmrr	45.98
	mmrm	45.85
	mmrr	45.76
	rmmr	45.05
mm	mmmr	44.94
	mmmm	44.92

spurious peak is made, the contribution of the area of peak G to the total area of the CH_2 resonance is 25%.

On the basis of the dyad distribution established above, m = 0.48 and r = 0.52, the Bernoullian tetrad distribution may be calculated as follows: mmm = 0.11, mmr and rmm = 0.24, rmr = 0.12, mrm = 0.13, mrr and rrm = 0.26 and rrr = 0.14. The poorly resolved CH_2 spectrum of PAA, except for peak G, Fig. 2, can be analyzed in terms of the tetrad distribution. Peak G may be assigned to one of the two major tetrads or a combination of two minor ones. On the basis of an approximate analysis of line width the former is more likely. The tetrad choice for G, mmr (and rmm) or mrr (and rrm), is not clear-cut based on the approximately equal areas for this polymer and conflicting earlier assignments[5-7].

In order to confirm the dyad distribution established above, the ^1H NMR analysis of CH_2, known to be useful for this purpose,[7] was undertaken. The ^1H NMR spectrum of PAA for the methylene proton at pH = 2, characterized by multiplets at 1.98, 1.79 and 1.65 ppm, is shown in Fig. 4a. The model compound, an equal molar mixture of m and r 2,4-dimethylglutaric aid, Fig. 4d, show the previously assigned peaks[20] at 2.02 and 1.54 ppm for the m configuration and 1.77 ppm for the r configuration. The peak areas, obtained from curve deconvolution are 23.1, 52.0 and 24.6% for the peaks centered at 1.98, 1.79 and 1.65 ppm, respectively. This result is in good agreement with the analysis of the methine carbon by ^{13}C NMR.

^{13}C NMR pH Titration. The ^{13}C NMR pH titrations of the methine carbon for each tacticity and the carbonyl carbon, one peak, are displayed in Fig. 5. Deprotonation with increasing pH resulted in a

Figure 4: The ^{1}H NMR spectrum of CH_2 of PAA at $80^{o}C$ in D_2O (0.05 M) at pH = 2 and for 2400 acquisitions; curve a) experimental spectrum, curve b) reconstructed spectrum from curve c) the deconvoluted spectrum based on the expected spin-spin coupling pattern. The ^{1}H NMR of CH_2 of a mixture of m and r 2,4-dimethylglutaric acid (curve d) at $25^{o}C$ in D_2O (0.5 M) at pH = 2 for 100 acquisitions with a pulse angle of 8 μs and a repetition rate of 5s.

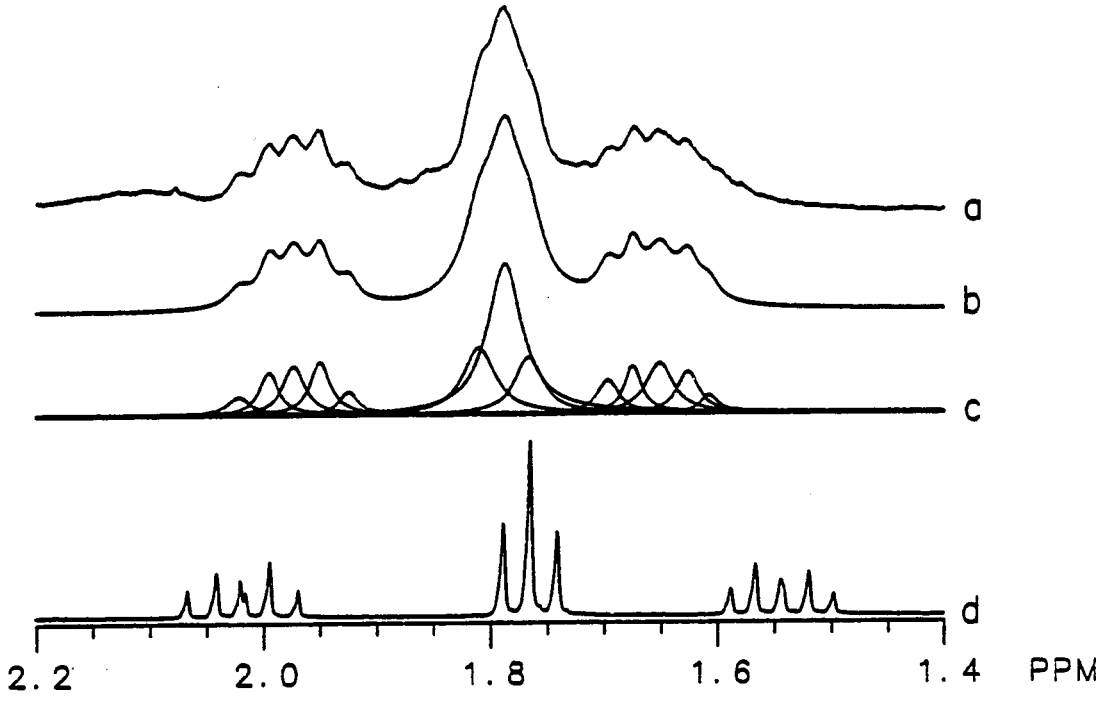
a
b
c
d
2.2
2.0
1.8
1.6
1.4
PPM

Figure 5: Chemical shift vs pH for the carbonyl carbon (a) and for the methine carbons (b = rr sequence, c = mr sequence, and d = mm sequence) of PAA at 25°C.

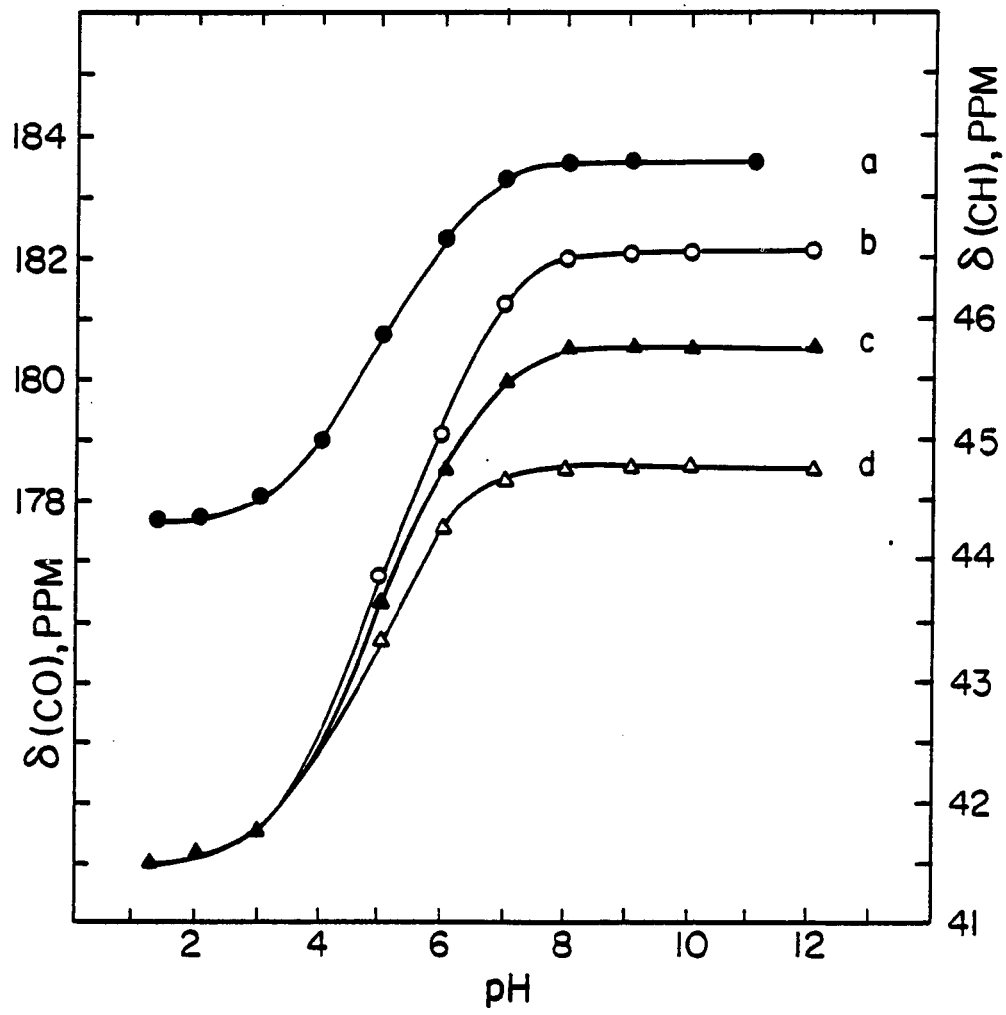
184
182
180
178
δ(CO), PPM
46
45
44
43
42
41
δ(CH), PPM
2
4
6
8
10
12
pH
a
b
c
d

downfield shift of each resonance. The extended HH treatment was used to calculate the pKA and $pK_{1/2}$ according to

$$pH = pK_{1/2} + n \log \frac{\alpha}{1 - \alpha} \qquad (1)$$

where α is calculated as the fraction of total chemical shift change given by

$$\alpha = \frac{\delta - \delta_{min}}{\delta_{max} - \delta_{min}} \qquad (2)$$

and where δ is the observed intermediate ^{13}C chemical shift at intermediate pH's, δ_{max} is the maximum chemical shift and δ_{min} is the minimum chemical shift at the extremes of pH. A linear regression fit of data to equation (1) gives $pK_{1/2}$ and n as the intercept and slope, respectively. The results for rr, mr and mm configurations of methine carbon and for the carbonyl carbon are given in Table III. The correlation coefficient in each case is very close to one which suggests that PAA does not change conformation abruptly during the course of titration.[12]

The $pK_{1/2}$ for each CH triad tacticity is slightly, but significantly, different. The most acidic tacticity corresponds to the mm sequence and the least acidic to the rr sequence. The CH mr (and rm) configuration and the carbonyl carbon are characterized by similar and intermediate values of $pK_{1/2}$. The slopes for each titration are also slightly different and indicate convergent pK's at low pH, i.e., low-charge state.

TABLE III

Acid Dissociation Constants of PAA

HH Equation	Methine Carbons			Carbonyl Carbon
	mm	mr(+rm)	rr	
$pK_{1/2}$	4.73	5.05	5.22	4.97
n	1.65	1.78	1.80	1.75
Correlation Coeff.	0.99	0.99	0.99	0.99
Mandel's Equation				
pK_i	3.91	4.09	4.22	4.03
a	1.93	1.99	2.08	2.09
b	-0.46	-0.18	-0.21	-0.42
n*	1.85	2.04	2.08	1.96
$pK_{1/2}$*	4.76	5.03	5.21	4.97

* HH parameters calculated from Mandel's equation

By another approach, Mandel[12] expressed pK_a (or $pH + \log\frac{1-\alpha}{\alpha}$) as a series expansion on α,

$$pK_a = pK_i + a\alpha + b\alpha^2 \qquad (3)$$

where pK_i is the intrinsic dissociation constant and a and b are the coefficients for the α terms. The results based on equation 3 are also shown in Table III, and they show the same trends in pK as described above. The self consistency of these two empirical equations[20] is made clear in the calculation of n and $pK_{1/2}$ of the extended HH equation from the a and b paramaters of Mandel's treatment by means of

$$n = 1 + 0.575\ (a + b). \qquad (4)$$

The results of these calculations for $pK_{1/2}$, but not for n (Table III), are consistent with the results obtained from the extended HH.

The $pK_{1/2}$ and n values obtained by ^{13}C NMR titration are close to the literature values obtained by potentiometric titration reported by Monjol and Champetier.[21] They found $pK_{1/2} = 5.35$ and $n = 1.7$ for atactic PAA at 10^{-2} M polymer concentration and 0.1 N NaCl salt concentration at $15^{\circ}C$. The results, theirs and ours, are surprisingly close given the difference in experimental conditions.

The effect of tacticity on the acid dissociation of PAA is small but the trends are clear $pK_{mm} < pK_{mr} < pK_{rr}$. The pK of the carboxyl associated with mr (and rm) sequence of CH is approximately equal to the pK determined from the CO titration and to the average of the other two carboxyl sequences. Our results, however, are at odds with the

potentiometric titration results of Kawaguchi and Nagasawa[22] who show the syndiotactic tactic polymer, r > m, to be a slightly stronger acid than the isotactic polymer, m > r. From Clark's report[23] on the potentiometric titration of 2,4,6-heptanetricarboxylic acid, the pka's equal 5.00, 4.87 and 4.90 for mm, mr and rr isomers, respectively. Since these values are so close, it is difficult to draw conclusions based on the different configurations. No doubt the conformational freedom of the low molecular weight model, and to a certain extent the polymer, moderate the configurational effects on pK_a.

REFERENCES

(1) Peat, I.R.; Reynolds, W.F. Tetrahedron Lett. 1972, 14, 1359.

(2) Wu, T.K.; Ovenall, W.F. Macromolecules 1974, 7, 776.

(3) Schaefer, J. Macromolecules 1977, 4, 105.

(4) Muroga, Y.; Noda, I.; Nagasawa, M. J. Phys. Chem. 1969, 73, 667.

(5) Schaefer, J. Macromolecules 1971, 1, 98.

(6) Matsuzaki, K.; Kanat, T.; Kawamura, T.; Matsumoto, S.; Uryu, T. J. Polym. Sci., Polym. Chem. Ed. 1973, 11, 1961.

(7) Watts, D.C. J. Biomed. Mater. Res. 1979, 13, 423.

(8) Prosser, H.T.; Richards, C.P.; Wilson, A.D. J. Biomed. Mater. Res. 1982, 16, 431.

(9) Morawetz, H. "Macromolecules in Solution"; John Wiley & Sons Inc.: New York, 1975; p. 344.

(10) Manning, G.S. J. Phys. Chem. 1981, 95, 870.

(11) Katchalsky, K.; Spitnik, P. J. Polym. Sci. 1947, 2, 432.

(12) Mandel, M. Eur. Polym. J. 1970, 6, 807.

(13) Freeman, R.; Kempsell, S.P.; Levitt, M.H. J. Magn. Reson. 1980, 38, 453.

(14) Kowalewski, J.; Levy, G.C.; Johnson, L.F.; Palmer, L. J. Magn. Reson. 1977, 26, 533.

(15) King, J.; Bower, D.I. Makromol. Chem. 1983, 184, 879.

(16) Randall, J.C. "Polymer Sequence Determination ^{13}C NMR Method"; Academic Press: New York, 1977; p. 71.

(17) Bovey, F.H. "High Resolution NMR of Macromolecules"; Academic Press: New York and London, 1972; p. 146.

(18) The sequencence distribution also fit first-order Markov statistics which is not surprising for this atactic polymer.

(19) The spurious peak is assumed to be an end group peak; however, at 9.4%, the calculated M_n is not consistent with a M_w of 15000. To refine this calculation it would be necessary to correct for T_1 and NOE.

(20) Fenyo, J.C.; Laine, J.P.; Muller, G. J. Polym. Sci., Polym. Chem. Ed. 1979, 17, 193.

(21) Monjol, P.; Champetier, G. Bull. Soc. Chim. Fr. 1972, 1313.

(22) Kawaguchi, Y.; Nagasawa, M. J. Phys. Chem. 1969, 73, 4382.

(23) Clark, H.K. Makromol. Chem. 1965, 86, 107.

CHAPTER III

HETERONUCLEAR CORRELATED TWO-DIMENSIONAL NMR SPECTROSCOPY APPLIED TO THE DYAD ASSIGNMENT OF VINYL POLYMERS

C. Chang, D. D. Muccio,* and T. St. Pierre
Department of Chemistry
University of Alabama at Birmingham
Birmingham, Alabama 35294

ACKNOWLEDGEMENT

The authors thank Drs. C. G. Overberger and C. C. Chen, Department of Chemistry and the Macromolecular Research Center, The University of Michigan, for providing us with samples of m and r DAP and Dynapol, Palo Alto, California for a sample of PVAm.

ABSTRACT

The dyad tacticity of poly(vinylamine) was determined for the methylene carbons by the use of heteronuclear correlated two-dimensional nuclear magnetic resonance experiments with and without broadband decoupling in the ^{1}H domain. The upfield resonances were assigned to the meso dyad and the downfield resonances were assigned to the racemic dyad. Experiments were also performed on the diasteromers of 2,4-diaminopentane, which confirmed the assignments made for the polymer. The approach used in this study was suggested to be a general one for the dyad assignment of other vinyl polymers.

INTRODUCTION

Nuclear magnetic resonance (NMR) spectroscopy has been widely used in past years as a practical method to analyze the configuration of polymers. Recently, two-dimensional (2D) NMR spectroscopy has been applied to this problem. Since 2D NMR experiments disperse the signals into two frequency domains, these techniques can, in principle, be used to resolve nearly degenerate resonances and make configurational assignments easier. For example, Bovey and coworkers[1] have used ^{19}F 2D J-correlated spectroscopy (COSY) to analyze the microstructure of poly(vinyl fluoride). Brown and coworkers have also made configurational assignments of poly(vinyl chloride)[2] and poly(vinyl alcohol)[3] by the use of ^{1}H 2D J-resolved experiments adapted for macromolecules (FOSY). Cheng and Lee[4] have employed ^{1}H-^{13}C heteronuclear shift-correlated 2D NMR (CSCM) to analyze the sequence distribution of ethylene-propylene copolymers. However, the use of this technique to study the configuration of polymers has not been reported. Recently, a broadband homonuclear decoupling variation of the heteronuclear shift-correlated 2D NMR experiment (CSCMBB) has been proposed by Bax.[5] This experiment eliminates the coupling among vicinal protons in the ^{1}H domain, and results in a contour plot with enhanced resolution and improved sensitivity. In this communication, we show that each of these experiments are extremely useful for the dyad assignment of the methylene carbon of poly(vinylamine) (PVAm) and further suggest that these techniques may be general ones for making these assignments in other vinyl polymers.

Normally, the configurational assignments of resonances are made by comparing the polymer NMR spectrum to the spectra of model compounds or reference polymers, one with a dominate configuration. However, each of these methods is beset with difficulties. The use of model compounds may lead to wrong resonance assignments in the polymer spectrum when the polymer chemical shifts are influenced by long-range interactions and conformational effects not present in the models. Furthermore, reference polymers, if available, may have unique steric or conformational properties not present in atactic polymers and also result in chemical shift changes in certain resonances.[6] Certainly, it will be more desirable to make tacticity assignments strictly on the basis of the fundamental properties of the polymer in question. The 2D NMR approach described in this communication utilizes this feature.

RESULTS AND DISCUSSION

It has been known for years that the methylene protons of the meso (m) isomer for both model compounds and vinyl polymers are chemically nonequivalent and lead to two multiplets, while the methylene proton resonances of the racemic (r) isomer are degenerate.[6,7] For instance, the

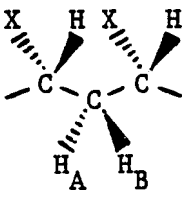

Meso Dyad

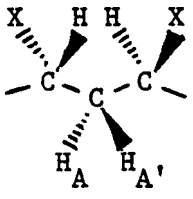

Racemic Dyad

^{1}H NMR spectra of 2,4-diaminopentane (DAP), in nearly a one to two molar mixture of m and r isomers at pH=1.5 (Fig. 1a) and pH=8.8 (Fig. 1b), illustrate these points. Two well-separated multiplets arise from the chemically nonequivalent methylene protons of m DAP. The central peaks are assigned to the methylene protons of r DAP. With increasing pH, the chemical shift difference between the two methylene m protons will become smaller, but not vanish (Fig. 1b). In principle, the nondegenerate methylene proton resonances can be used to determine the m and r content of vinyl polymers, as was recently shown for poly(acrylic acid)[8] as well as for other vinyl polymers.[6] Unfortunately, the ^{1}H NMR resonances of many vinyl polymers are obscured due to severely overlapped resonances. This is the case for the methylene proton resonances of PVAm, where virtually one broad peak appears at both pH=1.5 (Fig. 1c) and at pH=8.8 (Fig. 1d); even though, the methylene resonances in the ^{1}H NMR spectrum of PVAm at pH 8.8 suggest that both m and r resonances are contained within this peak (Fig. 1d).

Because of the poor resolution in the ^{1}H spectra of PVAm, the tacticity of PVAm was examined by ^{13}C NMR. The optimal configurational sensitivity for PVAm was found at pH=8.8 (Fig. 2b). The three most downfield regions (A, B and C) are assigned to the methine carbon resonances displaying triad and even some pentad resolution. The two upfield regions (D and E) are the methylene carbons displaying principally dyad resolution, but also contain some higher order configurations. The ^{13}C NMR spectrum between 35 and 55 ppm of the DAP mixture at pH=8.8 contains only three resonances (Fig. 2a, methyl resonances not shown). The resonances for the methine carbons of m and

Figure 1. The 300 MHz ^{1}H NMR spectra of 2,4-diaminopentane at pH=1.5 (a) and pH=8.8 (b), and of poly(vinylamine) at pH=1.5 (c) and pH=8.8 (d) in D_2O at room temperature. The 2,4-diaminopentane sample contained nearly a 1:2 mixture of meso and racemic isomers. The concentration of poly (vinylamine), was 0.05M. Chemical shifts are referenced internally to 3-(trimethylsilyl)-tetradeuteroproprionic acid, sodium salt.

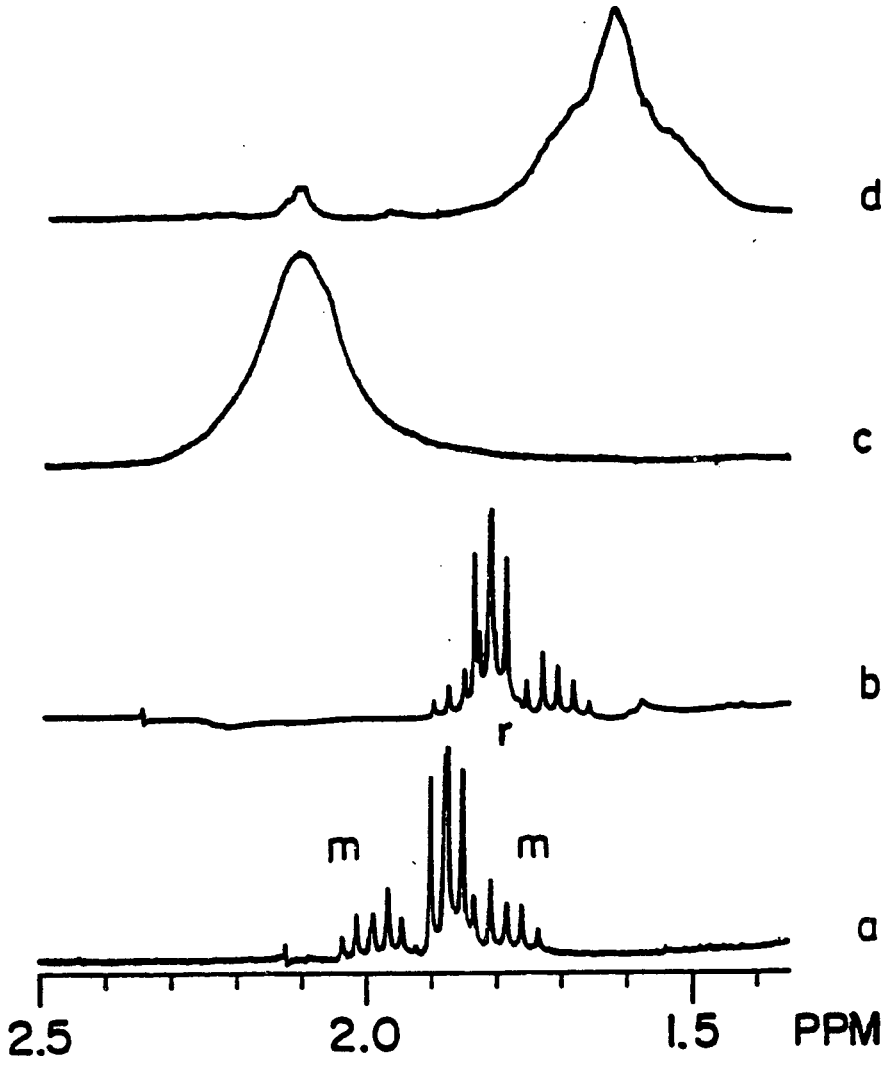
d
c
b
r
m
m
a
2.5
2.0
1.5
PPM

Figure 2. The 75.5 MHz ^{13}C NMR spectra with proton decoupling of 2,4-diaminopentane (1:2 molar mixture of meso and racemic isomers) at pH=8.8 (a) and poly(vinylamine) at pH=8.8 (b). The concentration of poly(vinylamine) was 10% (W/V) and the spectra were internally referenced to dioxane (66.5 ppm TMS).

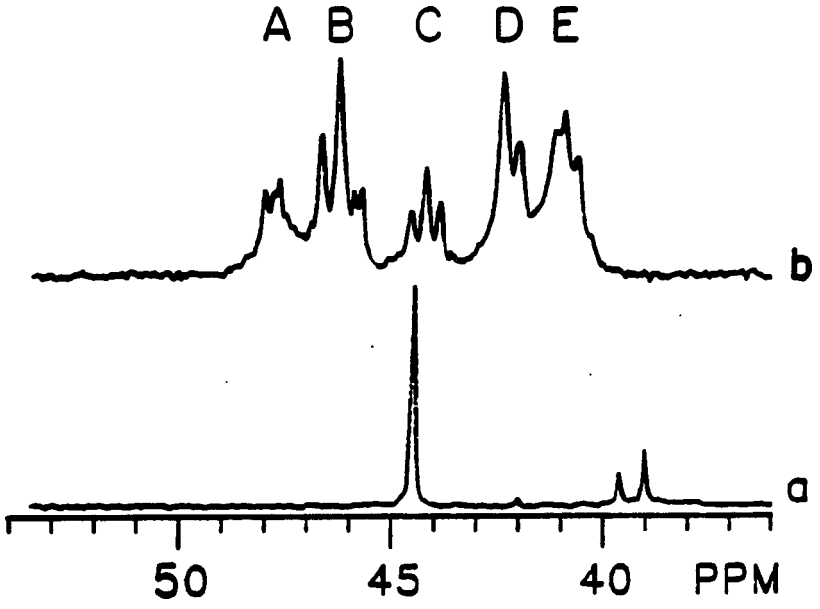
A B C D E
b
a
50
45
40
PPM

r DAP are overlapped at 44.44 ppm. The smaller downfield peak (39.55 ppm) is due to the methylene carbon of m DAP and the upfield peak (38.96 ppm) is due to this carbon in r DAP. According to the relative chemical shifts of the m and r methylene carbon resonances of the model compounds, the D peak of PVAm was initially assigned to the m dyad and the upfield E peak was assigned to the r dyad (Fig. 2).

In order to provide additional experimental evidence for these assignments, heteronuclear correlated 2D NMR experiments were used to examine the correlation between the carbon and proton resonances. Prior to studying PVAm, the CSCM and CSCMBB experiments were performed on the DAP mixture at pH=8.8 (Fig. 3). The contour plot shows a clear correlation of the methine carbon and proton resonances in each experiment. Likewise, the upfield r methylene carbon resonance displays a cross peak with the r methylene protons. The cross section of this correlation parallel to the ^{1}H axis is shown in Fig. 4a. For the methylene carbon resonance of m DAP in the CSCM experiment, a clear correlation occurred between this carbon resonance and the two nonequivalent methylene proton (Fig. 4b), reconfirming the assignments of the model compound resonances. A chemical shift difference of 68 Hz is estimated from this data, which is consistent with the separation found in the one-dimentional spectrum (Fig.1b). For the CSCMBB experiment, a drastic reduction occurs in the intensity of the m methylene carbon-proton correlation (Fig. 3). This fact is further reinforced in the projected data set (Fig. 3a) compared to the completely decoupled ^{13}C NMR experiment (Fig. 3c). Since the m methylene carbon resonance is only partially reduced as a result of the CSCM experiment (without homonuclear broadband decoupling, Fig. 3b),

Figure 3. The contour plot from the heteronuclear correlated 2D NMR experiment with broadband proton decoupling (CSCMBB) for a 1:2 molar mixture of meso and racemic isomers of 2,4-diaminopentane (pH=8.8). The ^{1}H NMR spectrum is above the ^{1}H axis. The projected data set from this experiment (a) and from the heteronuclear correlated 2D NMR (CSCM) experiment (b) as well as the proton decoupled ^{13}C NMR spectrum (c) are above the ^{13}C axis. These spectra have been scaled relative to the racemic methylene resonance for the purpose of comparison. The resonance at about 41.9 ppm is an impurity.

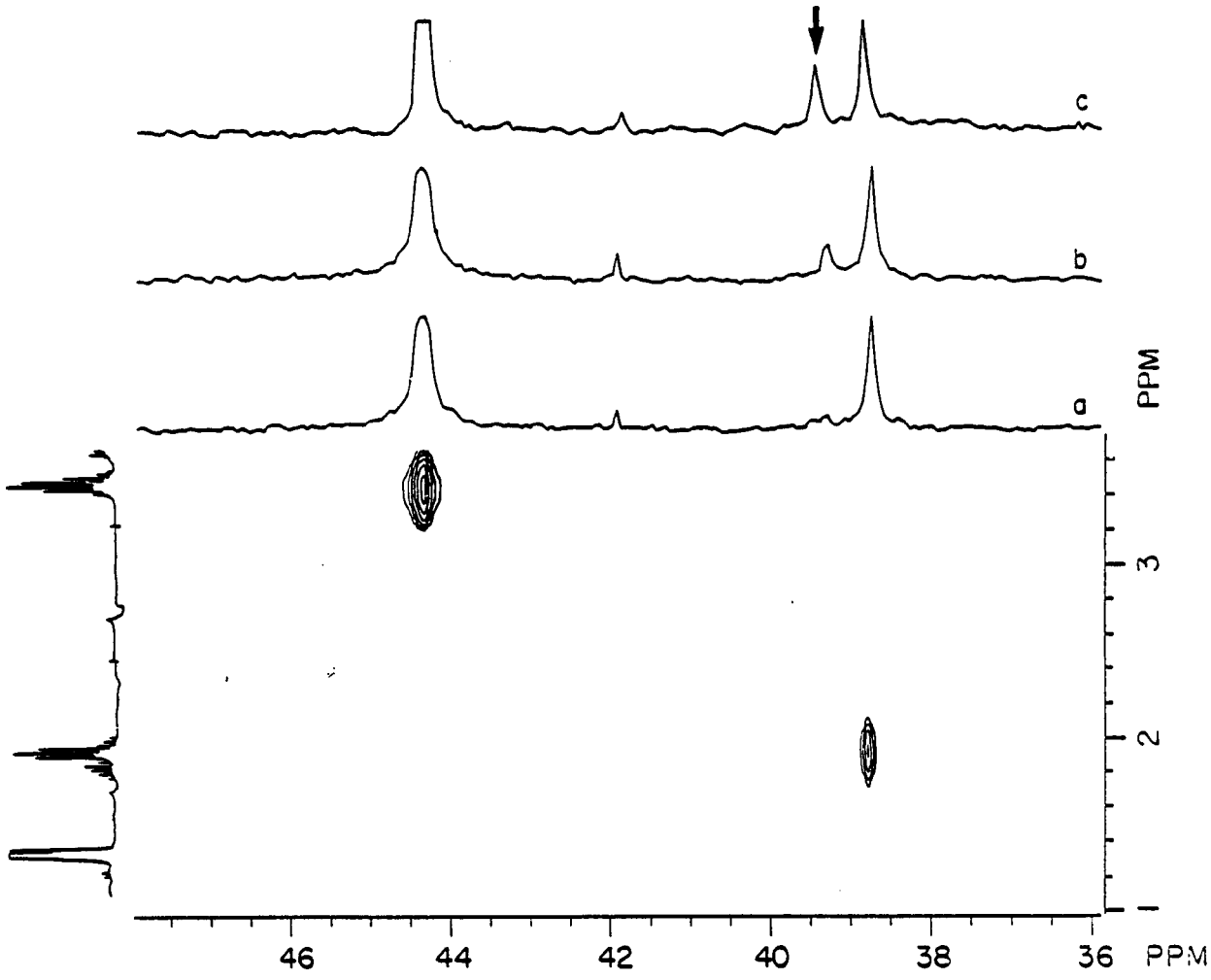
c
b
a
PPM
3
2
1
46
44
42
40
38
36
PPM

Figure 4. Cross sections parallel to the ^{1}H axis for the methylene carbons of 2,4-diaminopentane and poly(vinylamine) each at pH=8.8. The individual slices were processed from the F2T1 data set of the CSCM experiment with a double zero fill, exponential multiplication of 10Hz and phased to display absorption mode spectra. Spectra (a) and (b) correspond to the r and m methylene carbons of the model, respectively. Spectra (c) and (d) correspond to the D and E regions for the polymer, respectively. Since the ^{1}H chemical shifts of the model and polymer are different (Fig.1), the chemical shifts of the resonances of spectra (a) and (c) are set to zero Hz.

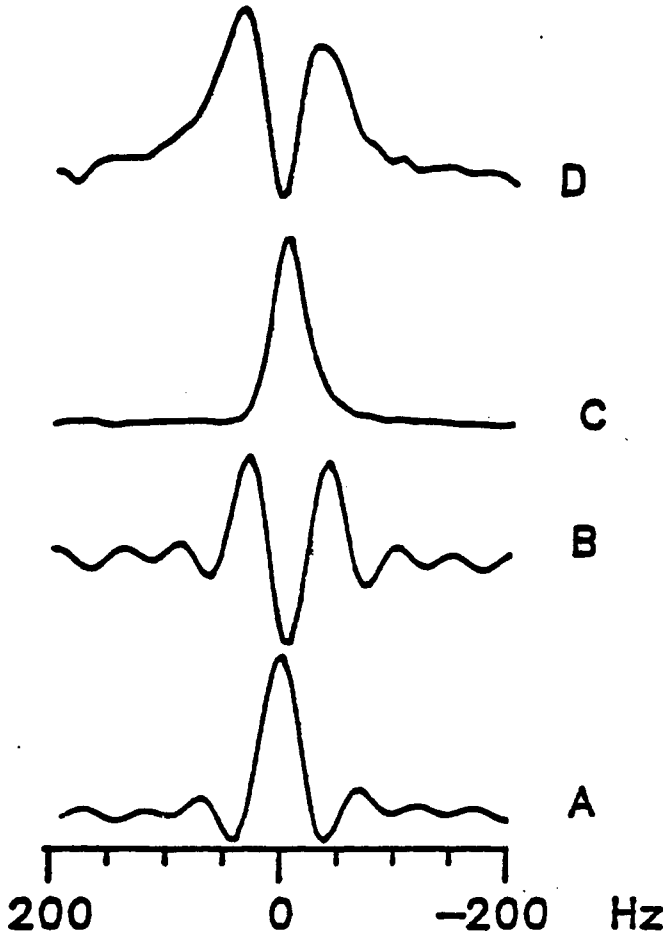
D
C
B
A
200
0
−200
Hz

this suggests that the ($\pi/2$, ^1H) - ($1/2J_{CH}$) - (π, ^1H,^{13}C) - ($1/2J_{CH}$) - ($\pi/2$, ^1H) pulse sequence is most responsible for the loss of correlation between the m resonances.

Pines and coworkers[9] have shown that this pulse sequence, referred to as a bilinear π rotation, refocuses the proton magnetization of the carbon satellites at the chemical shift of the non-satellite magnetization. This has a similar effect as the ^{13}C pulse used in the CSCM experiment.[10] The novel aspect of this pulse sequence lies in the elimination of vicinal proton coupling, hence achieving a broadband proton decoupled spectrum for methine carbons[5] as well as methylene and methyl carbons.[11] Optimal signal occurs when the delay value is set to $1/2J_{CH}$.[5] Error in this value decreases the intensity of the carbon-proton correlation peak.[11,12] However, since the delay used in the CSCMBB experiment on the DAP mixture was based on the measured J_{CH} value (127 Hz), we do not attribute the loss of the m methylene cross peak to this condition. Two other factors can also reduce the intensity of the carbon-proton correlation. Proton multiplet widths, which are greater than 20% of J_{CH}, result in significant intensity appearing in unwanted signals at $\pm J_{CH/2}$.[11,12] The multiplet proton width of m DAP is nearly 30 Hz, which is greater than that of r DAP (15 Hz). According to Wilde and Bolton,[12] the m methylene correlation should be reduced by about 20% with respect to the r methylene correlation. Another factor which influences the intensity of these correlations is the extent of strong coupling present among the satellite protons.[9] As shown by Bolton,[13] one of the ^{13}C satellites is often strongly coupled to other protons where the chemical shift range is compressed. Since the

chemical shift difference between the m methylene proton resonance is only 62 Hz (Fig. 1), it is expected that, for each methylene proton, there is a strongly coupled satellite. A single bilinear π rotation pulse sequence does not refocus the magnetization from strong proton-proton coupling and results in a loss of intensity of nonequivalent protons attached to the ^{13}C nucleus.[8] Apparently, a minimum of four bilinear π pulses are needed to completely decouple protons which are strongly coupled.[8] Thus, the loss of the m methylene carbon-proton correlation is consistent with the chemical nonequivalence, large multiplet width and probably strong coupling of these protons.

The CSCM and CSCMBB experiments were performed on PVAm at pH=8.8. For each of these experiments, a single correlation between the D methylene region and the center of the methylene protons was observed, as shown in the contour plot (Fig. 4) and as a slice along the D carbon resonance parallel to the ^{1}H axis (Fig. 4c). The E methylene region of PVAm contained two cross peaks in the CSCM experiment, separated by 63 Hz from each other (Fig. 4d). Even though these resonances are not resolved in the one-dimensional experiment, the 2D approach achieved clear separation of the resonances. This separation is consistent with that found for the model compounds (Fig. 4b) and indicates that the D region represents the r carbon dyad resonances, while the E region contains m dyad carbon resonances. Furthermore, the results of the CSCMBB experiment on PVAm indicate proton-carbon correlation for the D region is maintained, while that for the E region is much reduced (Fig. 5).[14] Again, the projected data sets of the CSCMBB (Fig. 5a) and the CSCM (Fig. 5b) experiments as well as the normal proton decoupled

Figure 5. The contour plot from the heteronuclear correlated 2D NMR experiment with broadband decoupling (CSCMBB) on a 10% (W/V) solution of poly(vinylamine) in D_2O at pH=8.8. The ^1H NMR spectrum is above the ^1H axis. The projected data set from this experiment (a), the heteronuclear correlated 2D experiment without broadband ^1H decoupling (b), and a decoupled ^{13}C NMR spectrum (c) are above the ^{13}C axis.

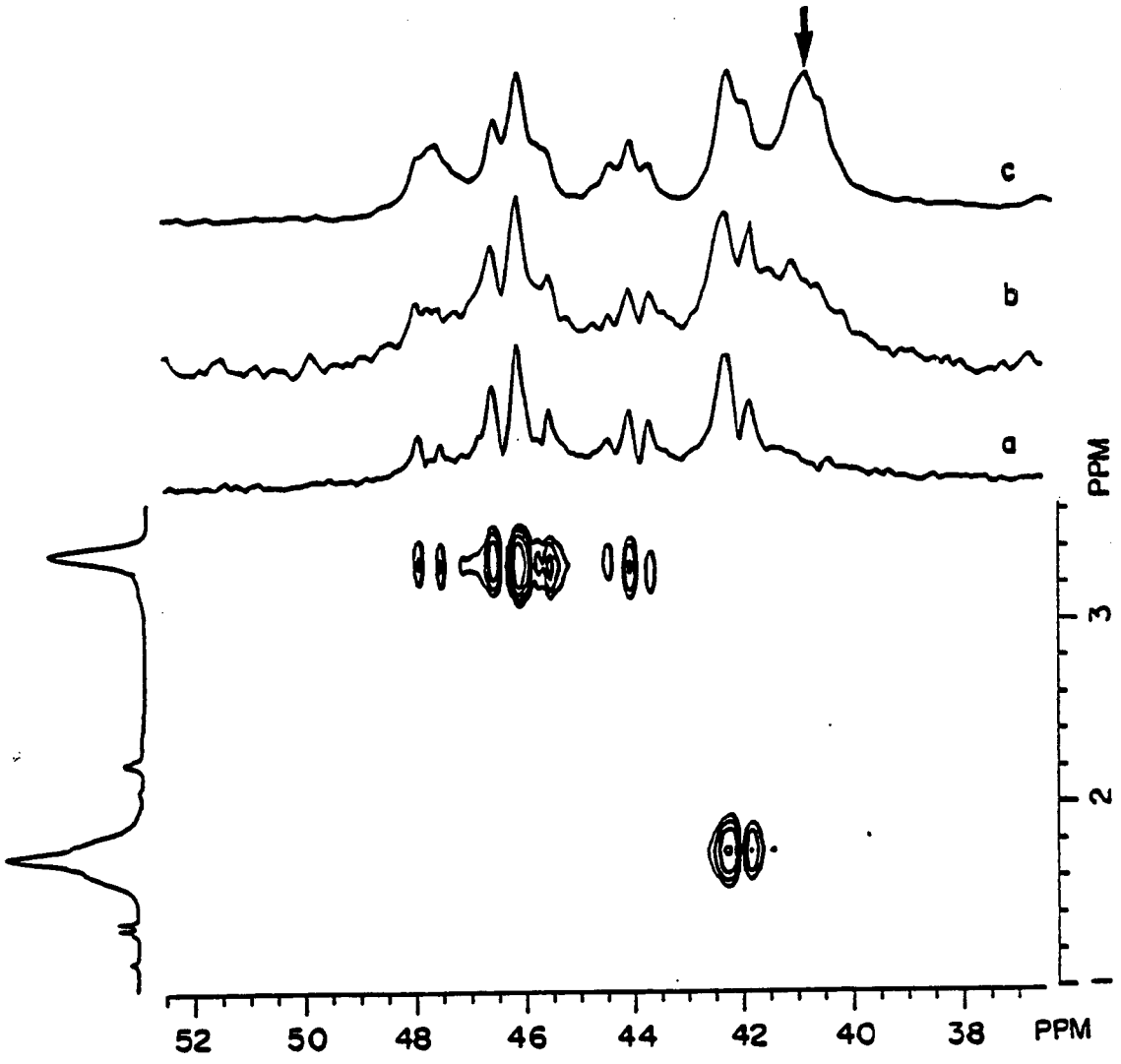
c
b
a
PPM
3
2
1
52
50
48
46
44
42
40
38
PPM

^{13}C spectrum (Fig. 5c) support this fact. This assignment is contrary to the assignments proposed above from the relative chemical shifts of the model compounds.

We show that the heteronuclear correlated 2D experiments (CSCMBB and CSCM) are able to provide valuable information leading to the dyad configuration assignment of PVAm. Since the phenomenon of chemically nonequivalent m protons and equivalent r protons is a general one for vinyl polymers, we suggest that these techniques may be useful for their dyad assignments. In many vinyl polymers, the chemical shift difference between the m methylene protons will be sufficient to have the satellite protons not strongly coupled to each other, resulting in each 2D experiment providing two clear correlations between the m methylene carbon and proton resonances; whereas, the r methylene carbon resonances should only exhibit a single cross peak. The great advantage of this technique is that the configurational assignment of vinyl polymers would rely on an intrinsic property of the polymer and can potentially be made independent of model compounds or reference polymers. A more complete configurational analysis of PVAm, based on these dyad assignments, will be presented elsewhere.

EXPERIMENTAL

The NMR spectra were recorded using a GE 300 WB spectrometer (NT series) equipped with a 1280 computer and 293c pulse programmer. The ^{13}C NMR spectra were obtained with complete proton decoupling on 10% (W/V) solutions in D_2O at 25°C, with dioxane as an internal chemical shift reference (66.5 ppm relative to tetramethysilane). Pulse

angles of 68° (19 μs), repetition rates of 2.5s, sweep widths of 2100 Hz and 2K data points were used to acquire the free induction decays. ^{1}H NMR spectra were obtained on 0.5% (W/V) in D_2O solutions at 25°C. Pulse angles of 75° (8 μs), sweep widths of 900 Hz and 8K data points were used to acquire the free induction decays. A broadband homonuclear decoupling heteronuclear correlated 2D NMR experiment used the following (CSCMBB) sequence:[5] $(\pi/2, {}^{1}H) - (t_1/2) - (\pi/2, {}^{1}H) - (1/2J_{CH}) - (\pi, {}^{1}H; \pi, {}^{13}C) - (1/2J_{CH})\ (\pi/2, {}^{1}H) - (t_1/2) - (\Delta_1) - (\pi/2, {}^{1}H; \pi/2, {}^{13}C) - (\Delta_2) -$ (FID, decoupling). Thirty-two spectra were acquired in 12 hrs with the spectral width of 2K data points. Processing involved an exponential multiplication in the F2 domain and sine multiplication and zero filling in the F1 domain. This produced a 1K x 64 point data set. The $\pi/2$ proton and carbon pulses were 40 and 25 μs, respectively. The delays Δ_1=4ms and Δ_2=1.9ms were used corresponding to J_{CH}=127 Hz. A hetero- nuclear correlated 2D NMR experiment (CSCM) uses the same sequence as CSCMBB only without $(\pi/2, {}^{1}H) - (1/2J_{CH}) - (\pi, {}^{1}H) - 1/2J_{CH} - (\pi/2, {}^{1}H)$ pulses. The parameters and processing procedures are the same as stated above for CSCMBB.

REFERENCES

1. Bruch, M. D.; Bovey, F. A.; Cais, R. E. Macromolecules 1984, 17, 2547.

2. Macura, S.; Brown, L. R. J. Magn. Reson. 1983, 53, 529.

3. Gippert, G. P.; Brown, L. R. Polymer Bull. 1984, 11, 585.

4. Cheng, H. N.; Lee, G. H. Polymer Bull. 1984, 12, 463.

5. Bax, A. J. Magn. Reson. 1983, 53, 517.

6. Bovey, F. A. "Chain Structure and Conformation of Macromolecules"; Academic Press: 1982; p 39-99.

7. Bovey, F. A.; Hood, F. P.; Anderson, E. W.; Snyder, L. C. J. Chem. Phys. 1965, 42, 3900.

8. Chang. C.; Muccio, D. D.; St. Pierre, T. Macromolecules (In press).

9. Garbow, J. R.; Weitekamp, D. P.; Pines, A. Chem. Phys. Lett. 1982, 93, 504.

10. Bax, A. In "Two-Dimensional Nuclear Magnetic Resonance in Liquids"; Reidel, Boston, Mass., 1982; p 50-65.

11. Rutar, V. J. Mag. Reson. 1984, 58, 306.

12. Wilde, J. A.; Bolton, P.H. J. Mag. Reson. 1984, 59, 343.

13. Bolton, P. H. J. Mag. Reson. 1983, 51, 134.

14. In the CSCMBB experiment, two resonances similar to that displayed in Fig. 4d were observed, but with much reduced intensity. Furthermore, we cannot on the basis of this analysis exclude the possibility of a high order m centered peak contributing to the r peaks and vice versa.

CHAPTER IV

A CONFIGURATIONAL STUDY OF POLY(VINYLAMINE) BY MULTINUCLEAR NMR

C. Chang, D. D. Muccio, and T. St. Pierre
Department of Chemistry
The University of Alabama at Birmingham
Birmingham, Alabama 35294

C. C. Chen and C. G. Overberger
Department of Chemistry and
the Macromolecular Research Center
The University of Michigan
Ann Arbor, Michigan 48109

ABSTRACT

The tacticity of poly(vinylamine) (PVAm), prepared from N-vinyl-t-butylcarbamate (PVAmI) and from N-vinylacetamide (PVAmII), was determined by C-13 NMR. The configurational sensitivity was optimal at pH=8.8 where nine well-resolved methine carbon resonances and five methylene carbon resonances were observed. Based on the meso (m) and racemic (r) assignments for the methylene carbon resonances of PVAm made previously by the use of heteronuclear correlated 2D NMR experiments, the dyad distribution for the PVAmI methylene regions was found to be 56% (r) and 44% (m). These results were extended to the tetrad analysis of the methylene peaks. The triad analysis were obtained from the relative area of the three distinct methine regions. The pentad assignments were made by a comparison of the nine methine peak areas with those calculated from first order Markov statistics and Bernoullian statistics. This analysis is supported, at the triad level, by N-15 NMR. Acetylated PVAmI, poly(N-vinylacetamide), was characterized by H-1 NMR for triad analysis of the $COCH_3$ group. This analysis gave internally consistent results with the C-13 analysis. A similar analysis for PVAmII gave 49% (r) and 51% (m).

INTRODUCTION

Compared to the studies of the titration behavior of poly-(vinylamine) (PVAm), only two reports have appeared concerning the tacticity of this polymer. Murano and Harwood[1] employed H-1 NMR to determine the tacticity of PVAmI, prepared from N-vinyl-t-butylcarbamate, indirectly by analysis of the acetyl derivative, poly(N-vinylacetamide) (PVAc). Based on the comparison of the methyl peaks of PVAc with the methyl peaks of acetylated meso (m) and racemic (r) 2,4-diaminopentane (DAP), they concluded that the PVAmI was essentially a syndiotactic (r > m) polymer. St. Pierre et. al.[2] investigated PVAmI by C-13 NMR. The assignments of the three methine peaks, mm , mr and rr from low to high field, were based on the changes of chemical shift with pH and the known assignments of poly(vinyl alcohol).[3] According to the relative areas of the methine peaks the polymer was judged to be atactic. An atactic polymer with opposite methine assignments, based on the relative C-13 chemical shift of m and r DAP, was recently reported by Chang et al.[4]

Because of the uncertainty of both the H-1 and C-13 peak assignments and the apparent discrepancy in tacticity, a systematic study of PVAm was undertaken. The methylene assignments for PVAm were based on C-13 analysis using heteronuclear correlated 2D NMR experiments and confirmed by applying the same experiments to m and r DAP.[5] In this study the tacticity of both PVAmI and PVAmII, the latter prepared from N-vinylacetamide, was determined by quantitative C-13 and N-15 NMR analysis. The comparison of the two slightly different

polymers was useful in confirming the peak assignments. Finally, the H-1 NMR analysis of PVAc was shown to be consistent with the C-13 and N-15 analyses of the parent polymer. Both Bernoullian and first order Markov statistics were used for fitting and testing the experimental results.

MATERIALS AND METHODS

PVAmI[6] was prepared from N-vinyl-t-butylcarbamate and PVAmII[7] was prepared from N-vinylacetamide. PVAc[8] was synthesized by adding acetic anhydride to a DMSO solution of PVA-nHOSu (HOSu=N-hydroxysuccinimide, n>6) at 25°C, and isolated by precipitation in acetone. The model compounds, m and r diaminopentane (DAP) were prepared by the method of Bosnich.[9] The NMR spectra were recorded using a GE 300 WB spectrometer (NT series) equipped with a 1280 computer and 293c pulse programmer. The C-13 NMR spectra were obtained with gated-decoupling (decoupler off during delay time) on 5% (W/V) solutions in D_2O at 25°C. The repetition rate for these measurements was ten times the longest spin-lattice relaxation time. The T_1 values were measured from the inversion recovery pulse sequence[10] employing a composite 180° pulse with delay values of 0.01, 0.05, 0.1, 0.2, 0.5 and 1.4 s. The T_1 values were calculated using a nonlinear, three-parameter fitting procedure.[11] C-13 NMR spectra were obtained with dioxane as an internal chemical shift reference (66.5 ppm relative to tetramethysilane). Pulse angles of 58° (19 μs), repetition rates of 2.5s, sweep widths of ± 7575Hz and 16K data points were used to acquire the free induction delays. The

N-15 NMR spectra of PVAmI were obtained with proton decoupling and gated decoupling on 10% (w/v) solutions in 10% D_2O at 25°C. Pulse angles of 75° (30 μs), repetition rates of 10 s, sweep widths of ± 1000 Hz and 2K data points were used to acquire the free induction decays. The T_1's were measured, as above, by using delay values of 0.01, 0.2, 0.7, 2.8 and 5.6 s. Nuclear Overhauser effects (NOE) were determined by the ratio of the peak intensity of the fully proton decoupled and gated decoupled (decoupler off during delay time) spectra. Ammonium chloride in 10M HCl was used as an external chemical shift reference (30.31 ppm from liquid ammonium at 25°C). H-1 NMR spectra were obtained on 0.3% (W/V) by weight in D_2O solutions with TSP as an internal reference at 25°C, 40°C, 60°C and 80°C. Curve deconvolution was accomplished with NMCCAP progam provided by the GE software using a completly Lorentzian line shape. The pH's were adjusted with NaOD and recorded on an Orion research model 701A pH meter with a microcapillary Ingold combination electrode.

RESULTS AND DISCUSSION

The C-13 NMR spectra of both PVAmI and PVAmII were recorded at pH=8.8 in D_2O by using a gated-decoupled pulse sequence in order to suppress the NOE. The configurational sensitivity is optimal at this pH. As the pH is lowered, the tacticity effects disappeared leaving a single but sharp peak for the methine carbon and a single but broad peak for the methylene carbon at pH=2, Fig. 1. At higher pH values, the configurational sensitivity is preserved; but the methine and methylene

Figure 1. C-13 NMR of PVAmI in D_2O at 25°C and at the indicated pH's.

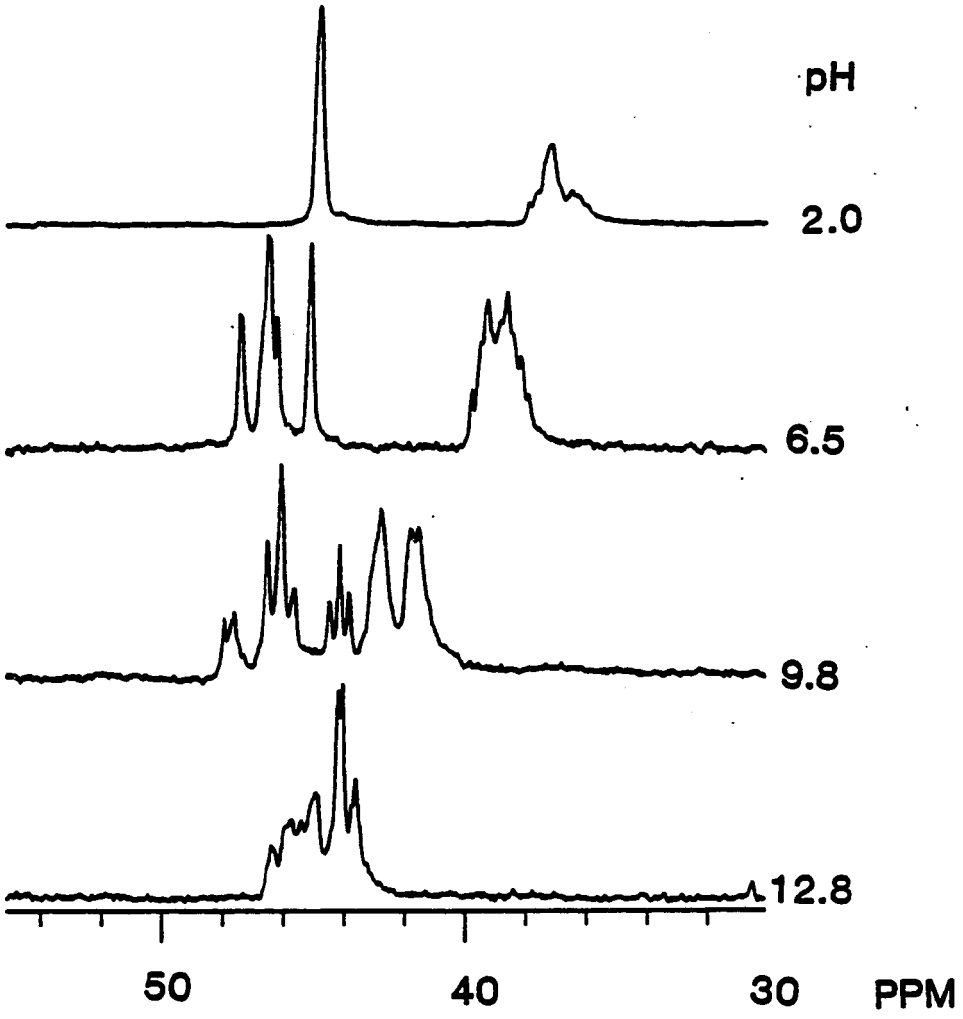
pH
2.0
6.5
9.8
12.8
50
40
30
PPM

carbon peaks are overlapped, Fig. 1. The C-13 NMR spectrum of PVAmI and its simulated spectrum are shown in Fig. 2. Five regions, labeled A through E, are observed. The A, B and C regions belong to the methine carbon resonances, and the D and E regions belong to the methylene carbon resonances. The areas of these five regions, obtained from curve deconvolution, are 17, 54 and 29% for the A, B and C triad distribution, respectively, and 55 and 45% for D and E dyad distribution, respectively.

In order to ensure a quantitative relationship between peak areas and the number of carbons, it is necessary to avoid saturation. Therefore, the T_1 values at pH=8.8 were measured and found to have almost equal values for the peaks in the methine carbon region (0.25 s) and the peaks in the methylene carbon region (0.13 s). Because nearly $10xT_1$ was used for the repetition rates in the acquisition of these gated-decoupled spectra, it is not necessary to correct the peak areas.

Initially the model compounds, m and r DAP, were used to assign the dyad configuration of the methylene carbon of PVAmI.[4] The fully proton-decoupled C-13 NMR spectrum of a one to two molar mixture of m and r DAP was recorded at 25°C and pH=8.8. The observed smaller CH_2 resonance at low field (39.59 ppm) was due to the m isomer and upfield resonance (39.00 ppm) due to the r isomer. The relative chemical shifts were first used to assign the m and r dyads of the polymer.[4] However, further studies employing heteronuclear correlated 2D NMR demonstrate convincingly the low field peak of m DAP corresponds to the upfield methylene peak of PVAmI and upfield peak of r DAP to the downfield peak of PVAmI.[5] Therefore, the D region

Figure 2. C-13 NMR of PVAmI in D_2O at 25°C and at pH=8.8 with CH_2 from 40-43 ppm and CH from 43-49 ppm. The top spectrum was observed and the middle and bottom spectra were calculated.

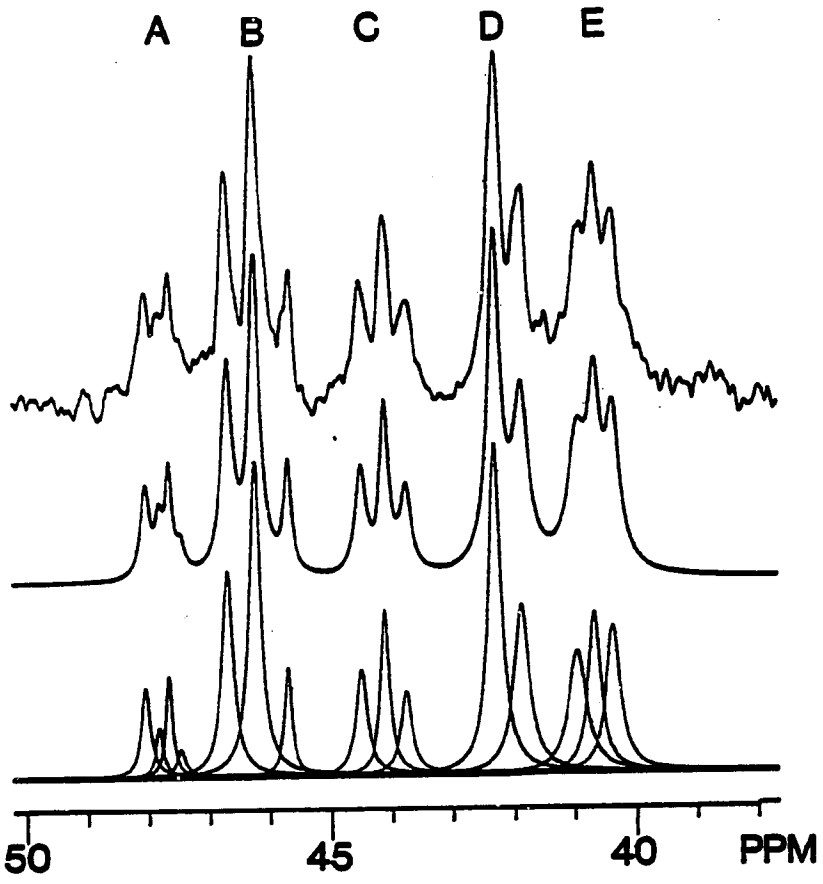
A
B
C
D
E
50
45
40
PPM

(55%) of PVAmI was assigned to the r dyad and the E region (45%) was assigned to the m dyad.

Our initial analysis assumes that all r and m centered peaks are grouped together in regions D and E respectively and likewise for the rr, mr, and mm centered peaks. Bernoullian statistics[12,13] were employed to test the triad sequence from these r and m probabilities which gave 29.9, 49.6, and 20.5% for the rr, mr, and mm triad sequences, respectively. A comparison of the calculated and experimental values for the triad analysis led to the tentative assignment of the mm sequence to the A region and the rr sequence to the C region. The experimental values for the three methine peaks were used to calculate the dyad sequence, 56% (r) and 43% (m), according to Bernoullian statistics.[14] First order Markov statistics were also used to fit the experimental results from the methine triad regions by the following relations:[13]

$$Pm/r = \frac{mr}{2(mm) + mr}$$

$$Pr/m = \frac{mr}{2(rr) + mr}$$

$$Pm = \frac{Pr/m}{Pm/r + Pr/m}$$

$$Pr = \frac{Pm/r}{Pm/r + Pr/m}$$

These calculations gave the dyad sequence 56% (r) and 44% (m). These two different statistics gave similar dyad distributions and values close to the experimental values of D and E.

The methine carbon appeared as nine peaks, suggesting pentad resolution. Based on either Bernoullian or first order Markov statistics, these calculated pentad values were compared to the experimental results. On the basis of matched areas, the high order assignments were made. Experimental and calculated pentad distributions with assignments and chemical shifts are given in the Table. Since the rr centered peaks were better resolved, they were examined by both Bernoullian and first order Markov statistics. Using this more critical test, we found little difference between these statistics, as expected for atactic polymers. Because the probabilities of rrrr, mrrm, mrrr, rmmm, rmmr and mmmm are very different, within their respective triads, their assignments were made with confidence (Table). For instance, if the positions of rrrr and mrrm were interchanged, a significantly poorer fit was observed. As to the mr centered triad (Table), suggested assignments are made but with less confidence. The standard deviation between calculated and experimental results was 1.1% for the first order Markov and 1.7% for the Bernoullian statistics.

The methylene carbon consists of five peaks, suggesting a tetrad resolution. Comparing the calculated tetrad sequences to the experimental results, it is obvious that the sequences cannot be assigned unambiguously. As mentioned above, the D region was assigned to the r dyad; however, it is also possible to have an m centered resonance contribute to the D region and vice versa, as reported by Ovenall for poly(vinyl alcohol).[15] We find in particular a better fit might

TABLE

C-13 NMR ANALYSIS OF POLY(VINYLAMINE)

Peak Assignments	.(ppm)	PVAmI First Order	PVAmI Zero Order[a]	PVAmI Exp.[b]	PVAmII First Order	PVAmII Zero Order[a]	PVAmII Exp.[b]
r		0.56		0.55	0.50		0.48
m		0.44		0.45	0.50		0.52
rr				0.29			0.23
mr				0.54			0.54
mm				0.17			0.23
mmm	40.40	0.07	0.09	0.10	0.10	0.13	0.11
mmr	40.67	0.21	0.22	0.21	0.25	0.25	0.31
rmr	40.97	0.17	0.14	0.15	0.15	0.12	0.10
rrr	41.89	0.15	0.17	0.16	0.10	0.12	0.14
mrr		0.28	0.28		0.25	0.25	
mrm		0.13	0.11		0.15	0.13	
mrrm	43.75	0.07	0.06	0.07	0.07	0.06	0.07
mrrr	44.10	0.14	0.15	0.14	0.11	0.12	0.11
rrrr	44.50	0.08	0.10	0.08	0.05	0.06	0.05
mrmm	45.67	0.10	0.10	0.07	0.14	0.13	0.11
mmrr		0.11	0.12		0.11	0.13	
rmrm		0.16	0.12		0.16	0.13	
rrmr	46.70	0.17	0.15	0.18	0.13	0.12	0.14
mmmm	47.43	0.03	0.04	0.02	0.05	0.07	0.05
mmmr[c]	47.73	0.08	0.10	0.09	0.12	0.13	0.11
rmmr	48.03	0.06	0.06	0.06	0.07	0.06	0.07

[a]Bernoullian; [b]Based on S/N = 20, the error is estimated to be + 5%; [c]Notice in Fig. 2, Region A consists of four peaks instead of the expected three peaks. Counting from left to right, Peaks 2 and 3 were combined in this assignment.

be obtained for the tetrad data by interchanging the rrr and rmr contributions to the D and E regions (Table), but based on our 2D results[5] the peak at 41.89 ppm belongs to an r centered tetrad.

The tacticity of PVamII was also analyzed by this procedure, and the results are shown in the Table. This analysis gave 49% r and 51% m for PVAmII based on first order Markov statistics. Although PVAmI and PVAmII did not have sufficiently different tacticities at the dyad level, they exhibited larger differences at the triad and pentad level. For instance, the rr and mm centered peaks reasonably decrease or increase and these trends are consistent with our assignments. For example, the rrrr and mmmm for PVAmII decreased and increased, respectively, according to the slight changes in r and m values between the two polymers (Table).

In addition to the C-13 results, we have used N-15 NMR to determine the tacticity of PVAm. The N-15 NMR spectrum of PVAmI and its simulated spectrum in 10% D_2O at 25°C are shown in Fig. 3. Six well resolved peaks at 46.5, 44.7, 44.2, 43.4, 42.9 and 42.4 ppm were observed, labeled A through F, respectively. The T_1 values of these six peaks were found to be almost equal (1.0 $\pm$ 0.1). The NOE of peak A is -3.7 $\pm$ 0.1, of peaks B and C is -3.5 $\pm$ 0.1 and of peaks D, E and F is -2.8 $\pm$ 0.1. The peak areas of these six peaks obtained with the NOE (better sensitivity than without NOE) are 20, 29, 29, 5, 12 and 5% for the peaks A through F, respectively. After the normalization of NOE, the respective peak areas of these six peaks are 18, 28, 29, 6, 14 and 6%. Based on the triad distributions obtained from the C-13 NMR results, we assign the A peak as the mm triad (18%), the B and C peaks as the mr triad (56%) and the D, E and F peaks as the rr triad (26%). It is worth

Figure 3. N-15 NMR of PVAmI in 10% D_2O at 25° and at pH=10.5. The top spectrum was observed and the middle and bottom were calculated.

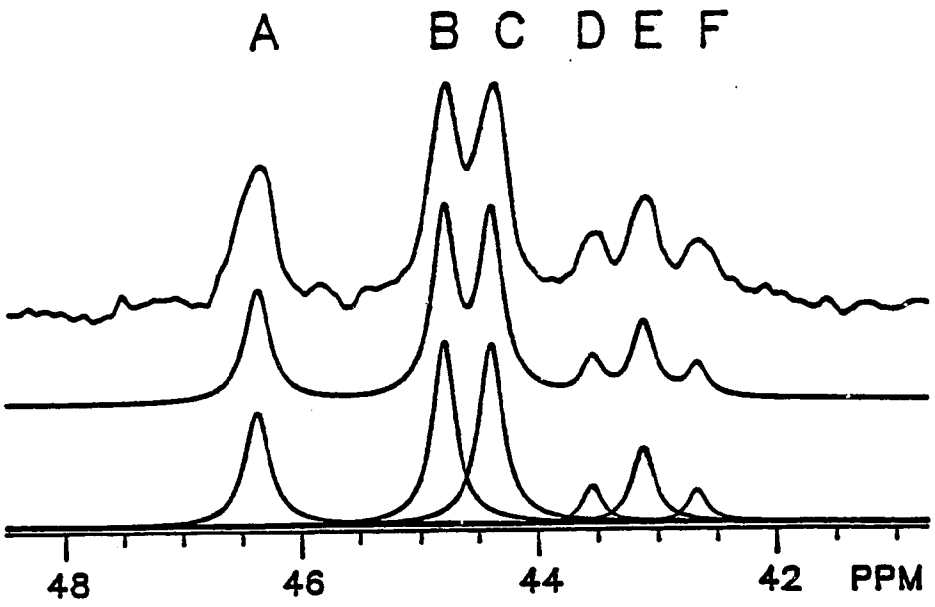
A
B C D E F
48
46
44
42
PPM

noting that the rr triad showed pentad sensitivity in the N-15 spectrum (Fig. 3) as detected in the C-13 results (Fig. 2). The assignments of rr centered peaks for N-15 NMR are the same as the C-13 NMR results, based on both relative areas.

In order to link this work with the earlier study of Murano and Harwood, [1] the H-1 NMR analysis of PVAm was undertaken. Unlike poly(acrylic acid),[16] the methylene proton resonances of PVAm are not resolved throughout the whole pH range and dyad analysis is not possible. Therefore, the tacticity of PVAc, acetylated from PVAmI, was determined by H-1 NMR assuming that PVAc and the parent polymer have the same tacticity. As first reported by Murano and Harwood, the H-1 NMR of PVAc at 100°C is expected to provide a triad analysis which would complement our C-13 analysis. The H-1 NMR spectra of the methyl peaks for PVAc at different temperatures, 25°C, 40°C, 60°C and 80°C at pH=2 are shown in Fig. 4. Clearly, the resolution for triad sensitivity was better at 25°C. The peak areas obtained from curve deconvolution for the three triad peaks are 16.0, 55.3 and 28.7%, ordered low to high field. Compared to the C-13 and N-15 triad results of PVAmI (Table), the assignments of PVAc for the methyl protons are mm, mr and rr from downfield to upfield.

It is clear from these results that 1) the ^{13}C NMR of PVAm solutions, adjusted to pH = 8-9, provides useful information concerning sequence distribution at the dyad and triad level and at higher levels with curve deconvolution, 2) the PVAm sequence distribution is close to random but significantly different depending on whether the polymer was prepared from N-vinylacetamide or N-vinyl-t-butylcarbamate and 3) ^{15}N NMR may also be used to analyze the sequence distribution of

Figure 4. H-1 NMR of PVAc in D_2O at the indicated temperatures (^oC) for CH_3 only. The bottom two spectra were were calculated from deconvolution.

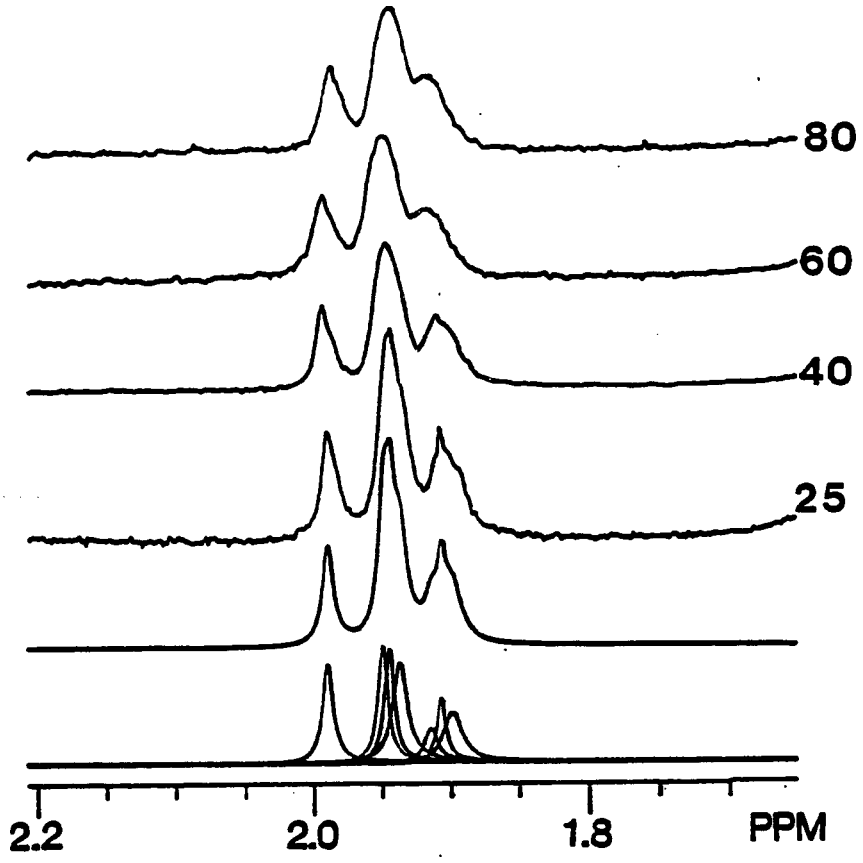
80
60
40
25
2.2
2.0
1.8
PPM

PVAm. It should also be noted that the ^{1}H NMR of the acetylated PVAm provides corroborating evidence for the triad analysis of PVAm and the configurational analysis of the latter is consistent with the configurational analysis of Poly(vinyl alcohol).

REFERENCES

1. Murano, M.; Harwood, H. J. Macromolecules 1970, 3, 605.

2. St. Pierre, T., Lewis, E. A.; Levy, G. C. in "Polymeric Amines and Ammonium Salts"; Goethals, E. T. (Ed.), Pergamon Press: Oxford 1980; P 245-8.

3. Wu, T. K.; Ovenall, D. W. Macromolecules 1973, 6, 582.

4. Chang, C.; Muccio, D. D.; St. Pierre, T.; Chen, C. C.; Overberger, C. G. Polym. Prepr., Am. Chem. Soc., Div. Polym. Chem. 26(2), 265, 1985.

5. Chang, C.; Muccio, D. D.; St. Pierre, T. Macromolecules (submitted).

6. Hughes, A. R.; St. Pierre, T. in "Macromolecular Synthesis"; Mulvaney, J. E. (Ed), John Wiley: New York, 1977; P 31-37.

7. Dawson, D. J.; Gless, R. D.; Wingard, Jr., R. E. J. Am. Chem. Soc. 1976, 98, 5996.

8. Overberger, C. G.; Chen, C. C. J. Polym. Sci., Polym. Lett. Ed. 1985, 23, 345.

9. Bosnich, B.; Harrowfield, J. M. J. Am. Chem. Soc. 1972, 94, 3425.

10. Freeman, R.; Kempsell, S. P.; Levitt, M. H. J. Magn, Reson. 1980, 38, 453.

11. Kowalewski, J.; Levy, G. C.; Johnson, L. F.; Palmer, L. J. Magn. Reson. 1977, 26, 533.

12. Randall, J. in "Polymer Sequence Determination ^{13}C NMR Method"; Academic Press: New York, 1977; P 71.

13. Bovey, F. A. in "High Resolution NMR of Macromolecules"; Bower, D. J. (Ed), Academic Press: New York, 1972; P 146.

14. The best values were calculated by a linear regression of the log form of $m^2 = 0.288$, $2mr = 0.541$ and $r^2 = 0.171$.

15. Ovenall, D. W. Macromolecules 1983, 17, 1458.

16. Chang, C.; Muccio, D. D.; St. Pierre, T. Macromolecules (accepted).

CHAPTER V

^{13}C AND ^{15}N NMR pH TITRATION STUDY OF POLY(VINYLAMINE)

C. Chang, D. D. Muccio, and T. St. Pierre
Department of Chemistry
University of Alabama at Birmingham
Birmingham, Alabama 35294

ABSTRACT

The ionization constants of each tacticity of poly(vinylamine) (PVAm), prepared from N-vinyl-t-butylcarbamate were determined by using ^{13}C and ^{15}N NMR pH titration experiments. The pKa values, obtained from the extended Henderson-Hasselbach and the Mandel equations applied to the ^{13}C CH_2 NMR data, are almost equal for the m and r dyad and consistent with the results obtained from the potentiometric titration. However, the ^{13}C CH NMR titration is described by a bell shaped curve which may not be reduced to pKa's but never the less indicates a strong triad configuration dependence for the acid dissociation process. This phenomena was investigated further by ^{15}N NMR pH titration. The discontinuity of these pH titration curves coincided approximately with the maximum of the ^{13}C CH NMR titration curve. We conclude that the electric field effect, hydrogen bonding and chemical shift effect are dominate factors in dictating the shape of the titration curves. Each tacticity according to the ^{15}N NMR titration exhibits significantly different pKa's.

INTRODUCTION

The titration of poly(vinylamine) (PVAm) has been studied extensively by means of potentiometric[1-3] and calorimetric titration.[4,5] There is general agreement in those studies that PVAm is subject to a strong neighboring group interactions (NGI) which is influenced by hydrogen bonding during the course of titration. However, none of the previous reports deal with the tacticity effect on pKa. Obviously, the tacticity of vinyl polyelectrolytes in aqueous solution plays an important role on the NGI and charged distribution. In the past few years, nuclear magnetic resonance (NMR) has proved to be the best tool to determine the configuration of vinyl polymers. The configuration of PVAm has been established by us using[6] ^{13}C and 2D NMR employing the model compounds, meso-(m) and racemic-(r) 2.4-diaminopentane (DAP).

Levy and co-workers[7,8] reported ^{13}C and ^{15}N NMR T_1 measurements at several pH's for PVAm[7] and DAP.[8] However they did not study the effect of tacticity on pKa. The advantage of using NMR to study the titration behavior of vinyl polyelectrolytes is that each tacticity can be studied independently in the same, single system. For instance, the titration of poly(acrylic acid) was studied by ^{13}C NMR and analyzed by the extended Henderson-Hasselbalch (H-H) and the Mandel equations.[9] The results are not only consistent with the result obtained from potentiometric titration but a small difference in pKa was observed for the syndiotactic, heterotactic and isotactic sequence.

For a limited class of polymers including PVAm, ^{15}N NMR may also be used to study the titration, just as Yu and Levy[8] used to study the titration of DAP. Their results show that the chemical shift for the indistinguishable nitrogens move downfield about 4 ppm on protonation. In this report, we explore the titration behavior of PVAm by using both ^{13}C and ^{15}N NMR. The chemical shifts with pH for CH gave a bell shaped curve whereas CH_2 and NH_x produced sigmoidal curves which were used to calculate the pKa's for the various dyad and triad tacticities.

MATERIALS AND METHODS

PVAm was prepared from N-vinyl-t-butylcarbamate[10] and the model compounds, m and r DAP were kindly provided by C. C. Chen and C. G. Overberger (Chemistry Department, University of Michigan). The NMR spectra were recorded using a GE 300 WB spectrometer (NT series) equipped with a 1280 computer and 293c pulse programmer. The ^{13}C NMR spectra of PVAm were obtained with complete proton decoupling on 0.5 M (5%,w/v) solutions in 10% D_2O at 25°C and with dioxane as an internal chemical shift reference (66.5ppm relative to tetramethysilane). J-modulated spin-echo spectra were acquired by attached proton test (APT) pulse sequence,[11] and J_{CH}=125 Hz was used to maximize the peak intensity. Pulse angles of 58°(19 μs), repetition rates of 1.5 s, sweep widths of +7575 Hz and 16k data points were used to acquire the free induction decay. The ^{15}N NMR spectra of PVAm were obtained with complete proton decoupling on 0.5M (5%,w/v) solutions

in 10% D_2O at 25°C. Pulse angles of 75° (30 μs), repetition rates of 3 s, sweep widths of ± 1000 Hz and 2k data points were used to acquire the free induction decays. Ammonium chloride in concentrated HCl was used as an external chemical shift reference (30.31ppm from ammonium at 25°C). The pH's were adjusted with concentrated NaOH and recorded on an Orion research model 701A pH meter with a microcapillary Ingold combination electrode and no corrections were made for the presence of D_2O. No attempt was made to control the ionic strength during the course of titration, but the ionic strength was generally high.

RESULTS

^{13}C NMR Titration The ^{13}C NMR spectra of PVAm were recorded as a function of pH. Both the methylene and methine carbon resonances shift downfield with increasing pH and the peak character of each change as well. The methine carbon begins to display triad sensitivity at pH=4.75, and pentad sensitivity at pH=8.22. The methylene carbon at the latter pH appears as a multiplet. The configurational sensitivity is optimal at pH=8.8 to 9.8. In this pH range, the methine carbon shows pentad sensitivity, and the methylene carbon shows dyad sensitivity with partial tetrad resolution.(6) Unfortunately, the methine and methylene carbon resonances overlap and eventually cross at higher pH. The model compound, m DAP, was used to examine this crossing phenomena. The ^{13}C NMR coupled spectra of m DAP at pH=2.0, 7.1 and 11.7, shown in Fig. 1a, 1b and 1c respectively, clearly show this crossing. The APT experiment(11) was employed in this pH region to identify the

Figure 1. The ^{13}C coupled spectra of m -2,4 diaminopentane at pH= (a) 11.87 (b) 7.1 (c) 2.0.

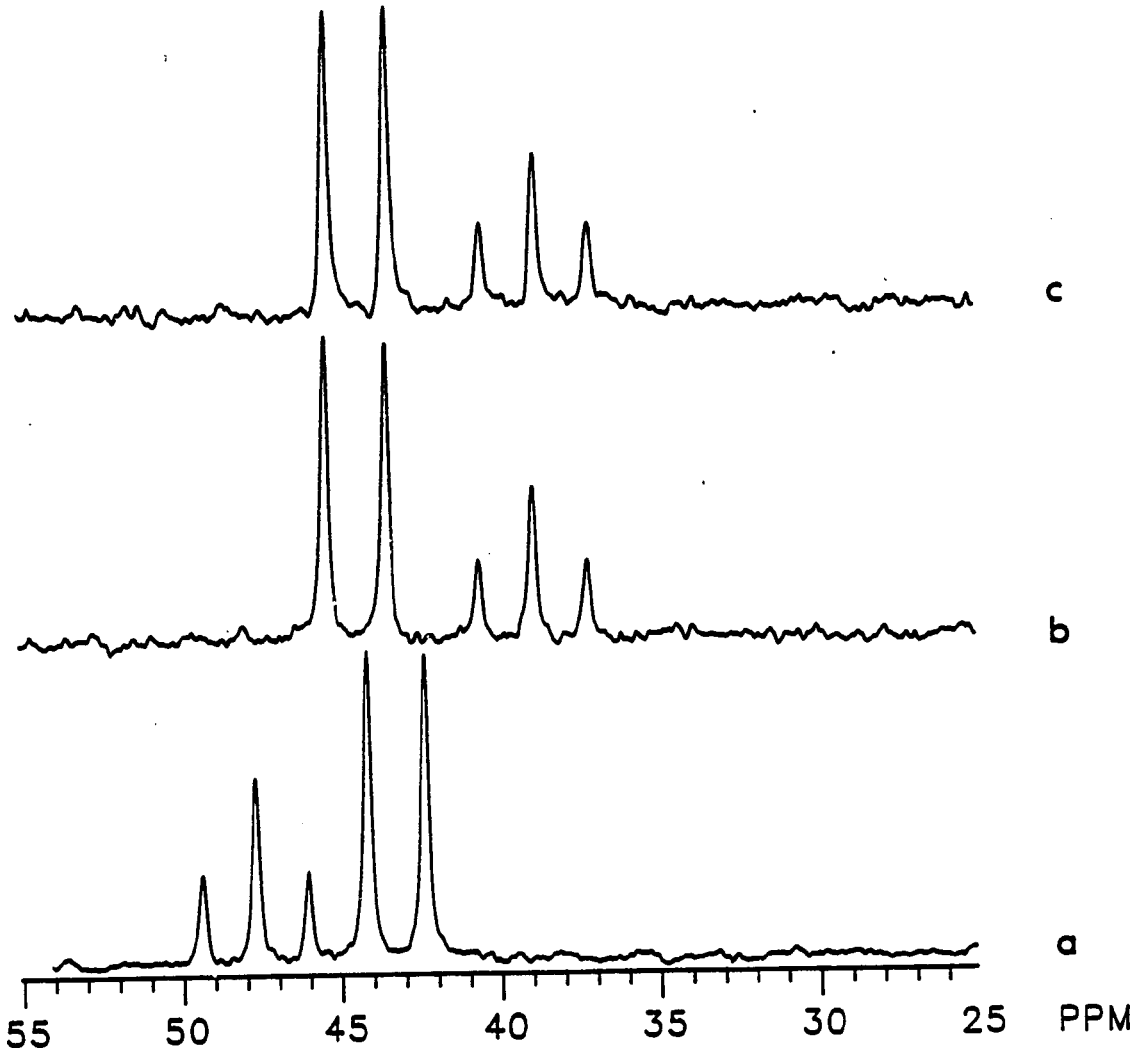
c
b
a
55
50
45
40
35
30
25
PPM

methine and methylene carbon resonances of the polymer, Fig. 2. By this technique the methylene carbon (positive peaks) and the methine carbon (negative peaks) may be distinguished in the pH range where they cross.

^{13}C Methylene NMR Titration The assignments of methylene carbon resonances of PVAm are based on our previous report.(6) At pH=8.8, the m dyad is upfield, compared to the r dyad. We assumed that this relationship between m and r resonances is preserved throughout the whole pH range. Furthermore, if the methylene carbon resonances exhibit a higher than dyad sensitivity, the average chemical shifts were selected for both the m and r resonances. This is the basis for the ^{13}C NMR pH titration curve of the m and r resonances shown in Fig. 3. The downfield shifts for m and r resonances are 8.5 and 8.8 ppm respectively. This result is close to that of the model DAP, about 9.5 ppm, established by Yu and Levy and confirmed by us in this study. The relatively larger downfield shift for the methylene carbon resonances of PVAm compared to PAA, about 4 ppm,(8) is not surprising because the carbon to the nitrogen is more influenced by deprotonation than is the corresponding carbon of the carboxylic acid.(12,13)

The sigmoidal titration curves for the m and r dyad were analyzed by the extended H-H and by the Mandel equation as referenced. The results of these two treatments are consistent with each other and are given in the Table. From von Treslong and Staverman's potentiometric study of PVAm,(2) the $pK_{1/2}$, the value of pKa at half neutralization, and the slope n from extended HH equation are dependent on the polymer concentration and ionic strength of the solution, the higher the polymer concentration and/or ionic strength, the lower the n value and the

Figure 2. The ^{13}C NMR APT spectra for PVAm at pH= (a) 10.7 (b) 11.3 (c) 11.8 (d) 12.3 (e) 12.83.

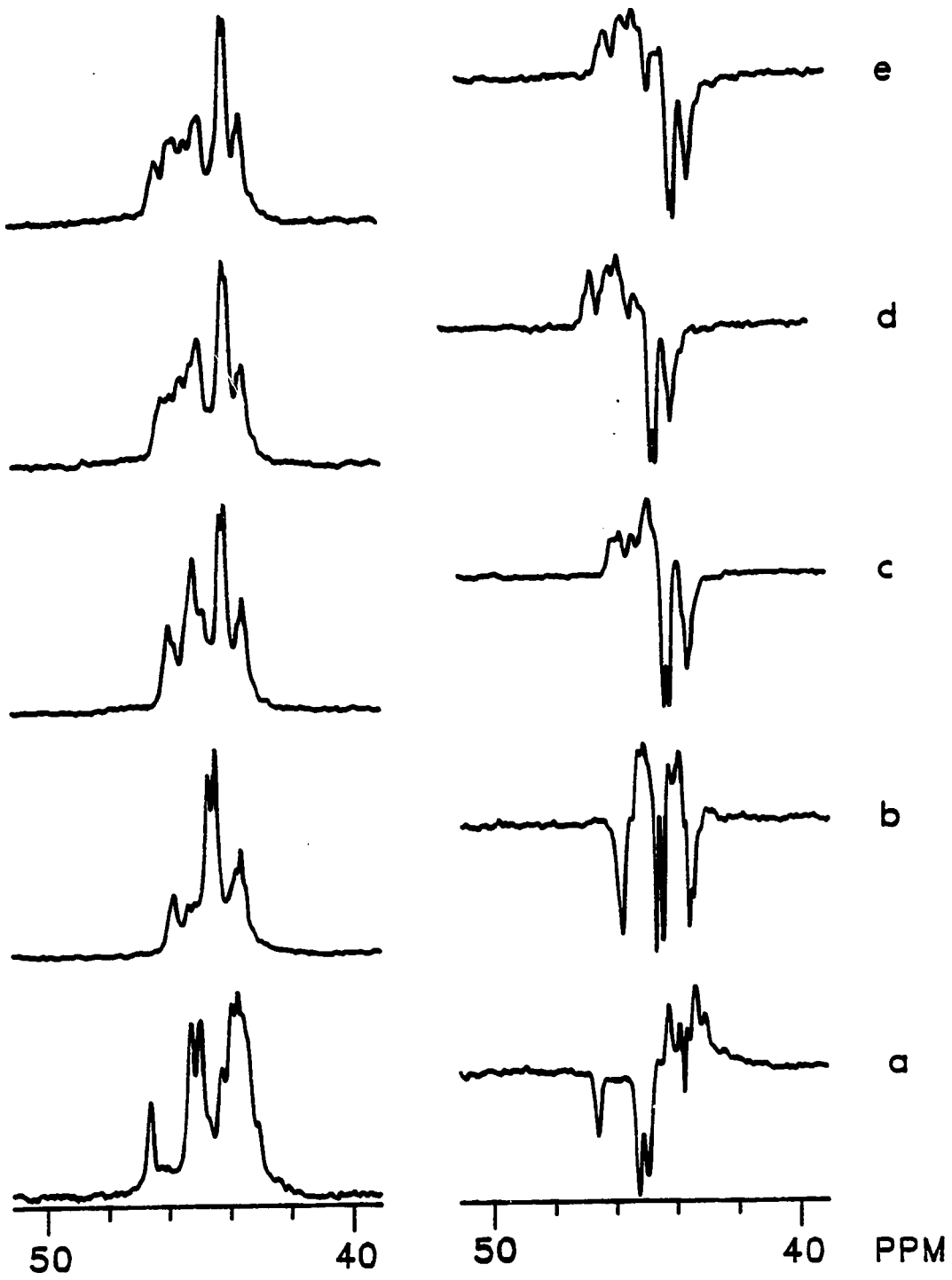
e
d
c
b
a
50
40
50
40
PPM

Figure 3. The ^{13}C NMR pH titration for CH_2 and CH of (a) m $-CH_2$ (b) r $-CH_2$ (c) rr $-CH$ (d) mr $-CH$ (e) mm $-CH$ configurations.

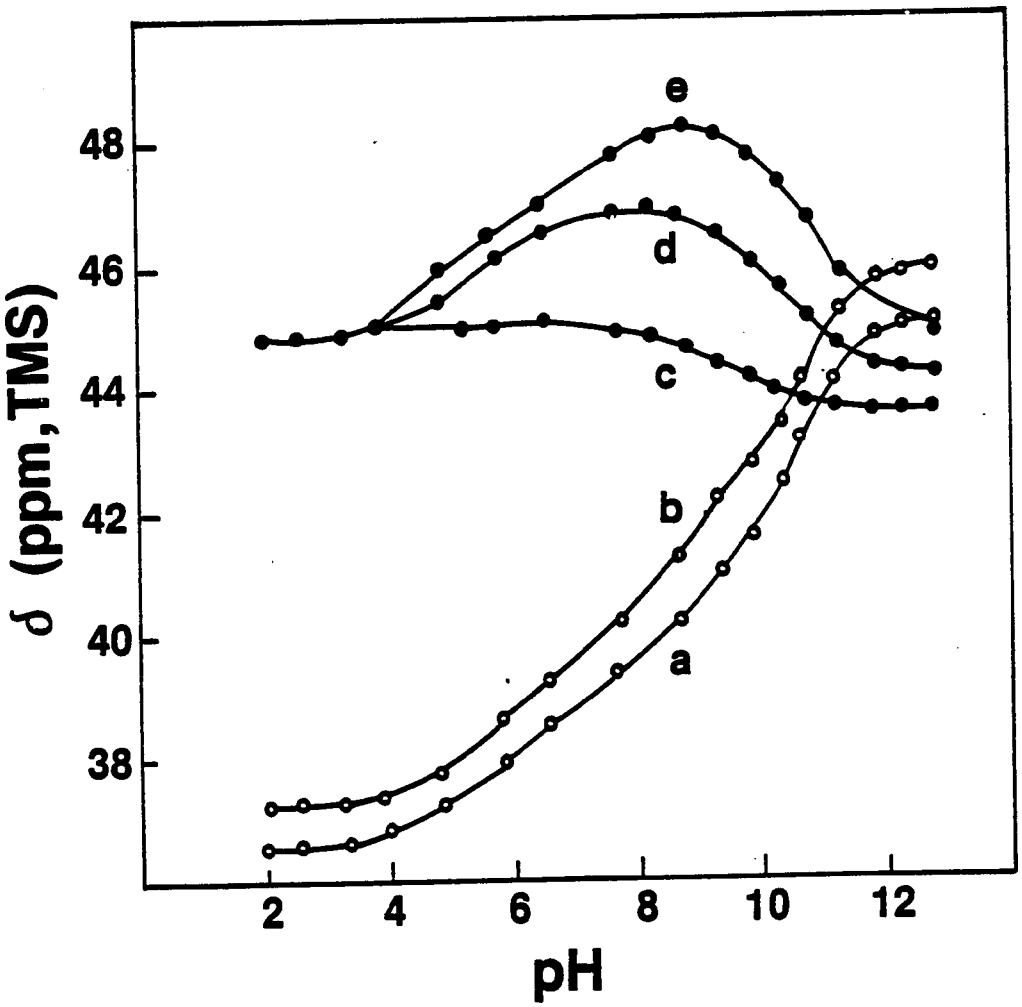
e
d
c
b
a
48
46
44
42
40
38
δ (ppm,TMS)
2
4
6
8
10
12
pH

TABLE ACID DISSOCIATION CONSTANTS FOR PVAm

Nuclei	Methylene Carbon			Nitrogen	
Configuration	m	r	mm	mr	rr
Slope[a]	-4.32	-4.08	-2.99	-3.06	-3.19
Intercept[a]	8.69	8.76	6.17	6.82	7.19
Correlation[a]	0.98	0.99	1.00	0.99	0.99
pKi[b]	9.94	10.47	9.80	9.32	9.56
a[b]	2.35	-0.39	-10.20	-5.99	-4.76
b[b]	-8.39	-5.30	5.55	1.64	0.04
n[c]	-4.47	-4.27	-3.69	-3.50	-3.71
$pK_{1/2}$[c]	9.02	8.95	6.09	6.74	7.19

a. These values are based on the H-H treatment, where slope = n and intercept = pK1/2.

b. These values are based on the Mandel treatment.

c. These are the H-H parameters calculated from pKi, a and b using the equations of Fenyo et.al. J. Polym. Sci., Polym. Chem. Ed., 1979, 17, 193, but with appropriate changes in sign due to our particular definition of ,i.e., α = fraction of charged sites instead of α = fraction of base.

higher $pK_{1/2}$. Accordingly, their results at 0.15M polymer concentration and 1M salt concentration, which gives $pK_{1/2}$=8.1 and n=4.87, is reasonably consistent with the values presented in the Table. The effect of the configuration (m and r dyad) on pKa of PVAm is negligible. The relative high n values, compared to PAA (n=1.7),[14] confirm that the titration of PVAm exhibits the strong NGI which gives rise to strong dependence of pKa on α, where α is the mole fraction of charged sites.

^{13}C Methine NMR Titration The assignment[6] of the methine carbon configurations for the triad level are isotactic (mm), heterotactic (mr) and syndiotactic (rr) sequences from downfield to upfield. Where the resonances were more complex, i.e. pentad resolution at pH 8.2 to 9.8, the average chemical shifts were used for each triad sequence to plot the titration curves. Bell-like titration curves are observed for the methine carbon, Fig. 3. The initial chemical shift at low pH is 44.8 ppm. The maximum chemical shift for mm is 48.2 ppm, at pH=8.68, for mr is 46.8 ppm, at pH=8.22 and for rr is 45.1 ppm, at pH=6.45. The final chemical shifts at high pH are 44.9, 44.1 and 43.6 ppm for mm, mr and rr respectively. Apparently, these three sequences exhibit different acidity, however, these titration curves, due to their complex nature, can not be used to obtain pKa directly. The magnitude and direction of the change in chemical shift of the carbon of an amine on protonation may not be rationalized on the basis of simple inductive effects.[15]

For a simple amine the protonation shift, analyzed in terms of a linear electric field effect,[13] predicts -2.36 ppm for an

methine, 4.82 ppm for a methylene and 0.26 ppm for a methine where upfield shifts for protonation are positive. The protonation shift for m DAP are CH = -1.2 and CH_2 = 9.2 ppm and for r DAP are CH = -1.5 and CH_2 = 9.7 ppm (this work). Using simple additivity rules for this diamine and neglecting configurational effects the protonation shift for DAP may be calculated, CH = -2.1 and CH_2 = 9.6 ppm. There is good argument for the CH_2 shift but not for the CH. The same is true of PVAm. The experimental values are m CH_2 = 8.5, r CH_2 = 8.8, mm CH = 0.1, mr CH = -0.7 and rr CH = -1.5 ppm and the calculated values are CH_2 = 9.6 and CH = -1.8 ppm. It is clear that the more complex amines represented in this study may not be accomodated by the linear electric field theory. The CH of DAP and PVAm are subject to both and amine protonation and the latter will no doubt depend strongly on conformation effects dictated by hydrogen bonding and configuration. Following the argument of Yu and Levy based on T_1 studies of DAP intramolecular hydrogen bonding increase with pH. The conformational course of titration would follow:

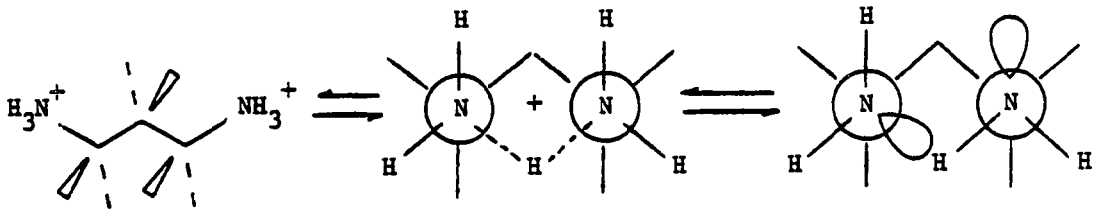

DAP^{+2} DAP^{+1} DAP^{o}

With respect to the CH the first stages of deprotonation would represent a change in the electric field effect and change in conformation of the NH_x group, trans to gauche. The electric field effect for the CH predicts an upfield shift for deprotonation. We assume the observed

downfield shift is due the effect. In the final stages of deprotonation the CH experiences only a change in the electric field effect which produces the observed upfield shift. If the intramolecular hydrogen bond which preserves the six membered ring is weak, then this form would be sensitive to the relative configuration of the methines. As the intramolecular hydrogen bond becomes stronger the configurational effects decrease. This describes the configurational effects on the measured T_1 of DAP, (pH=10 entry of Table 1 of Yu and Levy) and the CH titration of PVAm, Figure 3.

<u>^{15}N NMR Titration</u> Due to the uncertainty of the ^{13}C NMR pH titration for the methine carbon resonances, ^{15}N NMR pH titration was employed to determine the pKa for the various triad sequences. The assignments of the ^{15}N resonances are based on our previous report.(6) The average chemical shifts are selected for each triad sequence, where the configuration exhibits pentad resolution, i.e. pH = 10.45. Fig. 4 shows the titration curves for the ^{15}N NMR chemical shifts as a function of pH. The configurational assignments at low pH (pH<5) are somewhat arbitrary. This is not a critical point and the average chemical shift and chemical shift range could have been used as well. The ^{15}N NMR chemical shifts move upfield, with increasing pH, opposite to the ^{13}C NMR shifts. The upfield shifts with increasing pH are smooth in the pH range of 2 to 8 for these three sequences. However, at the pH range of 8.0 to 9.5 for the <u>mr</u> and <u>rr</u> triads and 8.0 to 11.5 for <u>mm</u> triad, the shifts change abruptly and this may be due to the conformational transition at these pH ranges. The discontinuity begins at about the same pH where the CH resonances begin to experience

Figure 4. The ^{15}N NMR pH titration of PVAm for the (a) rr (b) lmr (c) mm configurations.

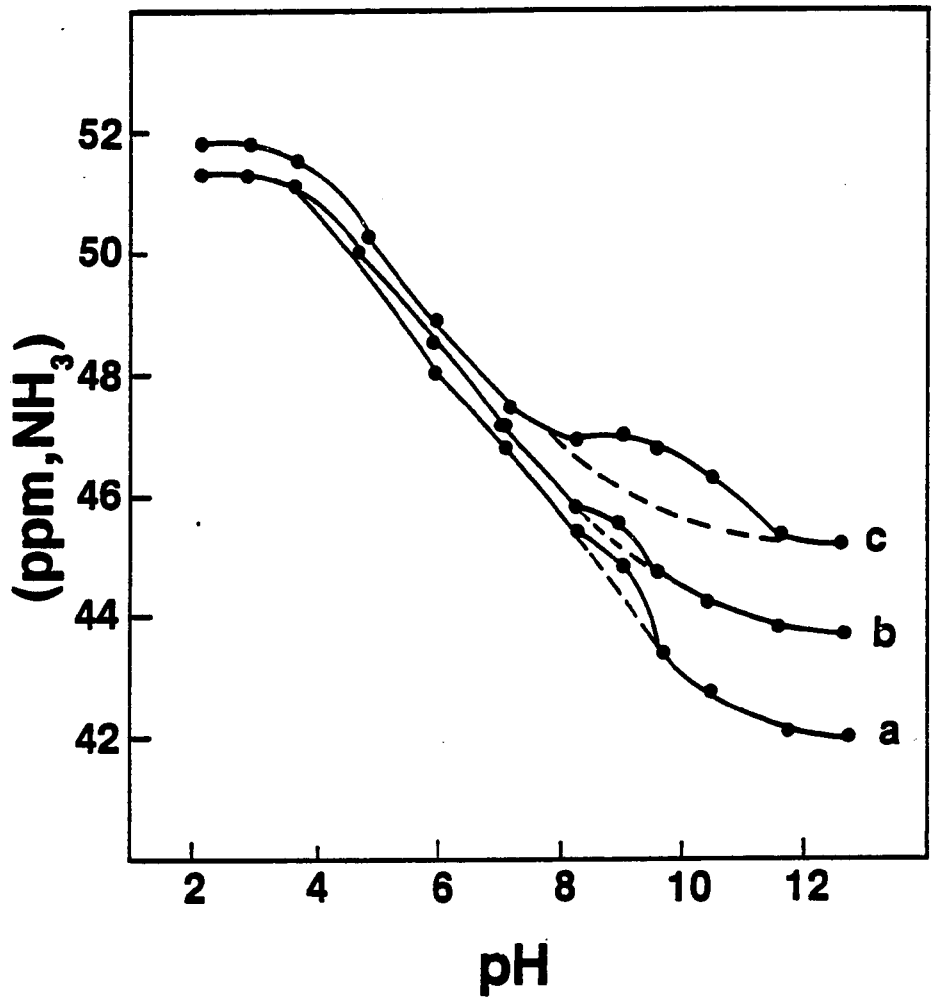
52
50
48
46
44
42
(ppm,NH3)
2
4
6
8
10
12
pH
c
b
a

an upfield shift with increasing pH, Figure 3. The effect on these pH ranges for each triad suggests that each triad experiences a little different NGI and pKa. The total protonation shifts for mm , mr and rr are 6.56, 7.6 and 9.31 ppm respectively.

These three titration curves are also treated with the extended H-H and the Mandel equation, using the artificially smoothened titration curves and the results are summarized in the Table. The titration behavior of the methylene carbon can not be compared with nitrogen titration. The former leads to a pKa which is consistent with the macroscopic pKa obtained by potentiometric titration and the latter leads to a pKa for the hypothetical polymer for which there is no conformational effects. The nitrogen titration curve gives strong indication of two distinct pKa's for each configuration, one higher and one lower than the nitrogen based pKa's reported in the Table. This may be taken as reasonable evidence for the proposition of Katchalsky[1] that the titration of PVAm may be viewed as the titration of two ammonium groups, the first and stronger acid, not hydrogen bonded, and the second and weaker acid, hydrogen bonded. Furthermore the first pKa could describe the ascending portion of the CH titration curve and the second, the descending portion of the CH titration curve.

REFERENCES

1. Katchalsky, A.; Mayur, J.; Spitnik, P. J. Polym. Sci. 1957, 23, 513.

2. Bloys von Treslong, C. J.; Staverman, A. J. Rec. Trav. Chim. Pays-Bas. 1974, 93, 171.

3. Bloys von Treslong, C. J. Rec. Trav. Chim. Pays-Bas. 1978, 97, 13.

4. Lewis, E. A.; Barkley, T. J.; St. Pierre, T. Macromolecules 1981, 14, 546.

5. Lewis, E. A.; Barkley, T. J.; Reams, R. R.; Hansen, L. D.; St. Pierre, T. Macromolecules 1984, 17, 2874.

6. Chang, C.; Muccio, D. D.; St. Pierre, T. Macromolecules (submitted).

7. Rinaldi, P. L.; Yu, C.; Levy, G. C. Macromolecules 1981, 14, 551.

8. Yu, C.; Levy, G. C. Org. Magn. Reson. 1984, 22, 131.

9. Chang, C.; Muccio, D. D.; St. Pierre, T. Macromolecules (in press).

10. Hughes, A. R.; St. Pierre, T. "Macromolecular Synthesis"; Mulvaney, Hugo (Editor), John Wiley and Sons: New York, 1970; p. 31.

11. Patt, S. L.; Shoolery, J. N. J. Magn. Reson. 1982, 46, 535.

12. Batchelor, J. G. J. Am. Chem. Soc. 1975, 97, 3410.

13. Rabenstein, D. L.; Sayer, T. L. J. Magn. Reson. 1976, 24, 27.

14. Fenyo, J. C.; Laine, J. P.; Muller, G. J. Polym. Sci. Poly. Chem. Ed. 1979, 17, 193.

15. Morishima, I.; Yoshikawa, K.; Okada, K.; Yonezuwa, T.; Goto, K. J. Am. Chem. Soc. 1973, 1065.

CHAPTER VI

DETERMINATION OF THE SEQUENCE DISTRIBUTION AND IONIZATION CONSTANT OF POLY(ACRYLIC ACID-CO-VINYLAMINE) BY ^{13}C NMR

C. Chang; D.D. Muccio; T. St. Pierre*

Department of Chemistry
University of Alabama at Birmingham
Birmingham, Alabama 35294

ACKNOWLEDGEMENT

The authors are grateful to C.G. Overberger and C.C. Chen for providing samples of m and r DAP and to H.J. Harwood for calculating the relative rate constants based on results of Table I.

ABSTRACT

Three copolymers of poly(acrylic acid-co-vinylamine) containing 12% (SP12), 30% (SP30) and 52% (SP52) amino groups were synthesized from poly(acrylic acid) by means of the Schmidt reaction. These copolymers were analyzed by C-13 NMR and the results compared to the previously analyzed homopolymers. The various comonomer sequence distributions were identified and by means of peak areas it was determined that 1) the reactivity was not significantly influenced by the triad tacticity of the parent poly(acrylic acid), 2) the final copolymer is characterized by an essentially alternating sequence, and 3) there is extensive lactam formation between neighboring carboxyl and amino groups. In terms of nearest neighbor effects the relative rates of amine formation are $k_1/k_o \approx 0.3$ and $k_2/k_o \approx 0$. A C-13 NMR pH titration of SP12 showed that the carboxyl group with a neighboring amino group is more acidic than a carboxyl group flanked by two carboxyl groups.

INTRODUCTION

The Schmidt reaction[1] which converts carboxyl groups (A) to amino groups (B) is a well known organic reaction. This reaction has been applied to poly(acrylic acid) (PAA) resulting in the Schmidt product (SP), a copolymer of both acrylic acid and vinylamine, Eq. 1.[2] Generally, polymer reactions of

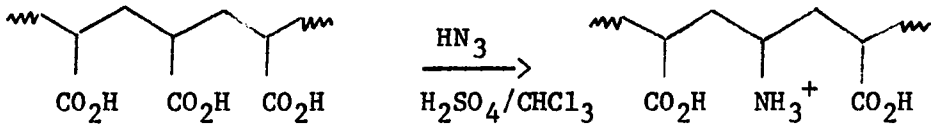

(1)

this type are subject to nearest-neighbor effects (NNE),[3-5] which, for the early stages of the reaction, are mainly configurational effects. Using a copolymer where 12% of the carboxyl groups have been converted to amino groups (SP12) and based on our recent configurational studies of PAA,[6] we explore in this study the question of configurational effects on reactivity.

It was previously found that the conversion of carboxyl groups to amino groups, even in the presence of excess HN_3, stops at about 50%. The conversion and sequence distribution of the copolymers, in principle, will depend on the NNE and will be reflected in the rate constants for the reaction of the central A units,[7] i.e. A$\underline{\text{A}}$A (k_o), A$\underline{\text{A}}$B + B$\underline{\text{A}}$A, (k_1) and B$\underline{\text{A}}$B (k_2). If $k_o < k_1 < k_2$, the formation of an intermediate block-like copolymer will be favored. For rate constants which are nearly equal ($k_o = k_1 = k_2$), the sequence distributions of the resulting intermediate

copolymer will be random. If, on the other hand, $k_o > k_1 > k_2$, the copolymer will have a strong tendency toward alternation and the reaction will slow down or stop before complete conversion. For this reaction there is the additional complication of lactam formation[2] and simple NNE may not apply. Three copolymers were prepared for this study with molar ratios of NH_3^+/CO_2H of 12/88 (SP12), 30/70 (SP30) and 52/48 (SP52). We found C-13 NMR useful in determining both the sequence distributions and extent of lactam formation for these copolymers. The sequence distributions was then used to estimate the relative rate constants.[8-11]

For these copolymers, the acid dissociation constants (pKa) of the carboxyl groups are expected to be influenced by neighboring carboxyl or amino groups in the different sequence distribution AAA, AAB and BAB. Previously, we have determined the pKa's of the carboxyl groups of PAA by C-13 NMR pH titration.[6] The same approach was applied to the above copolymers. The advantage of using NMR for these studies lies in the ability to analyze the titration behavior of different configurations or sequence distributions in the same system. However, it was found that these copolymers are not soluble over the whole course of the titration and the insoluble pH range increases with increasing B content. Because the insoluble pH range of SP12 is relatively small, pH = 3.0 - 4.5, our quantitative results are restricted to this copolymer.

MATERIALS AND METHODS

PVA was prepared from N-vinyl-t-butylcarbamate[12]. PAA, MW = 15,000, (Celanese Water Soluble Polymers, A Division of Celanese Corp.)

was used as received. The copolymers were prepared from PAA by means of the Schmidt reaction. The molar ratios of the three copolymers are based on limiting stoichiometric amounts of HN_3 for low conversions and the natural limit of the reaction for 50% conversion. The C-13 NMR spectra were recorded at 25°C on a GE 300 WB spectrometer (NT series) equipped with an 1180e computer and 293c pulse programmer. The concentration of all polymer solutions was 5% (w/v) in D_2O for the studies of the sequence distributions and 10% D_2O for the studies of the NMR pH titrations. Pulse angles of 60° (20 s), repetition rates of 5.0 s, sweep widths of ±7575 Hz and 16K data points were used to acquire the free induction decays. Dioxane was used as an internal chemical shift reference (66.5 ppm relative to tetramethylsilane). J-modulated spin-echo spectra were acquired by the APT pulse sequence,[13] using a delay value of 7.5 ms to optimize the peak intensity for both the A-centered and B-centered carbons. 2,4-Dimethylglutaric acid and 2,4-diaminopentane were used as models to determine the heteronuclear coupling constants (J_{CH}). J_{CH} for $\underline{CH}$-COOH is 140 Hz and J_{CH} for $\underline{CH}$ - NH_3^+ is 125 Hz. The delay time used in these experiments is the reciprocal of the average of these two constants. The spin lattice relaxation times (T_1's) were calculated using a non-linear three parameter fitting procedure. Nuclear Overhauser effects (NOE) were determined by the ratio of the peak area of the fully proton decoupled and gated-decoupled (decoupler off during delay time) spectra. The repetition rate for this measurement was at least ten times the longest T_1. Curve deconvolution was accomplished with NMCCAP program provided by the GE software using a completely Lorentzian line shape. The pH's were adjusted with 5 μL additions of NaOD and recorded on an Orion

research model 701A pH meter and with a microcapillary Ingold combination electrode. The pH were not corrected for isotope effects. The insoluble pH range of the copolymers is pH 3.0-4.5, 2.5-5.6 and 3.6-9.0 for SP12, SP30 and SP52 respectively.

The elemental analysis found for the various copolymers is as follows. Found for SP12: C, 30.07%; H, 4.81%; N, 1.39%; Na, 14.63%. Found for SP30: C, 33.44%; H, 5.93%; N, 4.33%; Na, 14.19%. Found for SP52: C, 38.00%; H, 7.4%; N, 9.37%; Na, 7.80%. The percent conversion was calculated by best fitting the analytical data to $-(CH_2CH(CO_2Na))_x-(CH_2-CH(CO_2H))_y-(CH_2-CH(NH_2))_{1-x-y}\ (H_2O)_z$. The values of x,y,z for SP12 are 0.74, 0.17, 1.73; for SP30 are 0.60, 0.10, 1.18; and for SP52 are 0.27, 0.21, 0.87.

RESULT AND DISCUSSION

Configurational Effects on Reactivity The tacticity of the PAA used in this study has been reported elsewhere.[6] The triad distribution was determined to be 27,50 and 23% for the syndiotactic (rr), heterotactic (mr) and isotactic (mm) configurations, respectively. The reactivity may be different for each configuration under the Schmidt reaction conditions. The reactivity of each triad may be determined by a comparison of the ratio of the peak areas of rr:mr:mm of the methine carbon of the starting PAA with the same ratio of the unreacted AAA sequence of the low conversion polymer, SP12. Since the A sequence is configurationally resolved only at high pH, the C-13 NMR spectrum of SP12 was analyzed at pH=8.08, as shown in Fig. 1 along with its simulated spectrum obtained

Figure 1: The C-13 NMR of SP12 in 10% D_2O at 25°C and at pH = 8.8 for CH; a) actual spectra and b) reconstructed spectra from c) deconvoluted spectra.

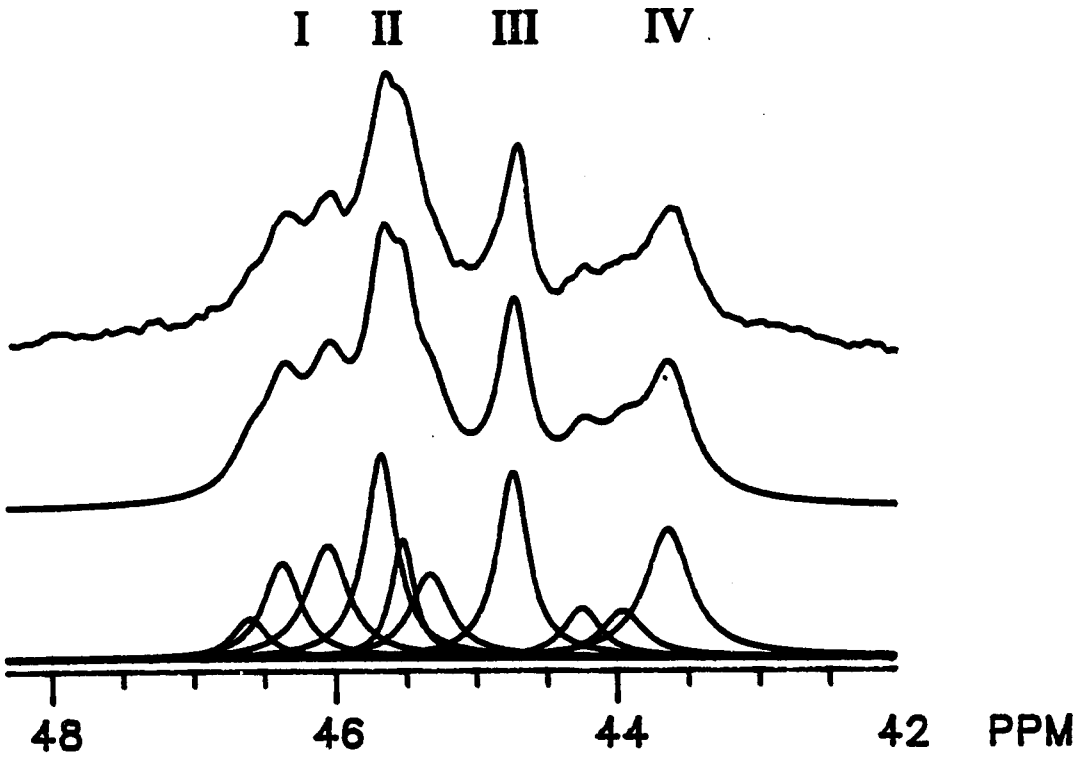
I
II
III
IV
48
46
44
42
PPM

from curve deconvolution. Four regions are observed at about 46.2, 45.6, 44.7, and 43.6 ppm and are labeled A through D, respectively. From the assignments of PAA, the regions A,B and C are assigned to the rr, mr and mm configurations of the AAA methine. The D region, as explained below, is the combination of the AAB and BAB methines. The peak areas of these four regions are 19, 33, 14, and 34% for A,B,C and D regions, respectively. After normalization of the regions A,B and C, the ratio of A:B:C is 29:50:21. This ratio is not significantly different from the rr:mr:mm ratio obtained for the parent PAA. This result indicates that the reactivities of the different configurations under the Schmidt reaction conditions are approximately equal.

Analysis of the Sequence Distributions The assignments of the methine carbon resonance of the copolymers were made from the attached proton test (APT),[13] by a comparison of the copolymer spectra with the PAA[6] and PVA[14] homopolymer spectra, from the principle of empirical additivity for C-13 chemical shifts,[15,16] from peak area changes as a function of composition[17] and from the C-13 NMR pH titration for each sequence. Because there is no apparent tacticity effect at low pH for PAA and PVA, the various peaks for the copolymers are assumed to be due to sequence distributions. The C-13 NMR spectra of the methine and methylene carbon regions for the SP at low pH are shown in Fig. 2 along with the spectra of PAA and PVA. The simple, but sharp, methine carbon resonance appear at 41.3 ppm for PAA (Fig. 2a) and 44.8 ppm for PVA (Fig. 2e). The single, but broad, methylene carbon resonance appear at 34.2 ppm for PAA and 37.2 ppm for PVA. Fig. 2 (b-d) show the spectra of SP12, SP30 and SP52. Because of the complexity of the methine and methylene carbon resonances

Figure 2: The C-13 NMR for the CH and CH_2 of a) PAA, b) SP12, c) SP30, d) SP52 and e) PVA in D_2O at 25^oC and at pH = 2.

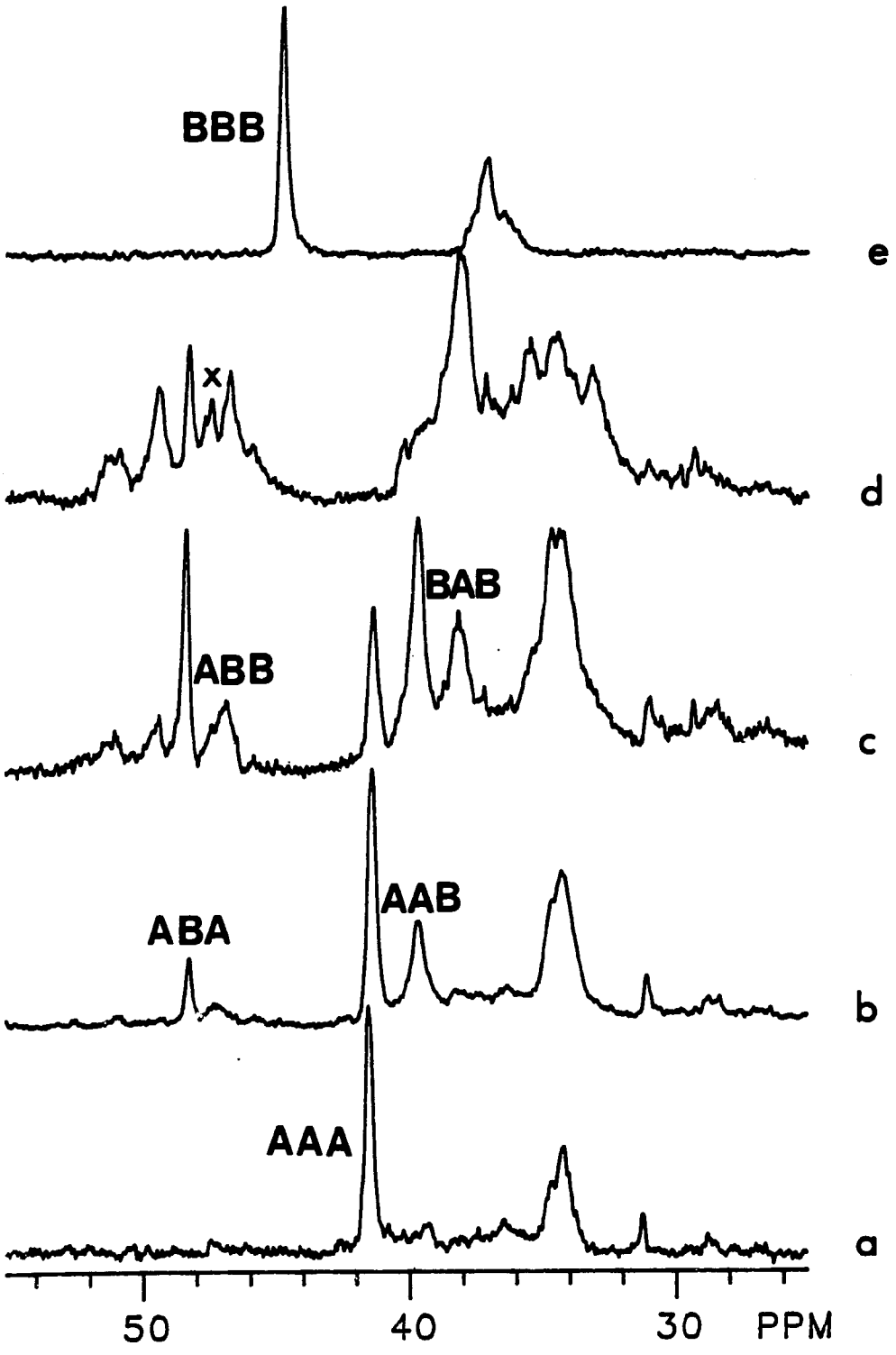
BBB
e
x
d
BAB
ABB
c
AAB
ABA
b
AAA
a
50
40
30
PPM

for the SP copolymers, the APT experiment was used to distinguish the methine carbon resonances from the methylene carbon resonances. The APT experiment results in positive resonances for both methylene and quarternary carbons, while the methine and methyl carbon resonances appear as negative signals. It is clear from Fig. 3 that peaks contained within 52-38 ppm represent the methine carbons, and the peaks between 38-32 ppm represent the methylene carbons. A comparison of Fig. 2c and Fig. 3b clearly indicates that there is some overlap in these two regions. The peak at 38.2 ppm in Fig. 2c is missing in Fig. 3b. This may be rationalized on the basis of a roughly equal contribution of methine and methylene resonances in this region. We will return to this point in the quantitative analysis of these spectra.

The assignments of the methylene carbons to individual sequences are difficult because of broad and severely overlapped peaks. Therefore, we will concentrate on the sequence distribution of the methine carbons. The AAA sequence of SP12 is assigned by comparison with the methine carbon resonance of PAA at 41.6 ppm. The intensity of the AAA sequence decreased with increasing B content, and eventually disappeared for SP52, Fig. 2 (b-d). From the principle of additivity for C-13 chemical shift, the exchange of CO_2H with NH_3^+ should produce an upfield shift of about 2 ppm at the -carbon.[18] Accordingly, the chemical shifts of the AAB and BAB sequences should be upfield with the respect to the AAA sequence. Referring to Fig. 2 (b), the peak at 39.9 ppm, should be assigned to the AAB sequence. The chemical shift difference between the AAA and AAB sequences is about 1.7 ppm which is closed to the predicted value. The intensity of the AAB sequence increased from SP12 to SP30, but decreased

from SP30 to SP52. The resonance for the BAB sequence is expected to be further upfield than that of AAB. Based on the 1.7 ppm change from conversion of one COOH group to an NH_3^+ group, we would expect a resonance at about 38.2 ppm. This corresponds well with the peak at 38.1 ppm, clearly present in the spectra of SP30 and SP52. The intensity of the BAB sequence increased with increasing B content.

The methine carbon resonance (44.8 ppm) of PVA (Fig. 2e), representing the BBB sequence, is absent in these three copolymers. From the additivity rule described above the ABA and ABB sequences should be downfield with respect to the BBB sequence. For SP12, the most prominent peak should be assigned to the ABA sequence which appears at 48.4 ppm. The ABB sequence should appear between the BBB and ABA sequences, which is consistent with the peak at about 46.9 ppm. However, for SP30, instead of two resonances we found four resonances; the unexpected peaks at 51.0(A) and 49.4(B), and the two predicted peaks at 48.4(C) and 46.9(D) ppm. The intensity of these four peaks generally increased from SP30 to SP52. Furthermore, in the spectra of SP52 there appears to be one additional peak (X) of unknown origin at about 47.3 ppm. Because of the magnitude of the differences in chemical shift we exclude long range, next neighbor, effects as the origin of peaks A and B.

In the previous study,[2] there appears in the H-1 spectrum of these copolymers, in D_2SO_4, two NH peaks one of which is assigned to NH_3^+ (8.70 ppm) and the other to the NH (6.75 ppm) of the lactam. On this basis we assign peaks A and B to the lactam form of ABA and ABB respectively. Each derivative peak is about 2.5 ppm downfield from the parent peak. These assignments were confirmed with T_1 and titration data. The T_1 for peaks A

and B is 0.35 s and for peaks C and D is 0.25 s indicating two types of B-centered peaks. The C-13 NMR pH titration again reveals two types of B centered peaks. Peaks A and B experience very little change in chemical shift in the pH range 2-12, ($\Delta\delta_A$ = 0.7 ppm and $\Delta\delta_B$ = 0.5 ppm) whereas peaks C and D go through a chemical shift maxima during the course of titration. This latter titration behavior is typical of methines containing amines[19] and typical of PVA.[20]

It is worth noting that in the B-centered methine region resonances have been assigned to the lactam, whereas lactam resonances do not appear in the A-centered methine region. This is because the chemical shifts difference between HC-COOH and HC-CONH is relatively small compared to the chemical shift difference between HC-NHCO and HC-NH_3^+.[18] This is not the case for the carbonyl carbons. It is known that the resonances of the CONH are downfield from the resonances of the COOH in acidic solution.[21] In order to confirm lactam formation, the spectra of the carbonyl regions for the various copolymers and for PAA are shown in Fig. 4. Based on the procedures of assigning the A-centered sequences described above, the peaks at 178.6, 177.7 and 176.9 ppm are assigned to the AAA, AAB and BAB sequences, respectively. It is reasonable to assign the peak at 180.9 ppm for SP52 to the lactam carbonyl if it is assumed that the lactam C=O of AAB and BAB appear as a single broad peak and/or the BAB is disproportionately prone to lactam formation.

The assignments of the sequence distributions of the methine carbon can be determined quantitatively by the peak areas which can be obtained from curve deconvolution. It is necessary however to first measure the T_1's and NOEs for the various carbon resonances. The T_1 values for A-

centered methines are about 0.2 s and the B-centered sequences, grouped in two sets, are about 0.25 s and 0.35 s. The NOE values for the A-centered methines are 1.9±0.1 and the B-centered sequences are about 1.8±0.1 for the amine and 2.1±0.1 for the lactam. Because a $10xT_1$ pulse delay was used and NOE measurements showed only slightly different values, the peak areas were not corrected for the fully decoupled spectra with complete NOE. As mentioned above the BAB methine resonance overlaps with the methylene resonance. Therefore, the peak area of the APT spectrum for SP30 was also examined. The methine peak area for the BAB sequence of the APT spectrum (Fig. 3b) is about 20% of the peak area of the fully decoupled spectrum (Fig. 2c), which represents the excess methine contribution to that peak. The remaining 80% represents a 50:50 contribution of methine and methylene resonances. Applying this correction to the deconvoluted methine region, the sequence distribution was determined and the results are shown in Table I.

The fraction of A and B units obtained from the peak areas are consistent with the elemental analysis. Lactam formation accounts for 14% of the SP30 B-centered peaks and 42% of the SP52 B-centered peaks, weighted slightly in favor of ABA generated lactams. The calculated lactam contribution to the A-centered peaks is 6% and 46% for SP30 and SP52, respectively. The results for SP52 based on the methine analysis indicate BAB:AAB > 2:1 while the carbonyl spectra, Fig. 4d, indicate BAB:AAB ≈ 1:1. These apparently conflicting results can be reconciled if the A-centered lactams are formed predominantly from the BAB sequence leading to (<u>BAB</u> + BAB):AAB ≈ 2:1. This is consistant with the methine

Figure 3: The C-13 NMR APT spectra for CH and CH_2 of a) SP12, b) SP30 and c) SP52 in D_2O at 25^oC and at pH = 2.

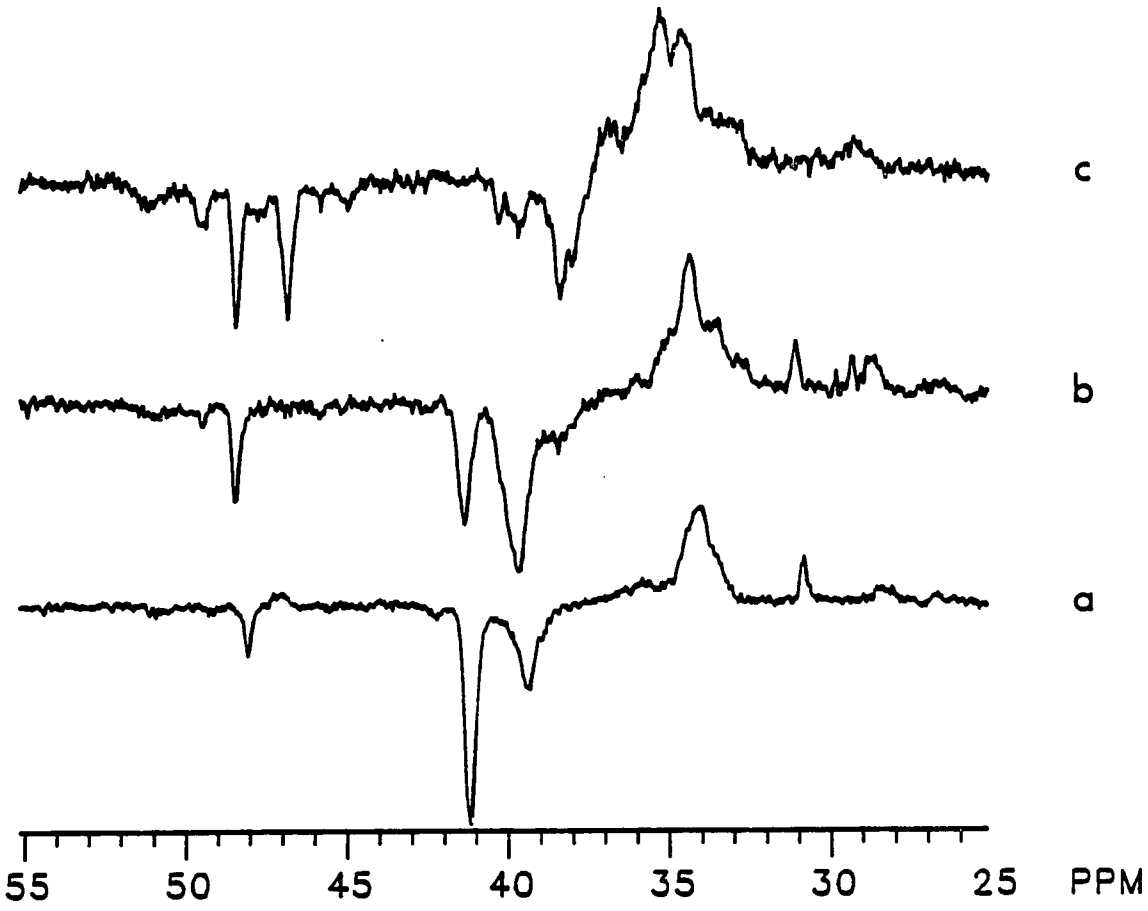
c
b
a
55
50
45
40
35
30
25
PPM

Figure 4: The C-13 NMR for the C=O of a) PAA, b) SP12, c) SP30 and d) SP52 in D_2O at $25^{o}C$ and at pH = 2.

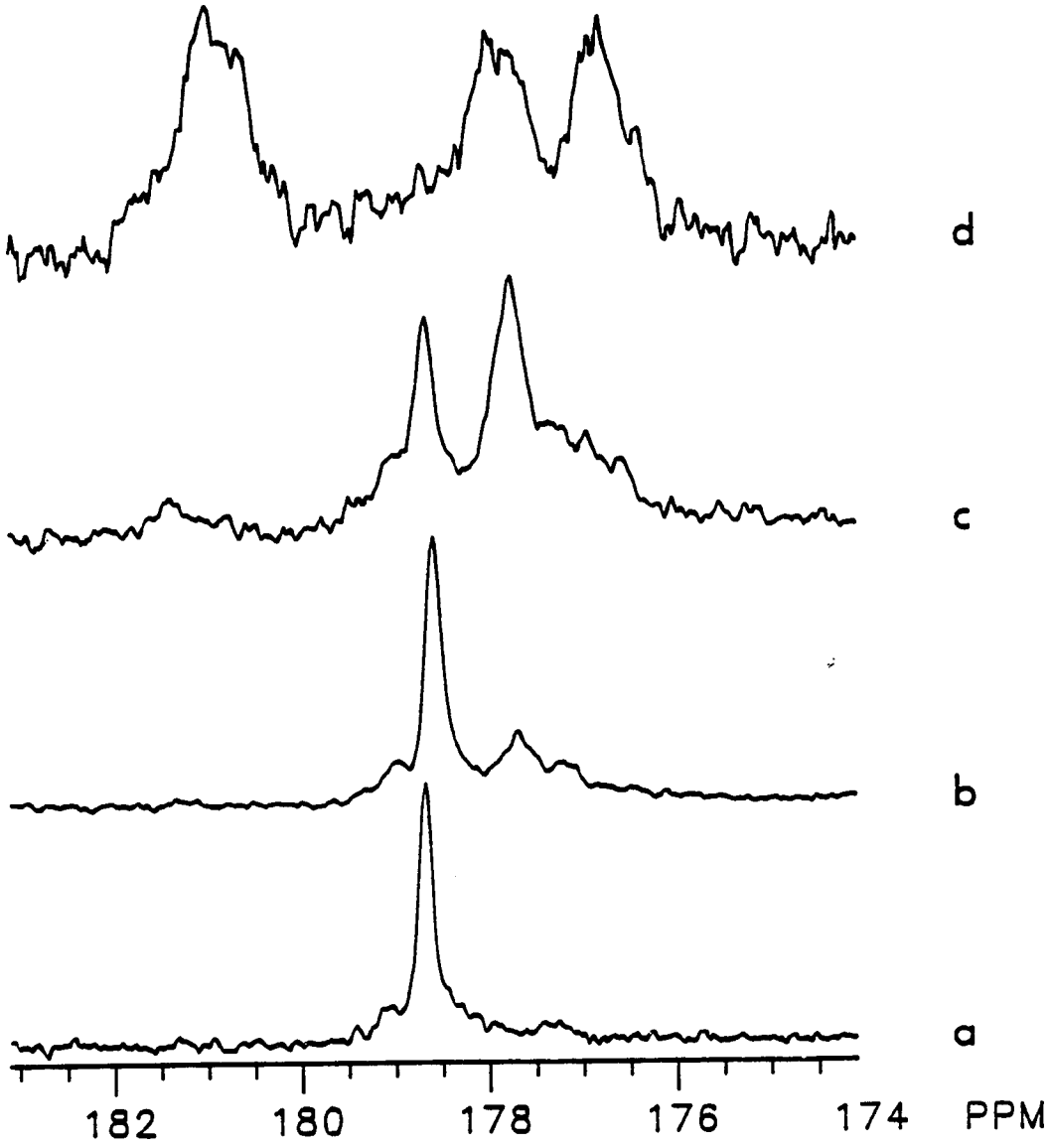
d
c
b
a
182
180
178
176
174
PPM

Table I. Triad Sequence Distribution for the Conversion of PAA Carboxyl Groups to Amino Groups via the Schmidt Reaction[a]

Chemical Shift	Assignment[b]	SP12 Exp	SP12 Calc[c]	SP30 Exp	SP30 Calc[c]	SP52 Exp	SP52 Calc[c]
51.0	<u>ABA</u>	0.0	-	2.0	-	14.8	-
49.4	<u>ABB</u>	0.0	-	2.9	-	7.5	-
48.4	ABA	8.8	9.3	15.5	14.7	8.8	12.0
46.9	ABB	3.0	2.6	14.1	12.6	22.0	26.0
44.8	BBB	0.0	0.2	0.0	2.7	0.0	14.1
41.6	AAA	60.3	68.1	12.2	34.3	0.0	11.1
39.9	AAB	23.8	18.6	35.1	29.4	14.3	24.0
38.1	BAB	4.2	1.3	18.2	6.3	32.6	13.0

[a]Based on the CH analysis. [b]Underlined sequences indicates lactam formation. [c]Calculated based on random statistics.

results which does not distinguish between A-centered amino acids and lactams.

Assuming lactam formation follows the primary reaction, i.e. the conversion of carboxyl to amino group, the sequence distribution may be analyzed in terms of the NNE. It is clear from the absence of AAA and BBB block sequences in SP52 that the relative rate constants $k_2/k_o > k_1/k_o > 1$ do not apply. The disparity between the observed and calculated sequences of Table I shows that the random case, $k_2/k_o \approx k_1/k_o \approx 1$, does not apply. In fact the analysis of the sequence distribution, according to Harwood,[9] for SP12, SP30 and SP52, combining ABA with ABA and ABB with ABB, are consistent with $k_2/k_o \approx 0$ and $k_1/k_o \approx 0.3$. These results indicate a strong tendency for an alternating sequence distribution.

C-13 NMR pH Titration The Schmidt products are water soluble in the basic or acidic form but water insoluble in the zwitterionic form. The insoluble range for SP12 is pH = 3.0 to 4.5, for SP30 is pH = 2.5 to 5.6 and for SP52 is pH = 3.6 to 9.0. Because of the relatively simple C-13 NMR spectrum for SP12 and its extended water solubility, SP12 was used for the C-13 NMR pH titration. Plots of chemical shifts versus pH for the AAA and AAB carbonyl carbons, for the ABA methine, for the AAA (rr, mr and mm sequences) methine and for the AAB methine are shown in Fig. 5. Curves a,d,e, and f correspond to various AAA sequences which experience a change in chemical shift only between pH = 2 and 8. Curves b and g represent the AAB sequences which experience a major change in chemical shift between pH = 2 and 8, but also displays a minor shift between pH = 9 and 12. Curve c representing the ABA methine responds in a more complex way to changes in pH and will not be discussed further in the context of this paper.[20]

Figure 5: The pH titration of SP12 at 25°C; a) the AAA carbonyl resonance, b) the AAB carbonylresonance,c) the ABA methine resonance, d) the ArArA methine resonance, e) the AmArA methine resonance, f) the AmAmA methine resonance and g, the AAB methine resonance.

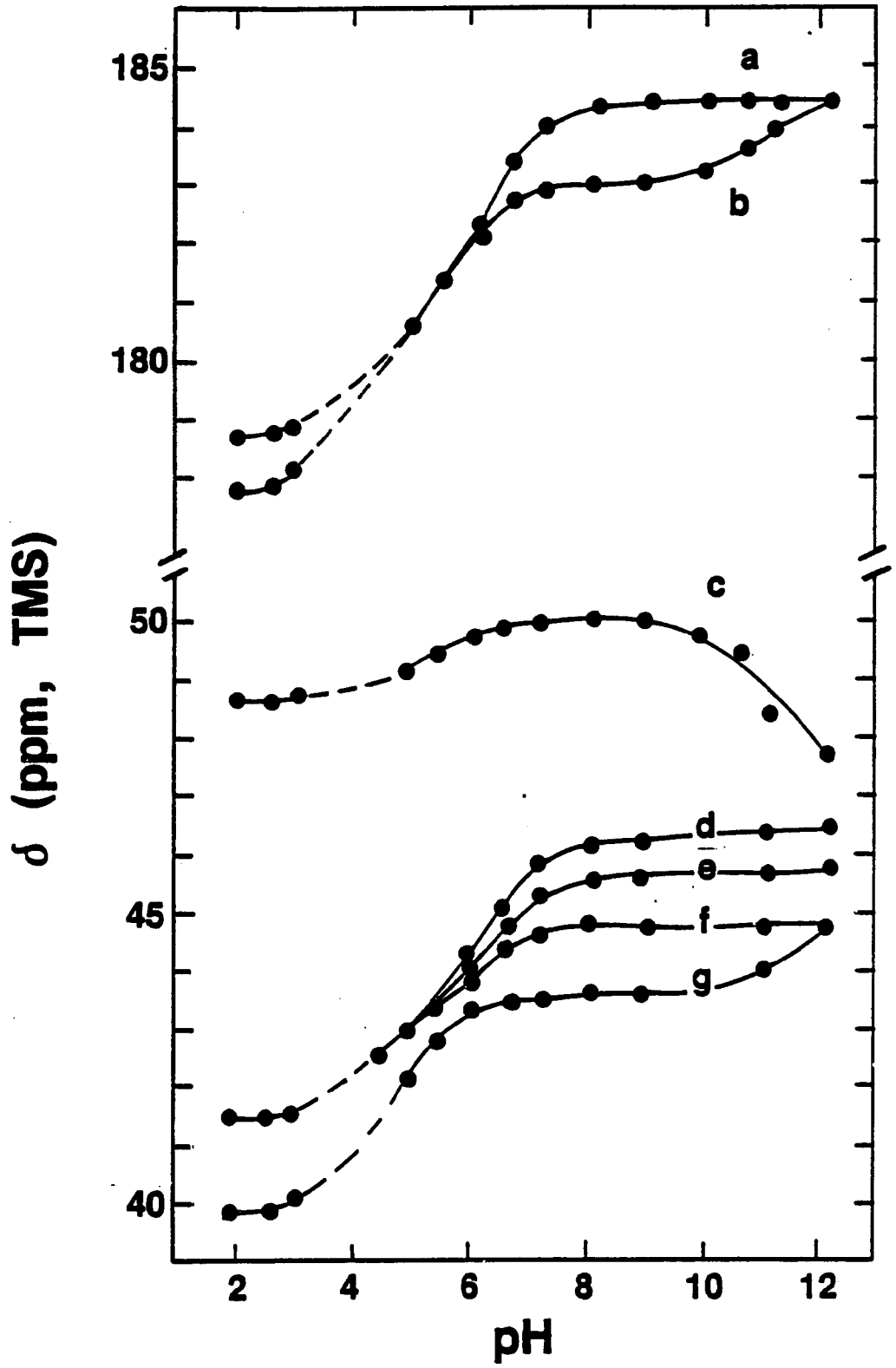
185
180
50
45
40
a
b
c
d
e
f
g
2
4
6
8
10
12
pH
δ (ppm, TMS)

Instead, we concentrate on the titration of the carboxyl group, i.e. A-centered peaks. These titration curves, for the pH range 2-8, were fit to the extended Henderson-Hasselbach (HH) equation or the Mandel equation. The procedures for evaluating $pK_{1/2}$ (pK_a at the titration midpoint) and n values (slope) for the extended HH equation and the coefficients a,b and pK_i (intrinsic pKa) for the Mandel equation are the same as already described for PAA.[6] These results are presented in Table II.

From the extended HH equation, the correlation coefficients for every set of data are close to unity, suggesting that this treatment is appropriate and that the polymers do not undergo a sudden conformational change during the course of the titrations.[6] The initial dissociation, represented by pK_i, appears to be very much the same for the AAA and AAB sequences of SP12 and for the AAA sequence of PAA. With the exception of the 4.30 value, the remaining nine values average to $pK_i = 4.05 \pm 0.1$. The polyelectrolyte effect expresses itself most in the latter stages of the titration, i.e. $pK_{1/2}$ (or intercept for the HH treatment). In these values we see a small trend for the configurational variations in the methine AAA sequences. The acidity of the carboxyl group depends slightly on the configuration of its neighbors in the order mm > mr > rr. The carbonyl group by NMR titration gives a $pK_{1/2}$ for the AAA sequence close to the average value determined for the three methine values. The more significant trend appears in the difference in acidity for the AAA sequence of PAA and SP12, and for the AAA and AAB sequence of SP12. The acidity of the carboxyl group increases in the order AAA-SP12, AAA-PAA and AAB-SP12. During the course of the titrations, the central A units of the sequence AAB will be deprotonated preferentially because the NNE provides

Table II. Acid Dissociation Constants for Copolymer SP12 and Homopolymer PAA

Polymer	SP12						PAA			
Carbon	Methine			- Carboxyl -			Methine			- Carboxyl -
Sequence	AAA	AAA	AAA	AAB	AAA	AAB	AAA	AAA	AAA	AAA
Configuration	mm	mr	rr	-	-	-	mm	mr	rr	-
Slope[a]	1.89	1.89	1.81	1.35	1.67	1.58	1.65	1.78	1.80	1.75
Intercept[a]	5.08	5.45	5.50	4.67	5.49	4.80	4.73	5.05	5.22	4.97
Correlation[a]	0.99	0.98	0.98	0.99	0.99	0.99	0.99	0.99	0.99	0.99
pK_1[b]	3.91	4.03	4.07	4.16	4.30	3.92	3.91	4.09	4.22	4.03
a[b]	2.93	3.90	4.83	1.23	3.00	2.09	1.91	1.99	2.08	2.09
b[b]	-0.92	-1.68	-2.86	-0.25	-1.14	-0.42	-0.46	-0.18	-0.21	-0.42
Xn[c]	2.16	2.28	2.13	1.56	2.07	1.96	1.85	2.04	2.08	1.96
$pK_{1/2}$[c]	5.15	5.56	5.77	4.71	5.52	4.86	4.76	5.03	5.21	4.97

[a]These values are based on the HH treatment where slope = pn and intercept = $pK_{1/2}$

[b]These values are based on the Mandel treatment [c]These are the HH parameters calculated from pK_1, a and b

electrostatic stabilization between the positive charge of the amino group and the negative charge of the carboxylate group. The AAA sequence, upon dissociation, will have a net negative charge and will be less favored. The same effect is well known for simple amino acids. It is not immediately obvious why the AAA sequence of SP12 is a slightly stronger acid than the AAA sequence of PAA. There are no convincing enthalpic argument to support this effect but one could argue on entropic grounds that the charge distribution would be more favorable for PAA lacking the fixed B units in the copolymer which would focus charge distribution.

The final comment concerning the titration behavior of SP12 is the obvious difference in the shape of the curves for the AAA and AAB sequences, Fig. 5. For the latter there is a change in chemical shift in the pH = 9 to 12 range in response to the titration of the neighboring amino group which is estimated at $pk_{1/2}$ = 10.9. This reinforces the assignment and provides a means for studying the amine titration.

REFERENCES

(1) Wolff, H. Org. Reactions 1946, 3, 307.

(2) Hughes, A. R. Ph.D. Dissertation, University of Alabama at Birmingham, Birmingham, AL, 1975.

(3) Keller, J. B. J. Chem. Phys. 1962, 37, 2584.

(4) Gunari, A.; Gundiah, S. Makromol. Chem. 1981, 182, 1.

(5) Halverson, F.; Lancaster, J. E. O'Connor, M. N. Macromolecules 1985, 18, 1139.

(6) Chang, C.; Muccio, D.D.; St. Pierre, T. Macromolecules (in press).

(7) Harwood, J. "Preparation and Properties of Stereoregular Polymers"; Leng, R .W. and Ciardelli, F. (Eds), D. Reidel Publishing Company, 1979; P 295.

(8) Klesper, E.; Strasilla, D.; Bartha, V. "Reactions on Polymers"; Moore, J.A. (Ed), Reidel, Boston, 1973; P 137.

(9) Harwood, H. J.; Kempf, K. G.; Landoll, L. M. J. Polym. Sci. Polym. Lett. Ed., 1978, 16, 1009

(10) Merle, Y.; Merle, L. Macromolecules 1983, 16, 1009.

(11) Merle, Y. J. Polym. Sci. Polym. Phys. Ed. 1984, 22, 525.

(12) Hughes, A. R.; St. Pierre, T. "Macromolecular Synthesis"; Mulvaney, J. E. (Ed), John Wiley: New York, 1977; 31.

(13) Patt, S. L.; Shoolery, J. N. J. Magn. Reson. 1982, 46, 535.

(14) Chang, C.; Muccio, D. D.; St. Pierre, T. Macromolecules (submitted).

(15) Grant, D. M.; Paul, E. G. J. Am. Chem. Soc. 1964, 86, 2984.

(16) Lindeman, L. P.; Adams, J. Q. Anal. Chem. 1971, 43, 1245.

(17) Klesper, E.; Gronski, W.; Barth, V. Makromol. Chem. 1970, 139, 1.

(18) Levy, G. C.; Lichter, R. L.; Nelson, G. L. "Carbon-13 Nuclear Magnetic Resonance Spectroscopy"; 2nd Ed, John Wiley: New York, 1980; P 62.

(19) Barbucci, R.; Casolaro, M.; Ferruti, P.; Barone, V.; Lelj, F.; Oliva, L. Macromolecules 1981, 14, 1203.

(20) Chang, C.; Muccio, D.D.; St. Pierre, T. (in preparation).

(21) Feeney, J.; Partington, P.; Roberts, G.C.K. J. Magn. Reson. 1974, 13, 268.

CHAPTER VII

CONCLUSION

In the first part of this study, the configurations of the homopolymers were determined principally from the analysis of ^{13}C NMR spectra and were supported by either ^{1}H or ^{15}N NMR spectral results, where appropriate. The ^{13}C NMR spectra of a PAA aqueous solution at the appropriate pH gave good resolution for the methine carbon enabling triad tacticity assignments; however, the poor resolution for the methylene carbons yielded little information as to the dyad tacticity of this polymer. The methine carbon appeared as three major peaks with relative areas of 27:50:23 corresponding to the rr, mr and mm triad sequences, respectively. Using Bernoullian statistics to analyze the two principle methylene peaks, the corresponding probabilities for the m and r dyad are 48% and 52%, respectively, indicating the atactic character of this polymer. This result is apparaent in the ^{1}H NMR spectrum of the polymer methylene protons, referenced to an equal molar mixture of m- and r-2,4-dimethylglutaric acid. Unlike that of PAA, the ^{1}H NMR spectrum of PVAm gave poor resolution and was not directly able to provide the dyad distribution. Instead, the dyad configuration of PVAm was based on the methylene carbon analysis only after using heteronuclear correlated two-dimensional (2-D) NMR experiments to make the m and r assignments. The dyad distribution based on the two methylene carbon peaks was found for PVAmI to be 44% m and 56% r, and the corresponding methine carbon analysis gave 17% mm, 54% mr and 29% rr, establishing the essentially

atactic character of PVAmI. PVAm was analyzed in more detail by taking advantage of the configurational sensitivity of its ^{13}C NMR spectrum which was optimal at pH = 8.8. At this pH nine well-resolved methine carbon resonances and five methylene carbon resonances were observed. On the basis of dyad distribution, the polymer configuration was analyzed for the tetrad and pentad distributions. The analysis of PVAmII was comparable to PVAmI except the dyad distribution is 52% m and 48% r. This analysis is supported, at the triad level, by ^{15}N NMR of PVAmI and ^{1}H NMR of the acetylated polymer, poly(vinyl acetamide), based on the reported analysis of the $COCH_3$ group.

At this point it is worth noting that the heteronuclear correlated 2-D NMR experiments established a new approach for the configurational assignments of vinyl polymers. This NMR technique may be a general one for the dyad assignment of the methylene carbons of other vinyl polymers. This approach is based on the chemical nonequivalence of the methylene protons of the m configuration and the equivalence of the r methylene protons. By means of the 2-D experiment, the dyad assignment of the methylene carbon is unambigously assigned as m or r depending on its correlation to the distinctive m or r proton pattern, two peaks for the former and one peak for the latter. This is true for resolved methylene dyad configuration even when the resolution is not apparent in the ^{1}H spectrum. The determination of the sequence distributions of the SP copolymers were made much easier suppressing after the tacticity effects. In contrast to the tacticity studies, the spectra were analyzed for the different sequences for solutions adjusted to low pH where the methine carbon of PAA and of PVAm each appeared as a single peak representing the

AAA and BBB sequence, respectively. Based on the peak area changes with composition and other considerations, the AAB, BAB, BBA and ABA sequences were easily identified. Copolymer shows a strong tendency for alternating vinylamine and acrylic acid units as the copolymer approaches 50% conversion. This tendency is consistent with the neighboring group effect that favors the conversion of AAA to ABA over the conversion of AAB to ABB and practically prohibits the conversion of BAB to BBB. This preference explains why the Schmidt reaction stops at about 50% conversion. It was also apparent in the sequence analysis of the B centered methines that neighboring amino acids tend to form lactams, to the extent of 46% for SP52.

In the last part of this study, the carboxyl and amino group proton ionization potentials were studied for each of the polymers. The effect of tacticity on the acid dissociation constant of PAA is small, but the trends are clear: pK_{mm}=4.73, pK_{mr}=5.05 and pK_{rr}=5.22, which are in consistent with the potentiometric data reported in the literature on polymers with preferred tacticity. These data, however, were obtained for an atactic polymer which would not be obtainable by other means except the ^{13}C NMR approach used here.

Since the SP copolymers are water soluble in the basic or acidic form but water insoluble in the zwitterionic form, only SP12 was used to study the ^{13}C NMR pH titration due to its extended water solubility of this copolymer. The titration curves for the AAA and AAB sequence are distinctly different. For the latter there is a change in chemical shift in the pH range 9 to 12. This is in response to the titration of the neighboring amino group of the AAB sequence. Moreover, the AAB sequence

is more acidic than AAA sequence just as the carboxyl group of an α-amino acid is more acidic than simple carboxylic acids. These results establish that the acid-base behavior of the polyelectrolytes in aqueous solution are subject to the neighboring group effects.

The analysis of the ionization of PVAm by NMR titration data is more complicated than that of PAA. The methylene carbon titration curves were typically sigmoidal and there is little difference in the pKa for the m and r dyads, and these results and the earlier potentiometric titration results. However, bell-shaped ^{13}C NMR titration curves for the methine triads and the abrupt change of ^{15}N NMR titration curves strongly suggest that PVAm does undergo a distinct conformational change during the course of titration at $\alpha = 0.5$, which was not present in PAA. For PVAm dissociation, the exact nature of the change in conformation with pH for PVAm has not yet been established but it is certain that the polymer configuration is an important factor. This is possibly due to the close proximity of the titrating groups and the more pronounced electric field effect, and /or hydrogen bonding associated with the NH_3^+ to NH_2 transition during the course of titration. The trend for pKa values based on the ^{15}N NMR fitration is significant, i.e. $pK_{mm} < pK_{mr} < pK_{rr}$.

Appendix A

^{13}C NMR of concentration study: The purpose of this study is to determine the most suitable concentration in terms of maximum efficiency of NMR time and minimum polymer concentration effects. PAA (MW = 15,000) was used as a standard polymer for this study. It is found that 0.5 M gave the same quality of spectra as did more dilute solutions.

Figure 1: Concentration study of PAA at pH = 12 and MW = 15,000 in 10% D_2O for about 2000 acquisitions with a pulse angle of 62° and a repetition rate of 3.5 s: (a) 0.1 M (CC058E.001), (b) 0.5 M (CC058F.001), (c) 1.0 M (CC059L.001), (d) 1.5 M (CC059J.001), (e) 3.0 M (CC059E.001).

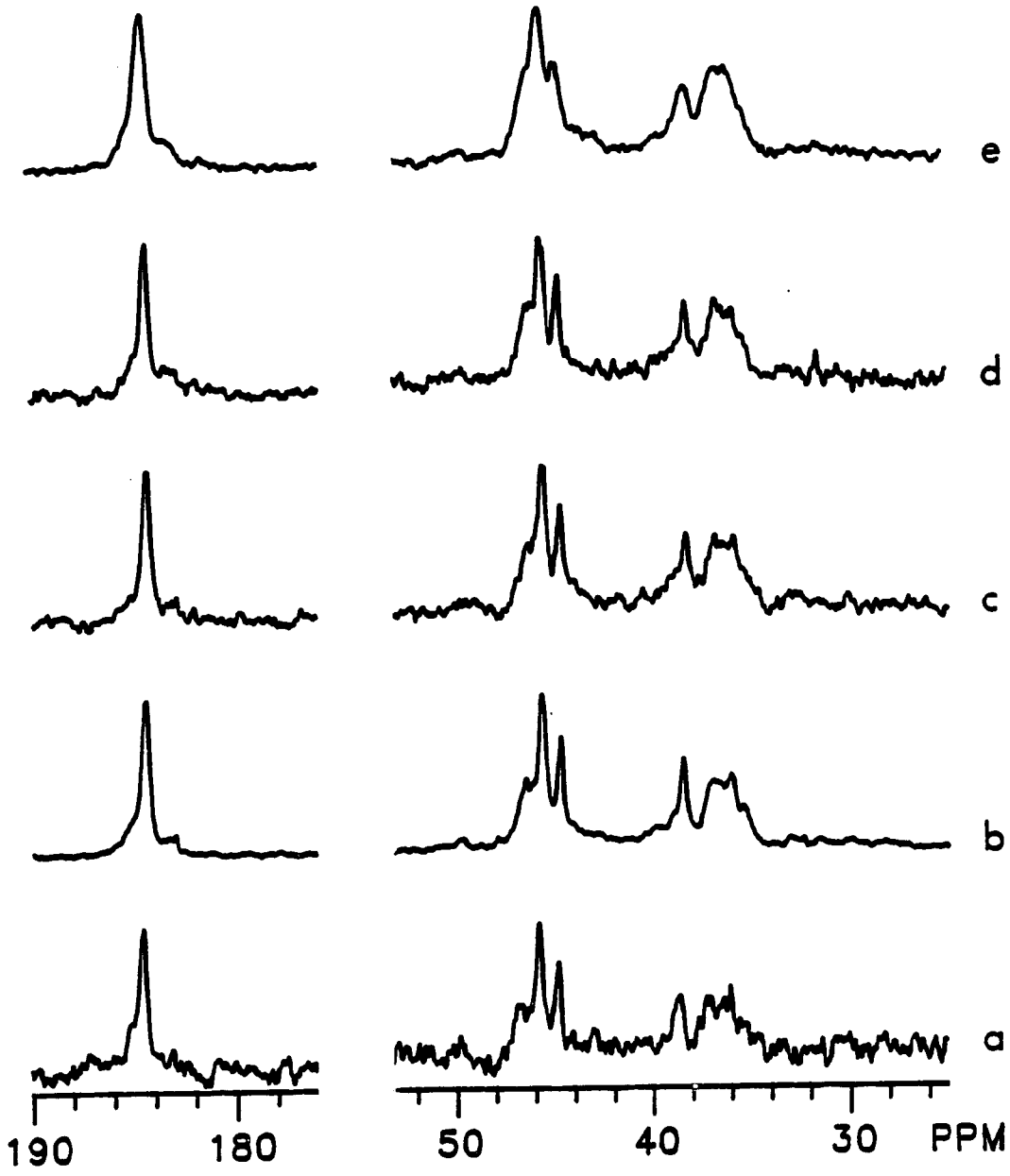
e
d
c
b
a
190
180
50
40
30
PPM

Figure 2: Concentration study of PAA at MW = 15,000 in 10% D_2O for about 2000 acquisitions with a pulse angle of 62^{o} and a repetition rate of 3.5 s: (a) 0.1 M (pH = 2, CC060B.001), (b) 0.25 M (pH =2, CC062A.001), (c) 0.5 M (pH =2, CC060C.001), (d) 1.5 M (pH = 4.52, CC059A.001), (e) 3.0 M (pH =4.64 CC059F.001).

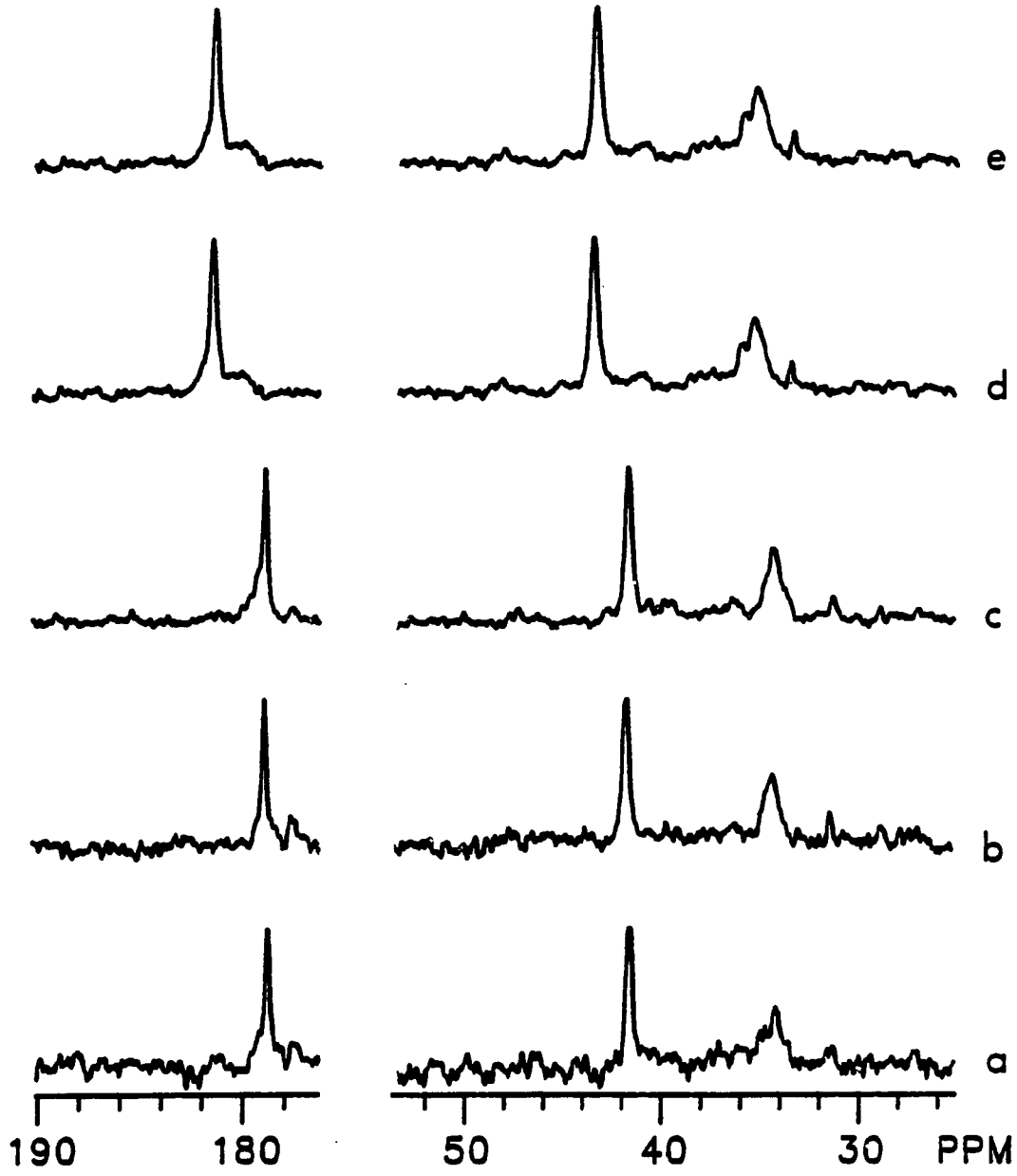
e
d
c
b
a
190
180
50
40
30
PPM

Appendix B

^{13}C NMR study of polymers with different molecular weight: In order to minimize polymer end-group effect, several different molecular weight of PAA were examined. It was concluded that the spectra of PAA at MW = 15,000 does not show significant end-group peaks and the use of higher MW polymers resulting in poorer resolution would not be justified. Therefore, PAA at MW = 15,000 was used to perform the PAA studies and to prepare the SP copolymers.

Figure 1: Molecular weight study of PAA for 0.5 M solutions in 10% D_2O at pH = 2 for about 2000 acquisitions with a pulse angle of 62^o and a repetition rate of 3.5 s: (a) MW = 1,000 (CC062B.001), (b) MW = 4,500 (CC066A.001), (c) MW = 15,000 (CC059A.001).

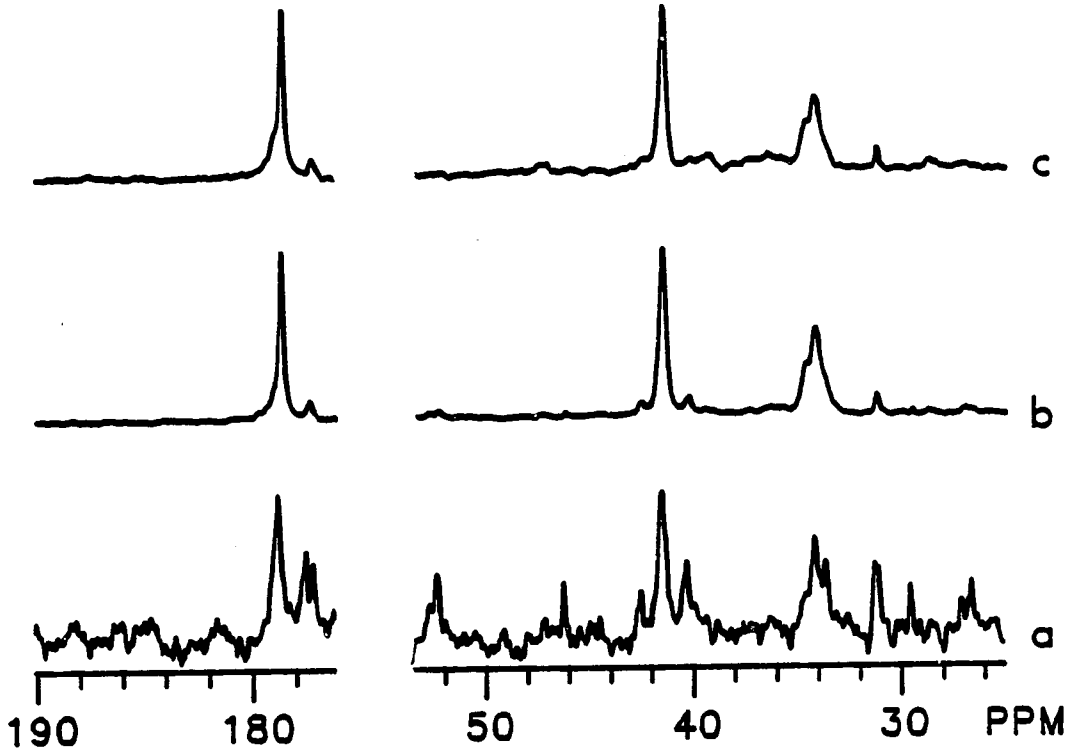
c
b
a
190
180
50
40
30
PPM

Figure 2: Molecular weight studyt of PAA for 0.5 M solutions in 10% D_2O at pH = 12 for about 2000 acquisitions with a pulse angle of 62^{o} and a repetition rate of 3.5 s: (a) MW = 4,500 (CC069B.001), (b) MW = 2,000 (CC068A.001), (c) MW = 4,500 (CC066A.010), (d) MW = 15,000 (CC065A.001).

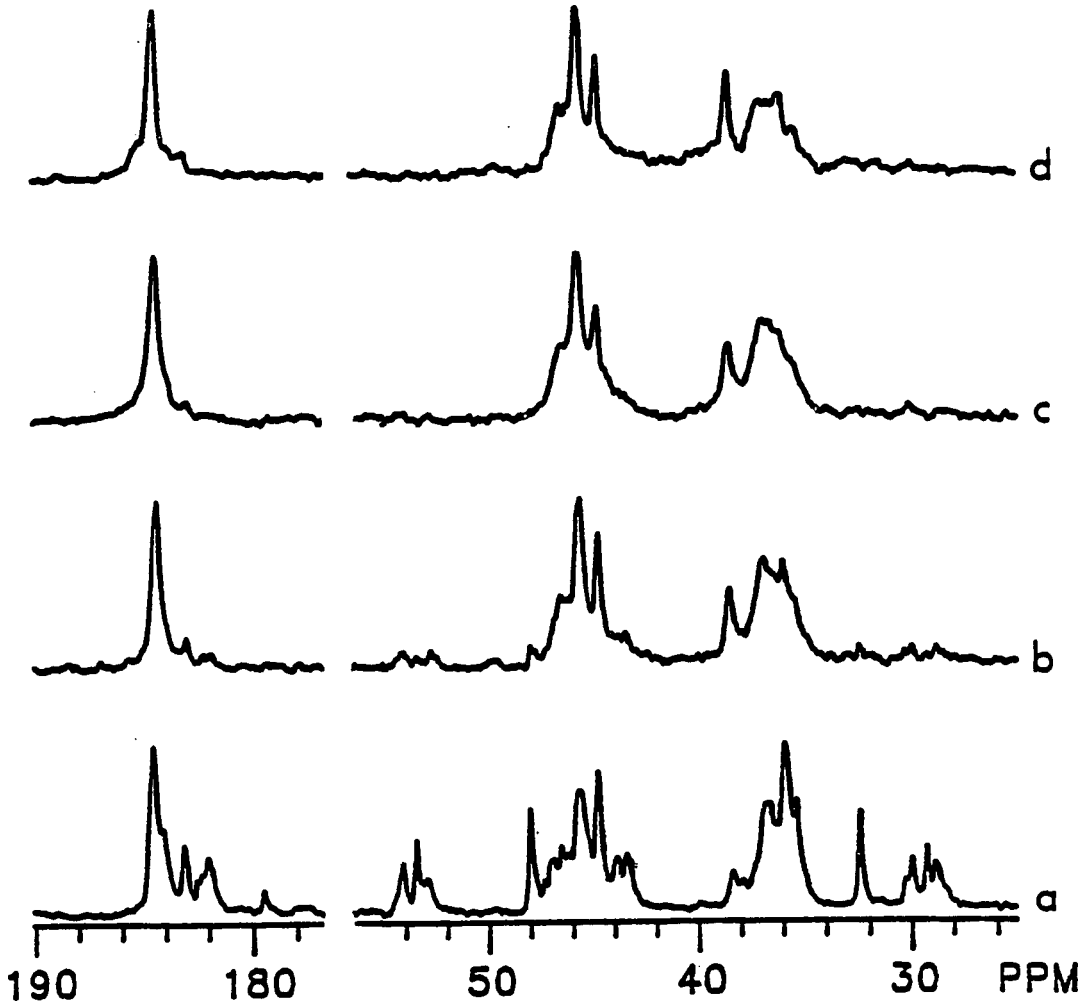
d
c
b
a
190
180
50
40
30
PPM

Appendix C

Temperature study: The chemical shifts and resolution of a polymer NMR spectrum will be influenced by temperature. PAA (MW = 15,000) was used to check these effects. The resolution increases wtih increasing temperature but chemical shifts remained unchanged for both the ^{1}H and ^{13}C NMR spectra. A temperature of 75°C was used for the PAA configurational study because of the improved resolution and 25°C for the remaining polymers. For all titration studies, a temperature of 25°C was also used because most of the reported titrations were performed at or near this temperature.

Figure 1: ^{1}H NMR of PAA at various temperatures for 0.05 M solutions in D_2O at pH = 12 for 3000 acquisitions with a pulse angle of 75° and a repetition rate of 3.5 s: (a) 25°C (CCA06C.005), (b) 75°C (CCA06B.005), (c) 80°C (CCA06D.005).

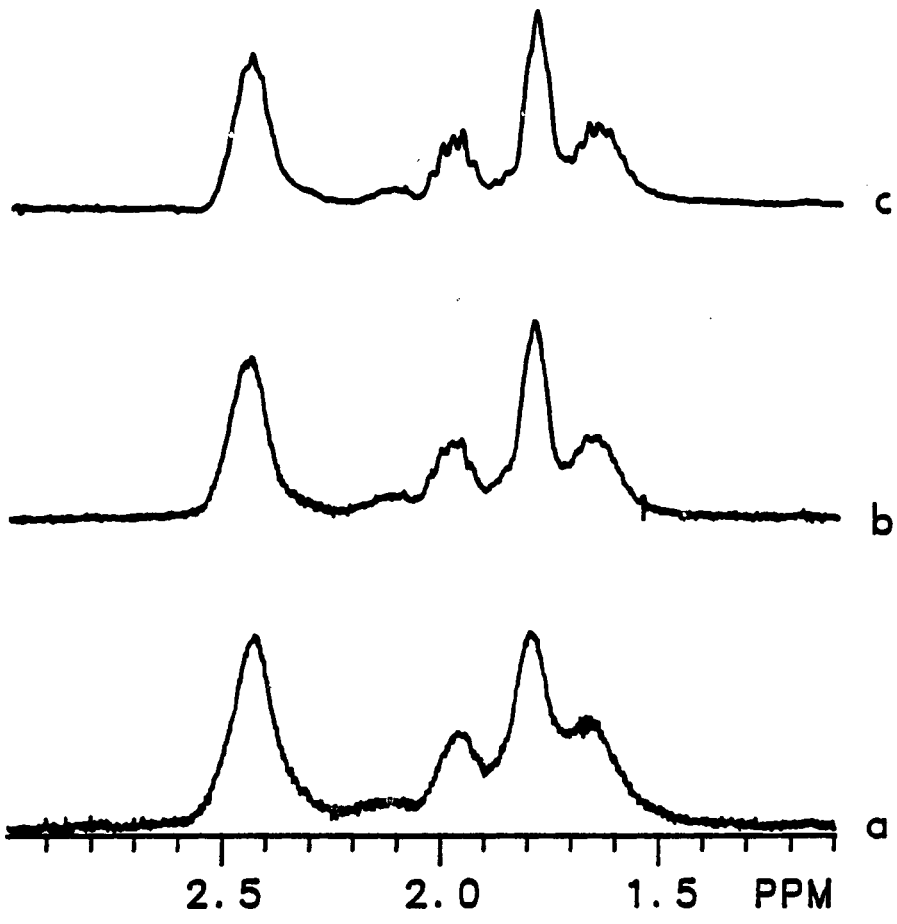
c
b
a
2.5
2.0
1.5
PPM

Figure 2: ^{13}C NMR of PAA at various temperatures for 0.5 M solutions in D_2O at pH = 12 for about 5000 aquisitions with a pulse angle of 62° and a repetition rate of 3.5 s: (a) 25°C (CC058F.001), (b) 60°C (CC070C.001), (c) 75°C (CC090X.001).

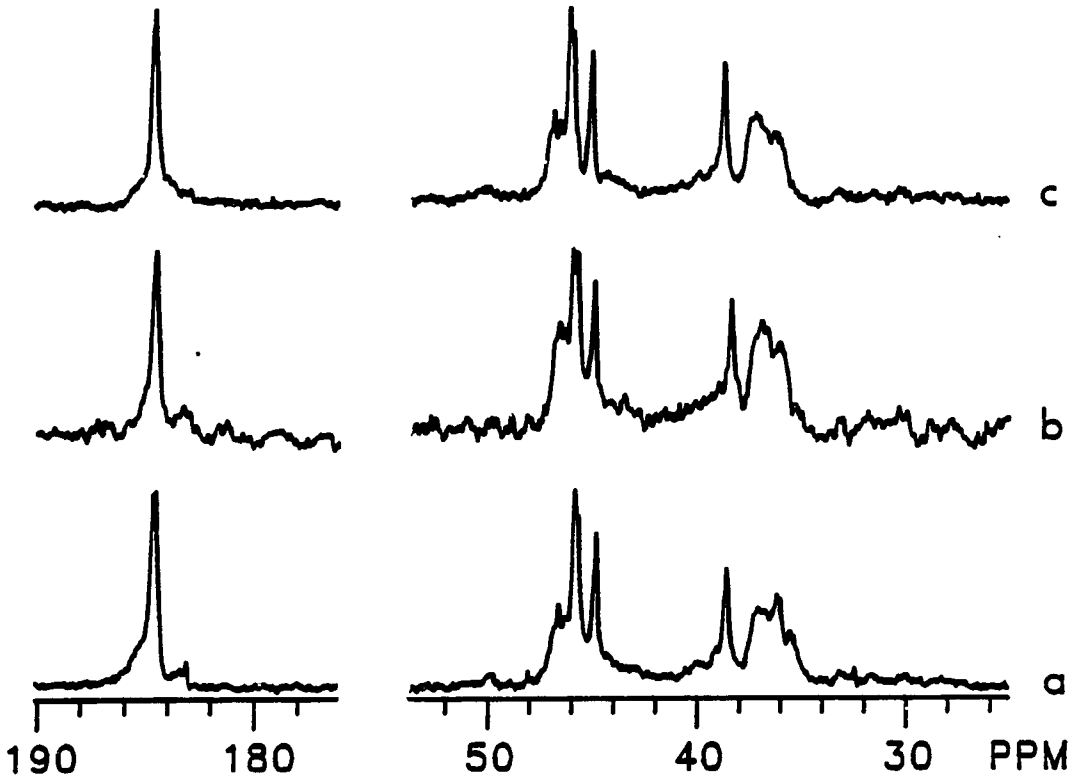
c
b
a
190
180
50
40
30
PPM

Appendix D

^1H NMR model study: The assignments of tacticity are made by the comparison of the polymer spectra to the spectra of the model compounds. A mixture of m and r 2,4-dimethylglutaric acid (DGA) was used as the model for PAA and m and r isomers of 2,4-diaminopentane (DAP) were used as model compounds for PVAm. The results indicate that the methylene protons of the m isomer for both model compounds are chemically nonequivalent and lead to two multiplets, while the methylene protons of the r isomer are degenerate. The experiments were performed on 0.1 M solutions in D_2O.

Figure 1: ^{1}H NMR spectra of a mixture of m and r DGA at pH = 2, 25°C (CCA06S.004) for 24 aquisitions with a pulse angle of 75° and a repetition rate of 7 s: (a) full spectrum scaled relative to the methyl protons, (b) methyl protons, (c) methylene protons, (d) methine protons. This result was used to establish the configuration study of PAA (Chapter I).

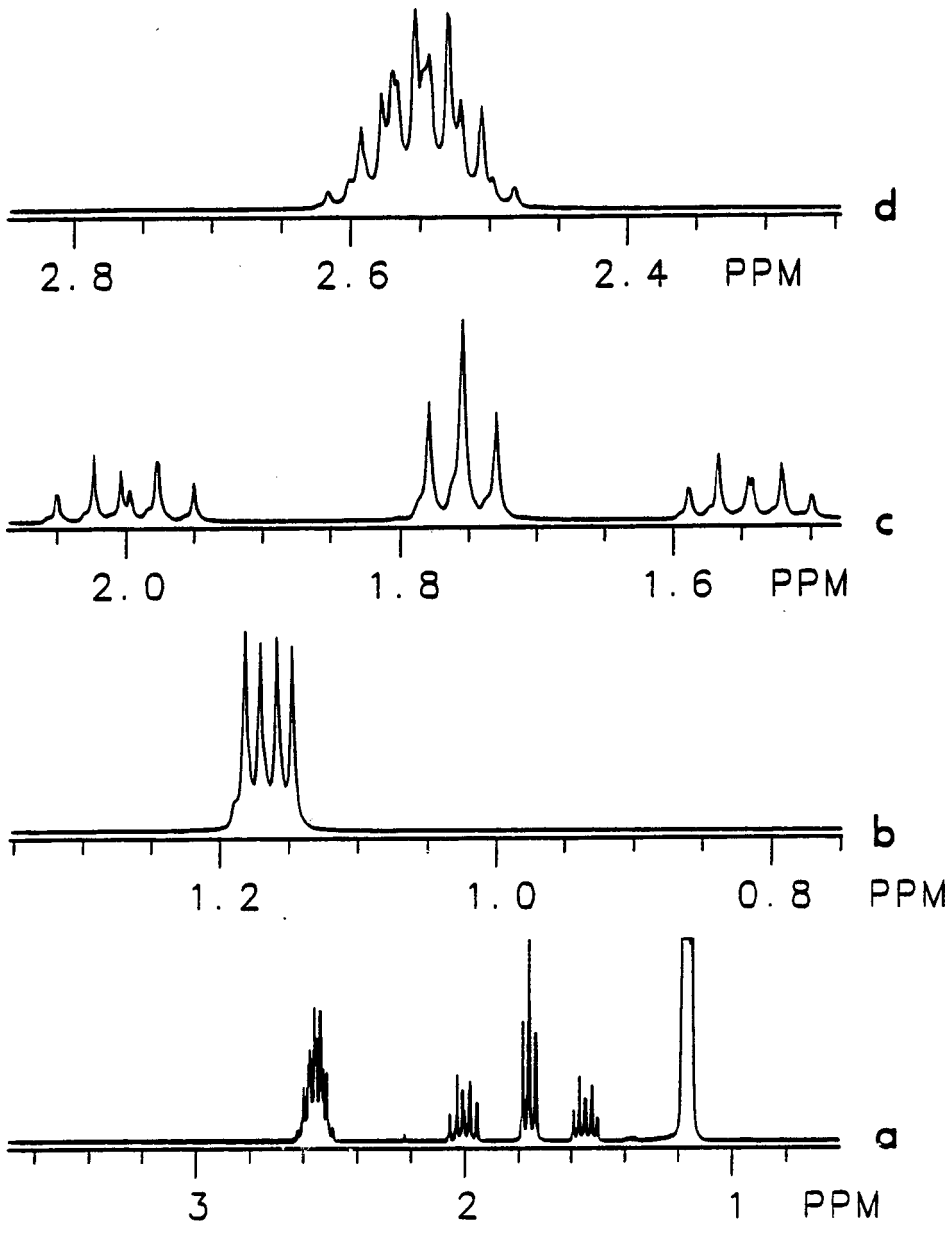
d
2.8
2.6
2.4
PPM
c
2.0
1.8
1.6
PPM
b
1.2
1.0
0.8
PPM
a
3
2
1
PPM

Figure 2: ^{1}H NMR spectra of a mixture of m and r DGA at pH = 2, 80°C (CCA06C.004) for 24 acquisitions with a pulse angle of 75° and a repetition rate of 7 s: (a) full spectrum scaled relative to the methyl protons, (b) methyl protons, (c) methylene protons, (d) methine protons. This result was used to establish the configuration study of PAA (Chapter I).

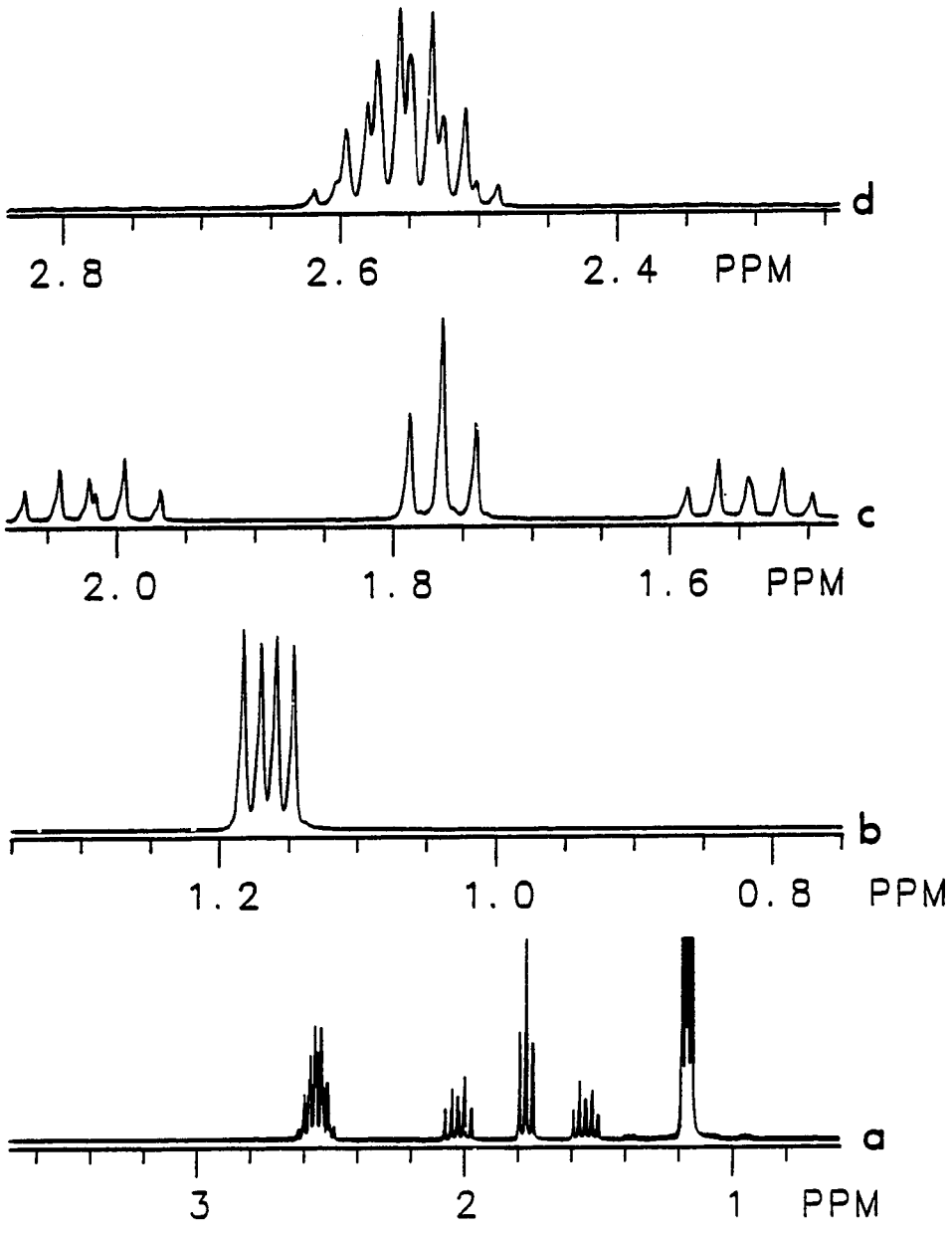
d
2.8
2.6
2.4
PPM
c
2.0
1.8
1.6
PPM
b
1.2
1.0
0.8
PPM
a
3
2
1
PPM

Figure 3: Spectrum of r DAP at pH = 1.8, 25°C (CCA06C.001) for acquisitions with a pulse angle of 75° and a repetition rate of 7 s: (a) full spectrum scaled relative to the methyl protons, (b) methyl protons, (c) methylene protons, (d) methine protons. This information was used in the configuational and 2-D studies of PVAm. (Chapter II and III).

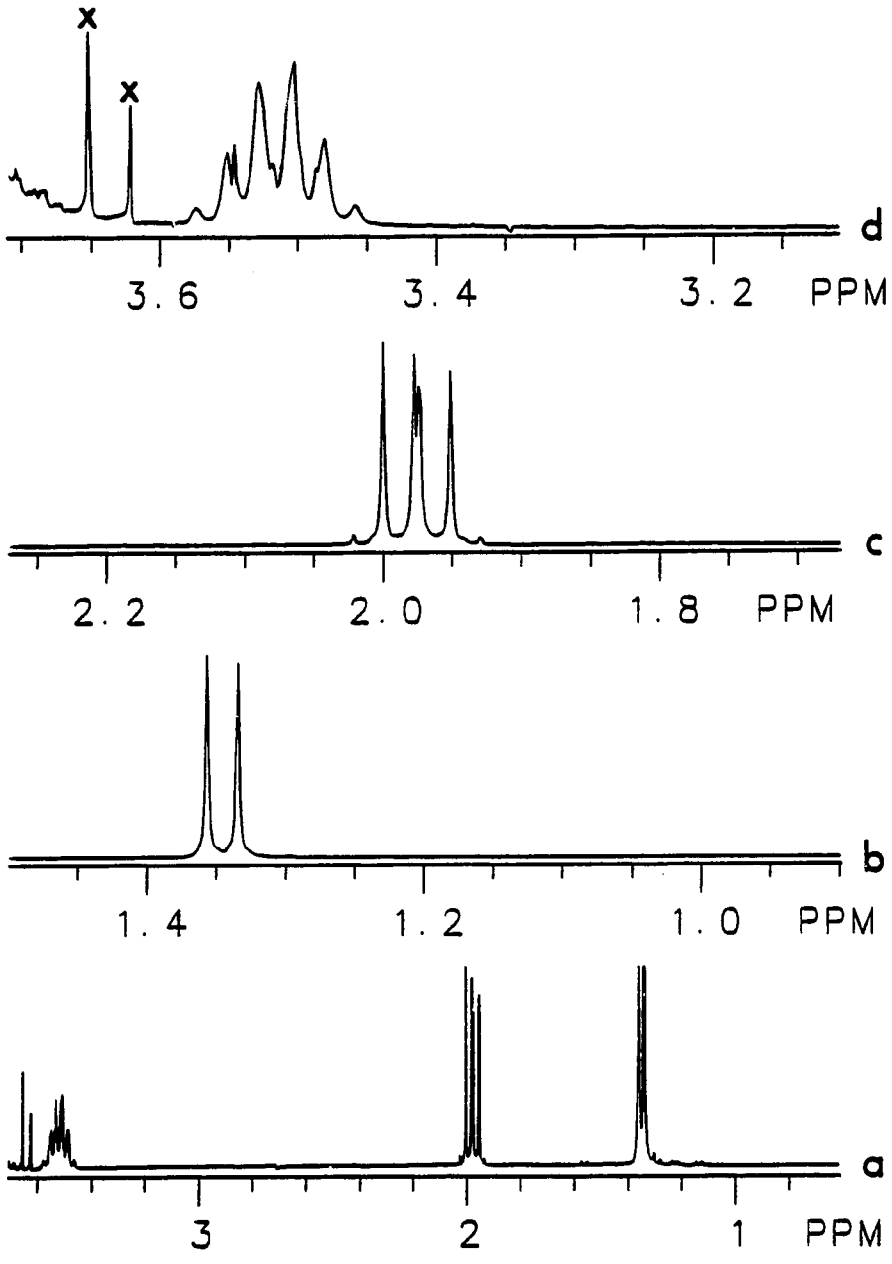
X
X
d
3.6
3.4
3.2
PPM
c
2.2
2.0
1.8
PPM
b
1.4
1.2
1.0
PPM
a
3
2
1
PPM

Figure 4: Spectrum of r DAP at pH = 11.8, 25°C (CCA06A.001) for 24 acquisitions with a pulse angle of 75° and a repetition rate of 7 s: (a) full spectrum scaled relative to the methyl protons, (b) methyl protons, (c) methylene protons, (d) methine protons.

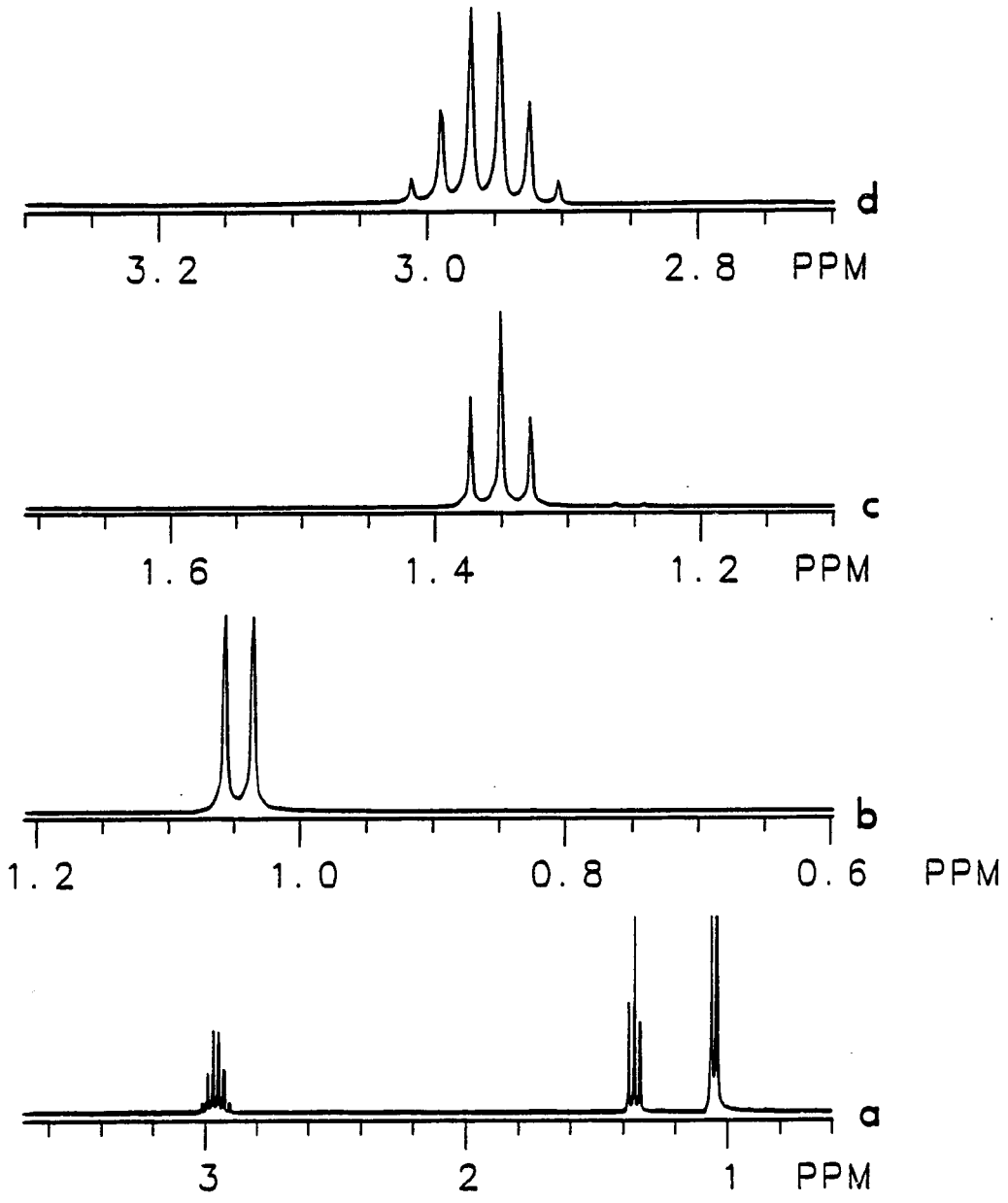
d
3.2
3.0
2.8
PPM
c
1.6
1.4
1.2
PPM
b
1.2
1.0
0.8
0.6
PPM
a
3
2
1
PPM

Figure 5: Spectrum of m DAP at pH = 1.8, 25°C (CCA06C.003) for 24 acquisitions with a pulse angle of 75° and a repetition rate of 7 s: (a) full spectrum scaled relative to the methyl protons, (b) methyl protons, (c) methylene protons, (d) methine protons. This information was used in the configurational and 2-D studies of PVAm (Chapter II and III).

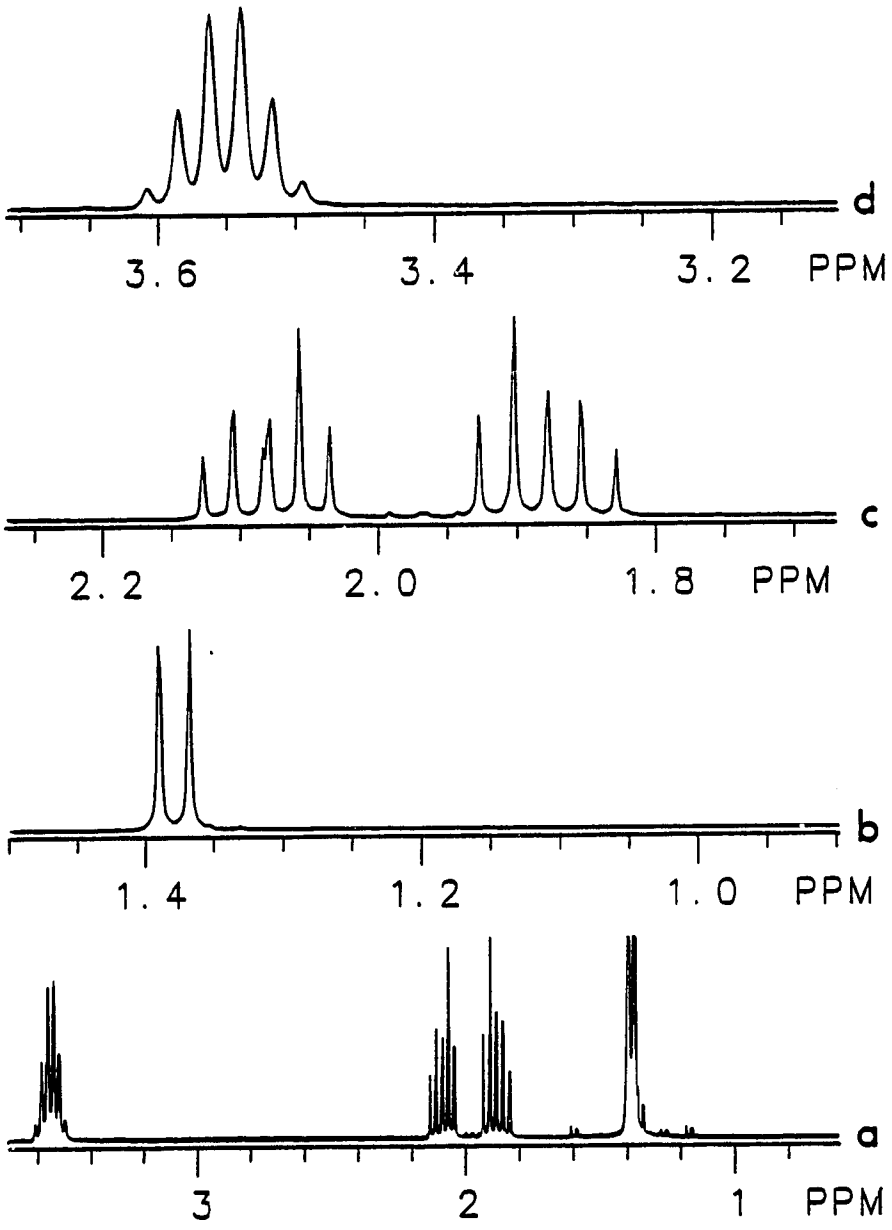
d
3.6
3.4
3.2
PPM
c
2.2
2.0
1.8
PPM
b
1.4
1.2
1.0
PPM
a
3
2
1
PPM

Figure 6: Spectrum of m DAP at pH = 11.8, 25°C (CCA06A.003) for 24 acquisitions with a pulse angle of 75° and a repetition rate of 7 s: (a) full spectrum scaled relative to the methly protons, (b) methyl protons, (c) methylene protons, (d) methine protons.

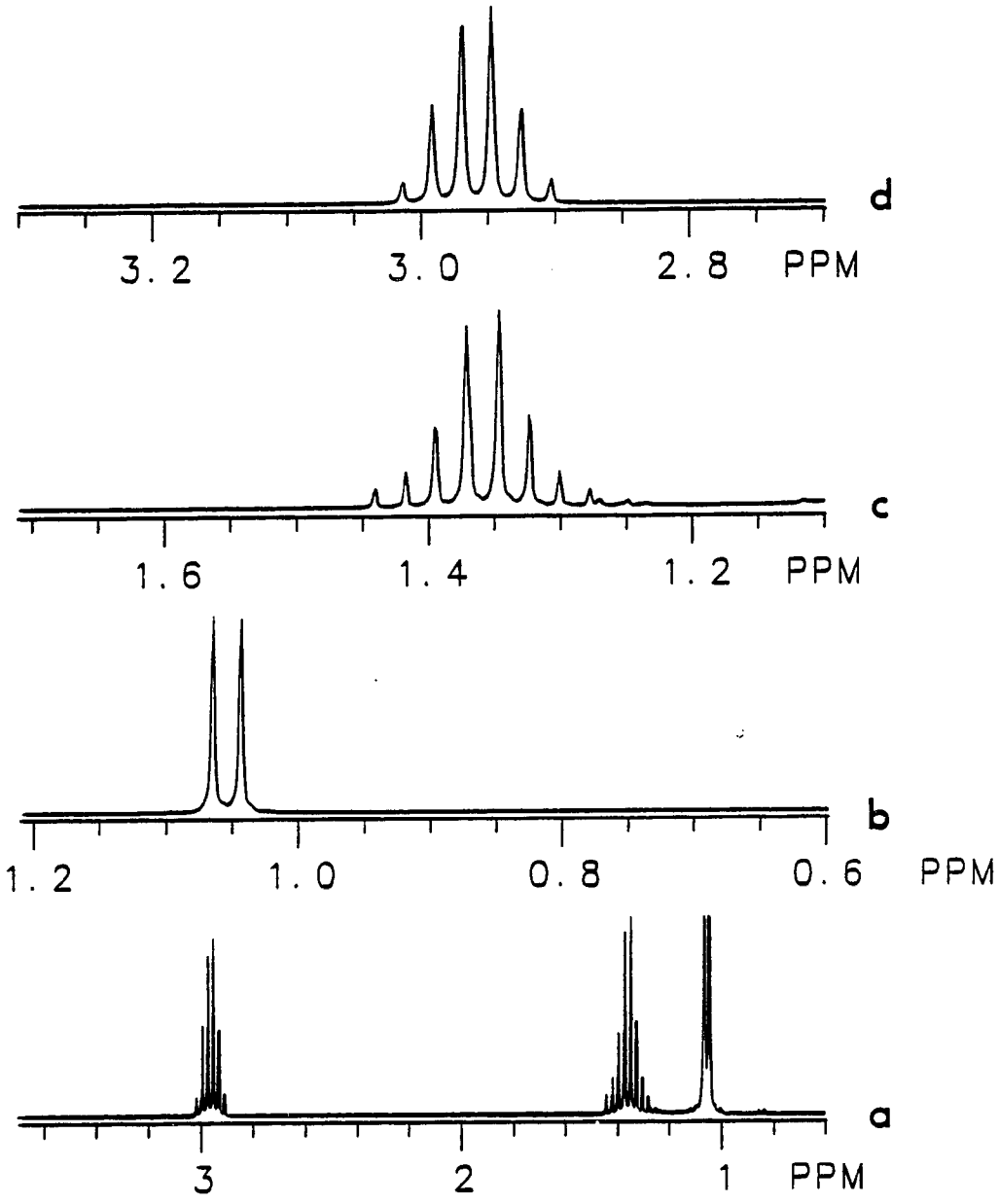
d
3.2
3.0
2.8
PPM
c
1.6
1.4
1.2
PPM
b
1.2
1.0
0.8
0.6
PPM
a
3
2
1
PPM

Appendix E

Nuclear Overhauser effect (NOE) study: The NOE was determined by the ratio of the peak intensity of the fully proton decoupled and gated-decoupled (decouper off during delay time) spectra. This information was used for the quantitative analysis of the polymer tacticity. The results show that there is no need for NOE corrections because the NOE was found to be essentially the same for different tacticity.

Figure 1: NOE as a function of correlation time for 75 MHz ^{13}C magnetic field strength. Isotropic rotation is assumed.

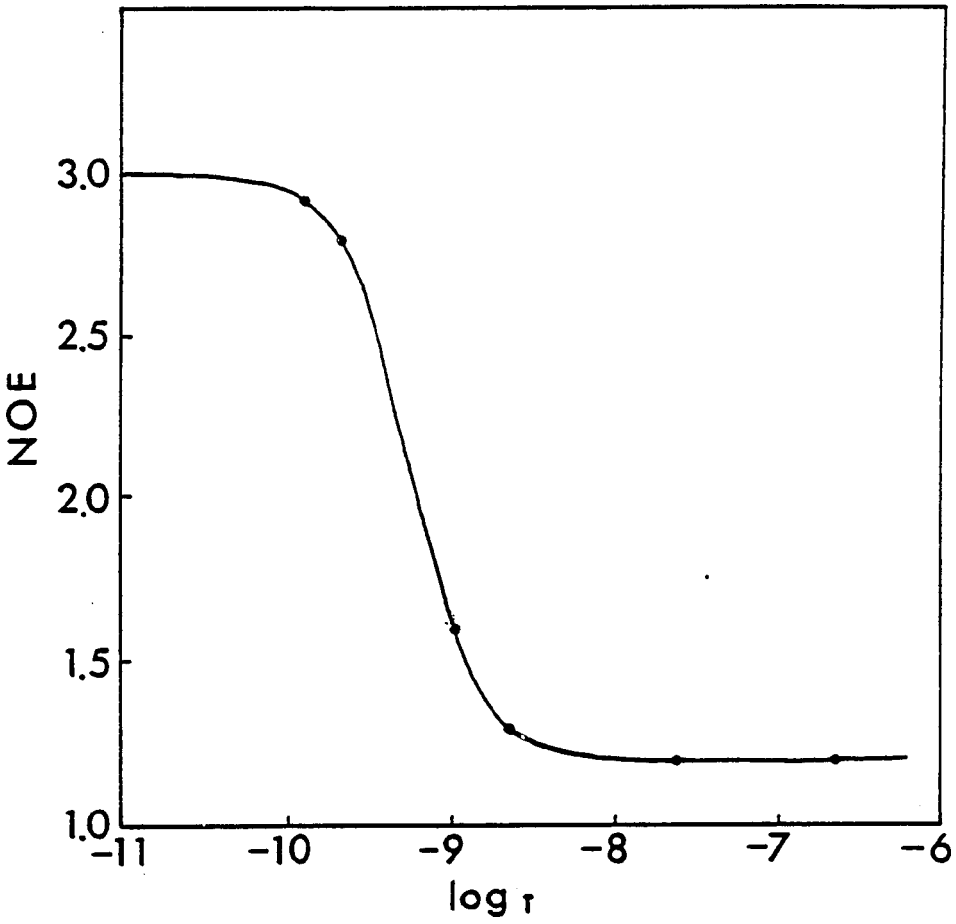
3.0
2.5
2.0
1.5
1.0
NOE
-11
-10
-9
-8
-7
-6
log τ

Figure 2: ^{13}C NMR spectra of PAA (MW = 4,500) for a 0.5 M solution in 10% D_2O at pH = 12, 25°C for 6000 acquisitions with a pulse angle of 62° and a repetition rate of 3.5 s: (a) with NOE (CC078.001) and (b) without NOE (CC078.002). NOE values: CO = 1.6 $\pm$ 0.1, CH = 2.4 $\pm$ 0.1 and CH_2 = 2.4 $\pm$ 0.1.

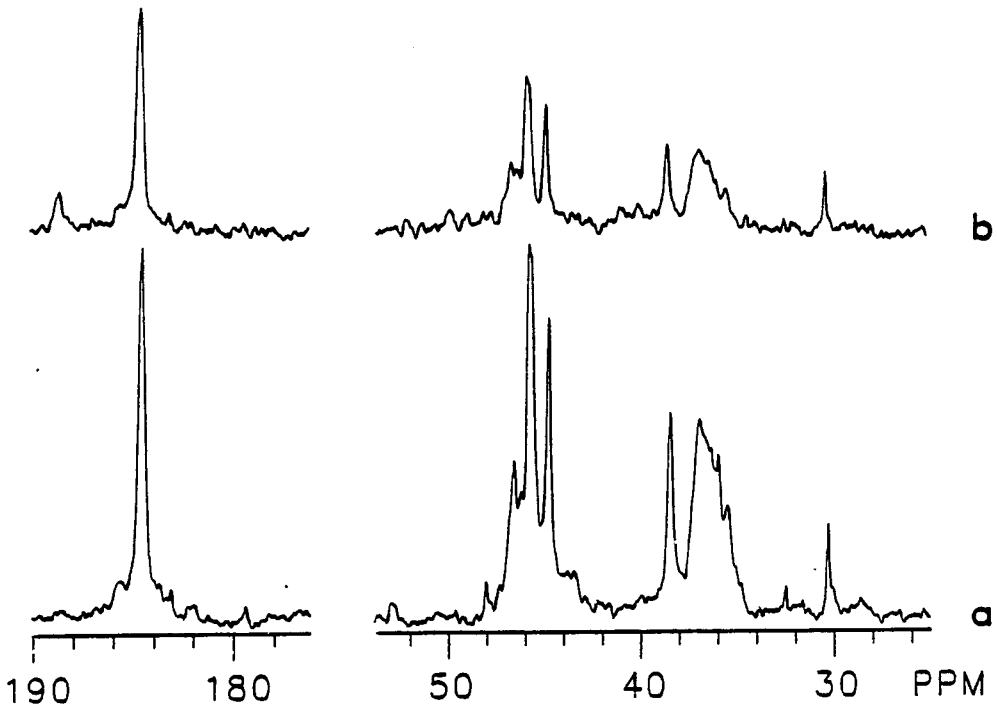
b
a
190
180
50
40
30
PPM

Figure 3: ^{13}C NMR spectra of PAA (MW = 15,000) for a 0.5 M solution in D_2O at pH = 12, 75°C for 6000 acquisitions with a pulse angle of 62° and a repetition rate of 3.5 s: (a) with NOE (CC090X.001) and (b) without NOE (C0090A.003). This information was used in the configuational study of PAA (Chapter I).

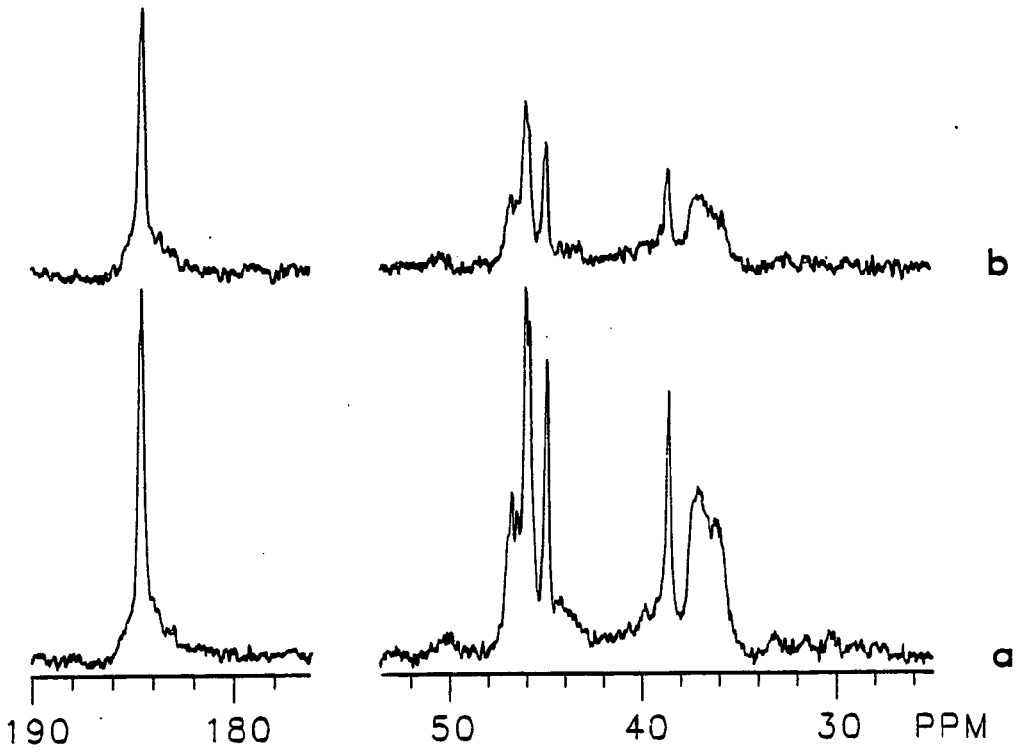
b
a
190
180
50
40
30
PPM

Figure 4: ^{13}C NMR spectra of PAA (MW = 15,000) for a 0.5 M solution in D_2O at pH = 2, 25°C for 2000 acquisitions with a pulse angle of 62° and a repetition rate of 1.5 s: (a) with NOE (CC097D.001) and (b) without NOE (CC097D.002). NOE values: CO = 1.1 $\pm$ 0.1, CH = 1.8 $\pm$ 0.1 and CH_2 = 1.8 $\pm$ 0.1.

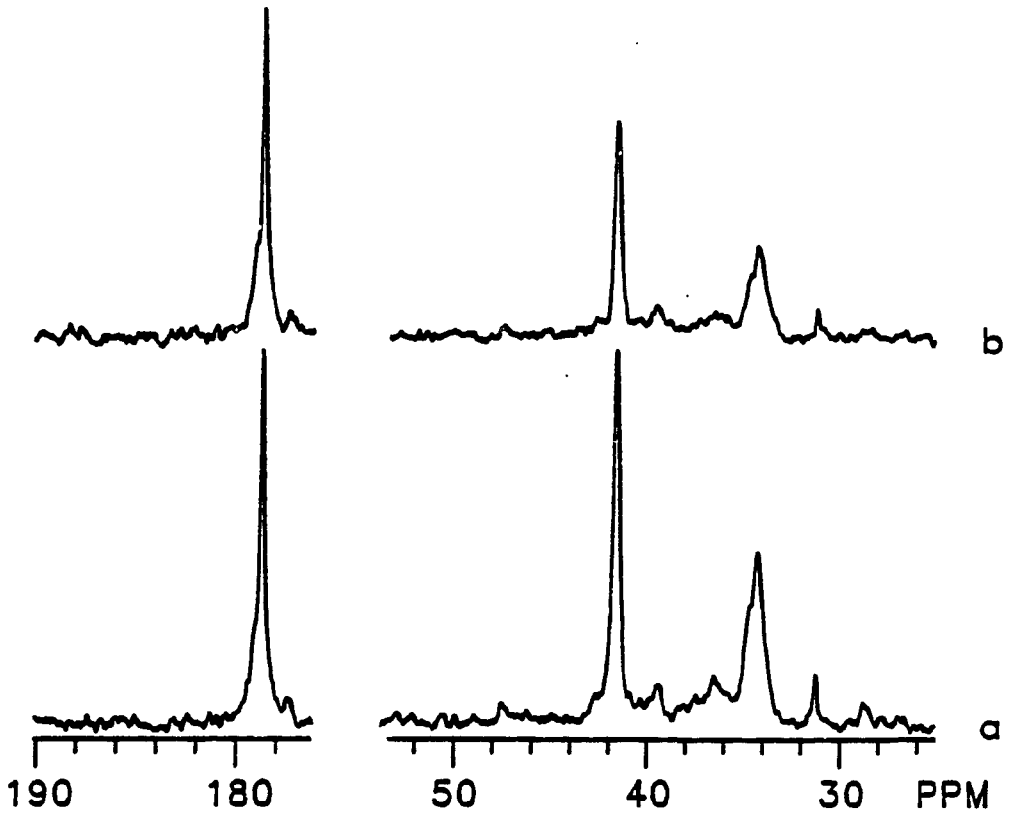
b
a
190
180
50
40
30
PPM

Figure 5: ^{13}C NMR spectra of SP12 for a 0.5 M solution in D_2O at pH = 2, 25° for 7424 acquisitions with a pulse angles of 62° and a repetition rate of 5.5 s: (a) with NOE (CCA014.003) and (b) without NOE (CCA014.004). These data were used in the sequence distribution study of SP12 (Chapter V).

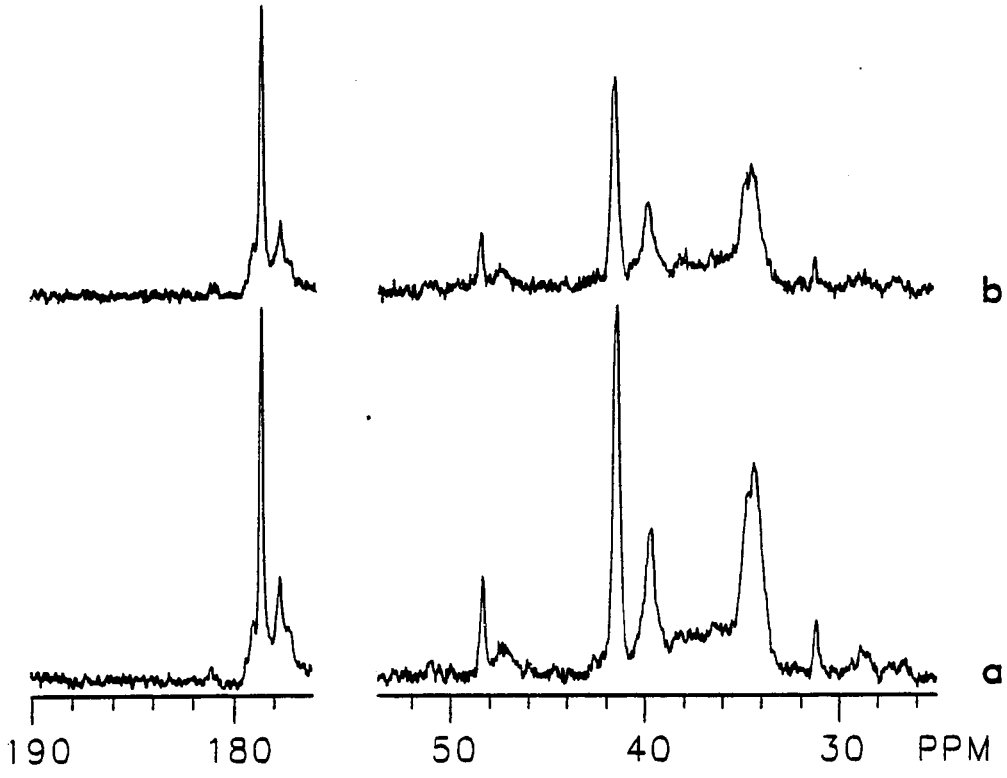
b
a
190
180
50
40
30
PPM

Figure 6: ^{13}C NMR spectra of SP30 for a 0.5 M solution in D_2O at pH = 2. 25°C for 14852 acquisitions with a pulse angle of 62° a repetition rate of 5.5 s: (a) with NOE (CCA020.001) and (b) without NOE (CCA020.002). These data were used in the sequence distribution study of SP30 (Chapter V).

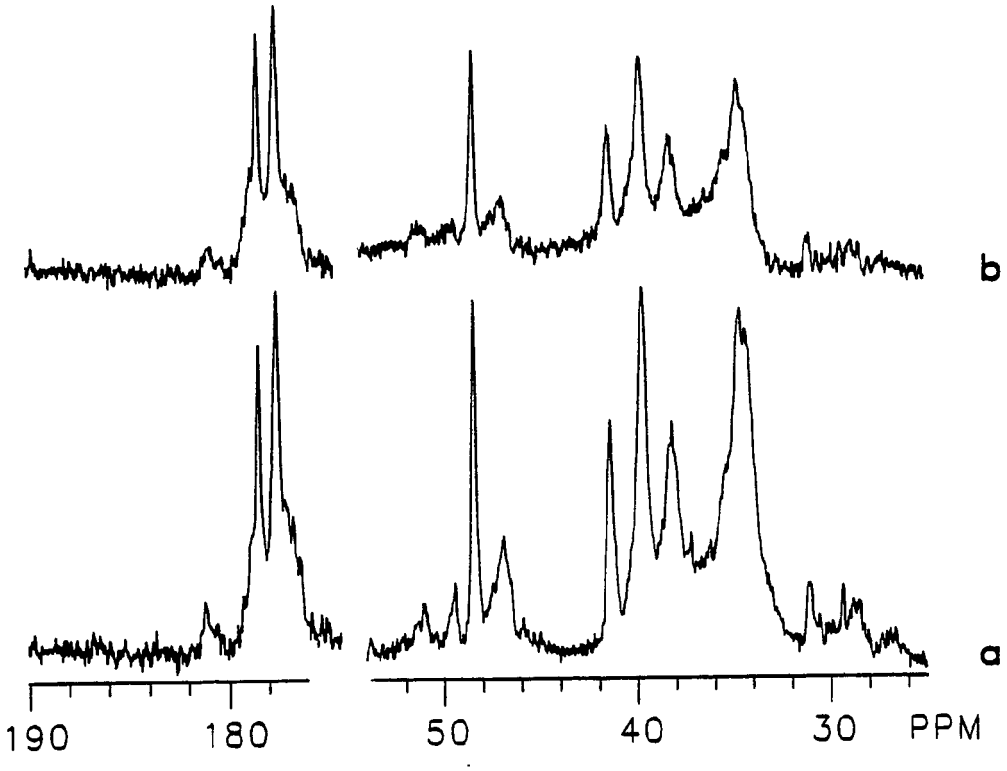
b
a
190
180
50
40
30
PPM

Figure 7: ^{13}C NMR spectra of SP52 for a 0.5 M solution in D_2O at pH = 2, 25°C for 16800 acquisitions with a pulse angle of 62° and a repetition rate of 5.5 s: (a) with NOE (CCA021.001) and (b) without NOE (CCA021.002). These data were used in the sequence distribution study of SP52 (Chapter V).

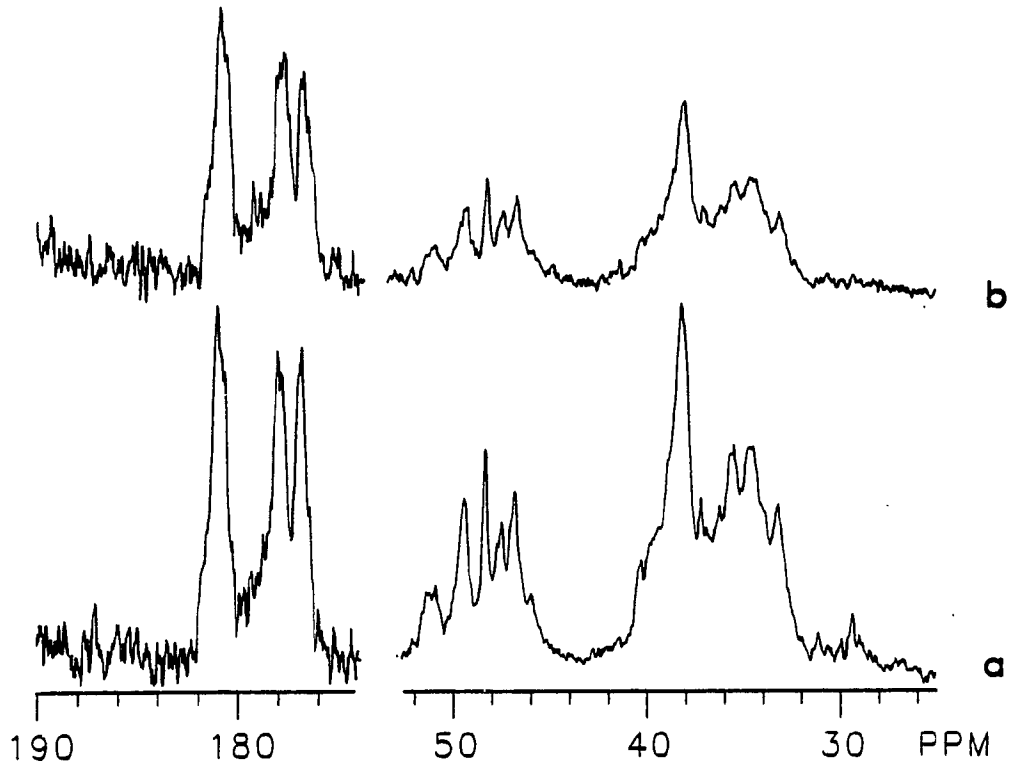
b
a
190
180
50
40
30
PPM

Figure 8: ^{13}C NMR spectra of PVAm for a 0.5 M solution in 10% D_2O at pH = 2, 25°C for 2000 acquisitions with a pulse angle of 62° and a repetition rate of 2.5 s: (a) with NOE (CCA03A.002) and (b) without NOE (CCA03.001). NOE values: CH = 1.7 $\pm$ 0.1, CH_2 = 2.0 $\pm$ 0.1.

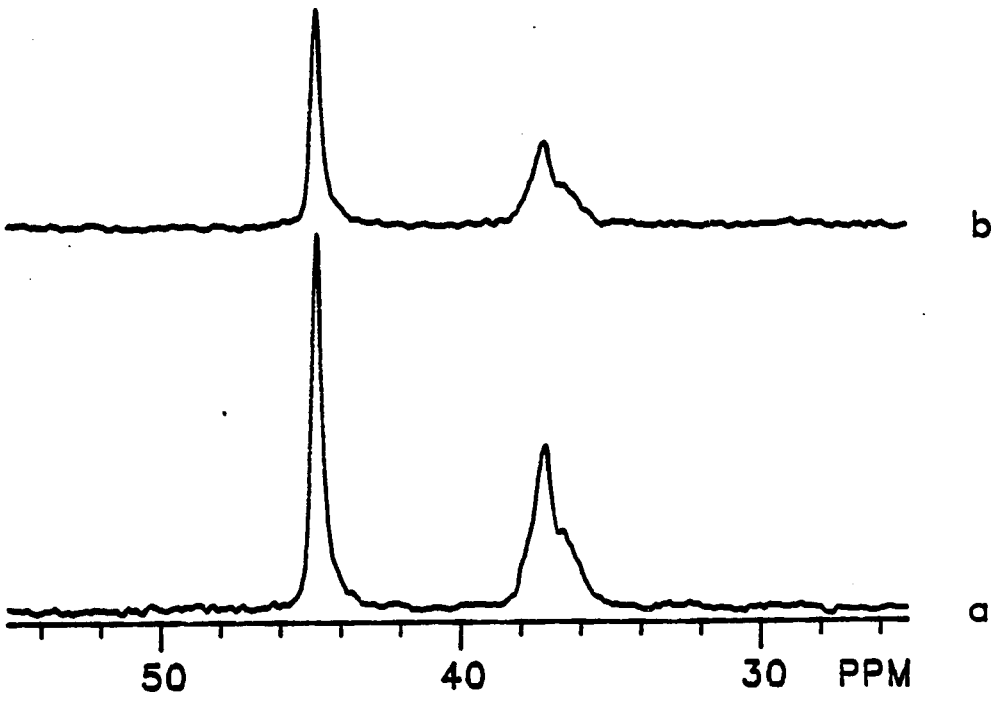
b
a
50
40
30
PPM

Figure 9: ^{13}C NMR spectra of PVAm for a 0.5 M in D_2O at pH = 7, 25°C for 12000 acquisitions with a pulse angle of 62° and a repetition rate of 2.5 s: (a) with NOE (CC095A.001) and (b) without NOE (CC095A.002). NOE values: CH = 1.9 $\pm$ 0.1 CH_2 = 2.0 $\pm$ 0.1

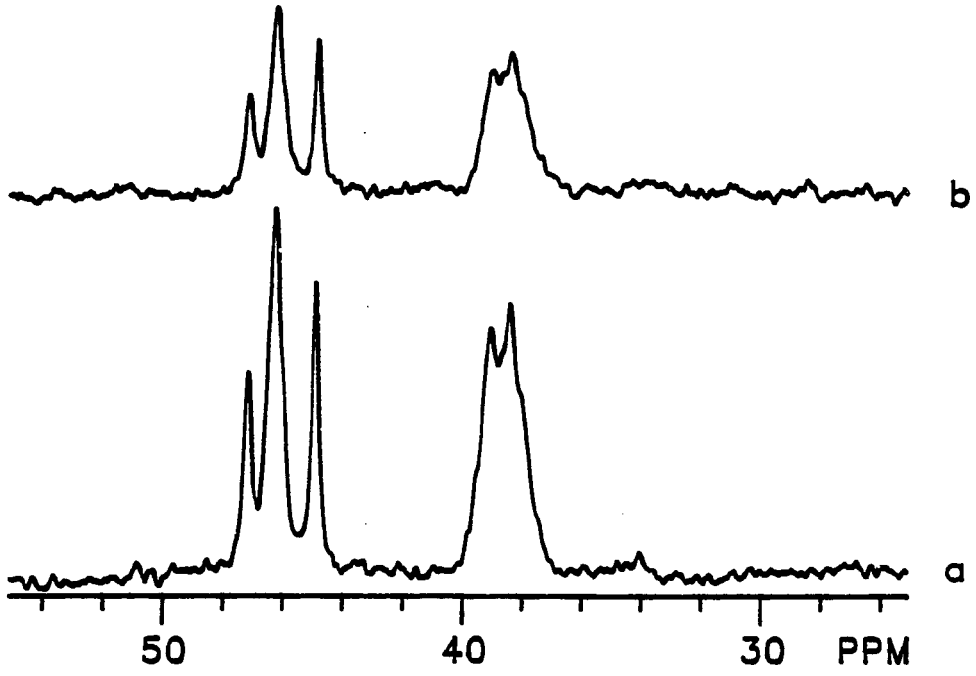
b
a
50
40
30
PPM

Figure 10: ^{13}C NMR spectra of PVAm for a 0.5 M solution in 10% D_2O at pH = 7, 25°C for 6000 acquisitions with a pulse angle of 62° and a repetition rate of 2 s: (a) with NOE (CC098A.001) and (b) without NOE (CC098E.001). NOE values: CH = 2.3 $\pm$ 0.1 CH_2 = 2.1 $\pm$ 0.1.

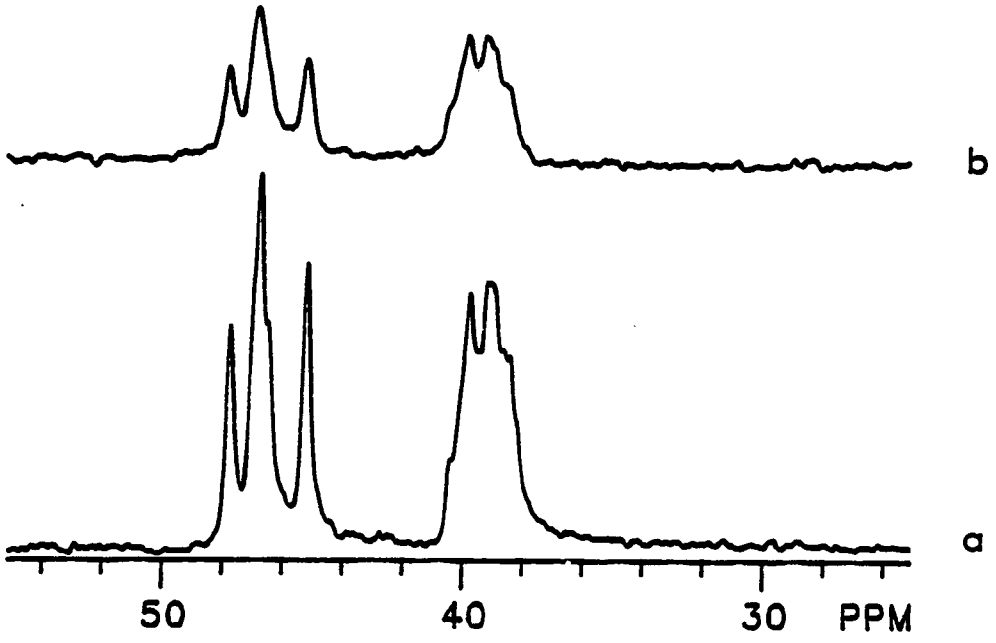
b
a
50
40
30
PPM

Figure 11: ^{13}C NMR spectra of PVAm for a 0.5 M solution in 10% D_2O at pH = 8.56, 25°C for 6900 acquisitions with a pulse angle of 62° and a repetition rate of 3.0 s: (a) with NOE (CCA010.001) and (b) without (CCA010.001). NOE values: CH = 2.2 $\pm$ 0.1 and CH_2 = 2.1 $\pm$ 0.1.

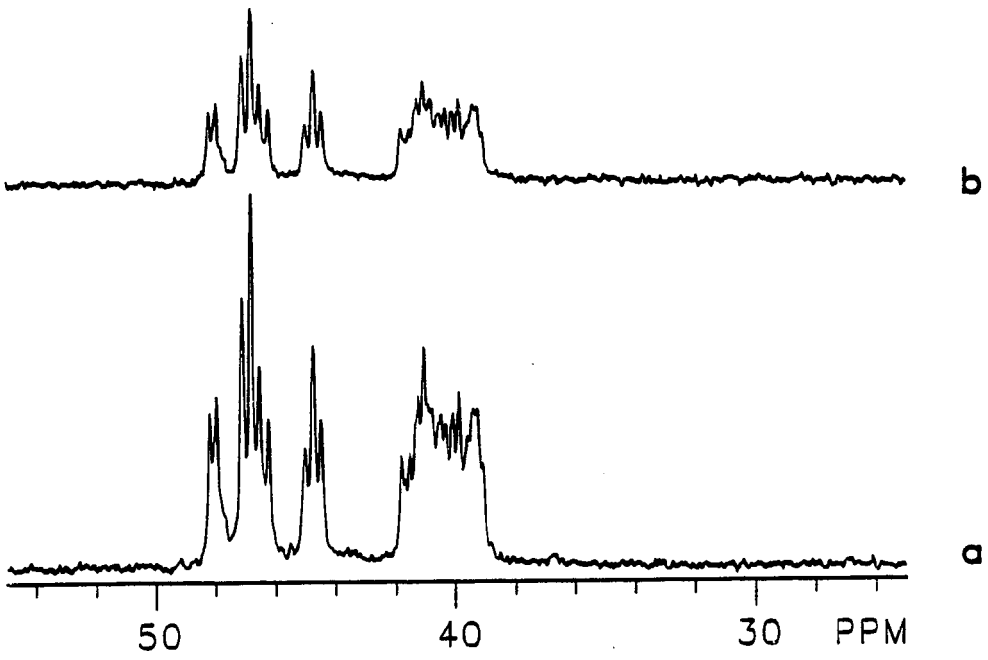
b
a
50
40
30
PPM

Figure 12: ^{13}C NMR spectra of PVAm for a 0.5 solution in 10% D_2O at pH = 8.68, 25°C for 6900 acquisitions with a pulse angle of 62° and a repetition rate of 1.5 s: (a) with NOE (CC098A.001) and (b) without NOE (CC098F.012). NOE values: CH = 2.3 $\pm$ 0.1 and CH_2 = 2.0 $\pm$ 0.1.

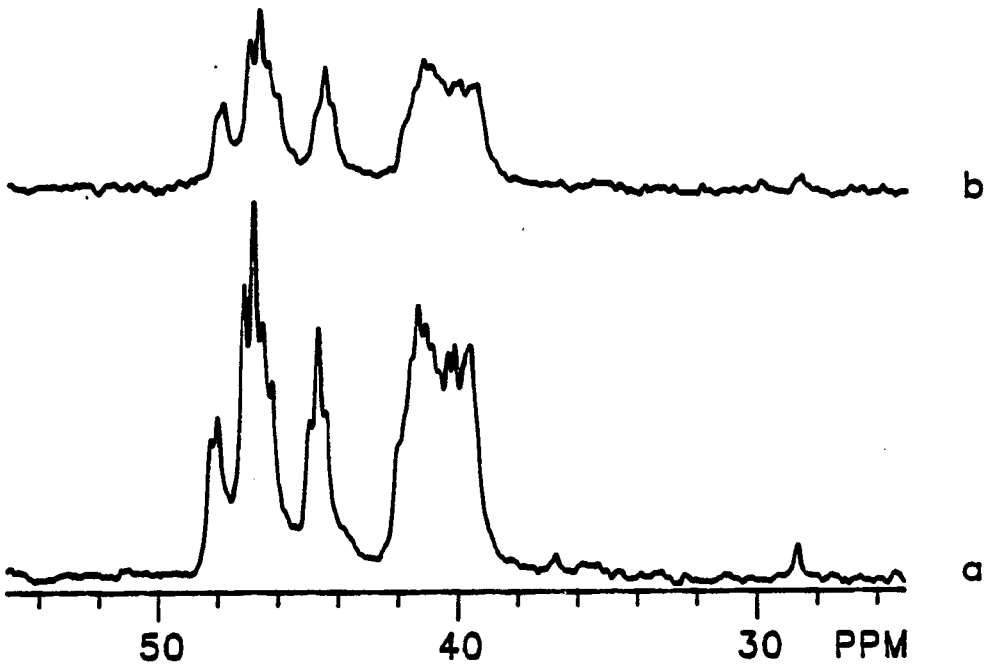
b
a
50
40
30
PPM

Figure 13: ^{15}N NMR spectra of PVAm for a 1 M solution in 10% D_2O at pH = 10.45 for 10000 acquisitons with a pulse angle of 75^2 and a repetition rate of 10.5 s: (a) with NOE (CC034C.001) and (b) without NOE (CC034C.002). These data were used in the configurational study of PVAm (Chapter 3).

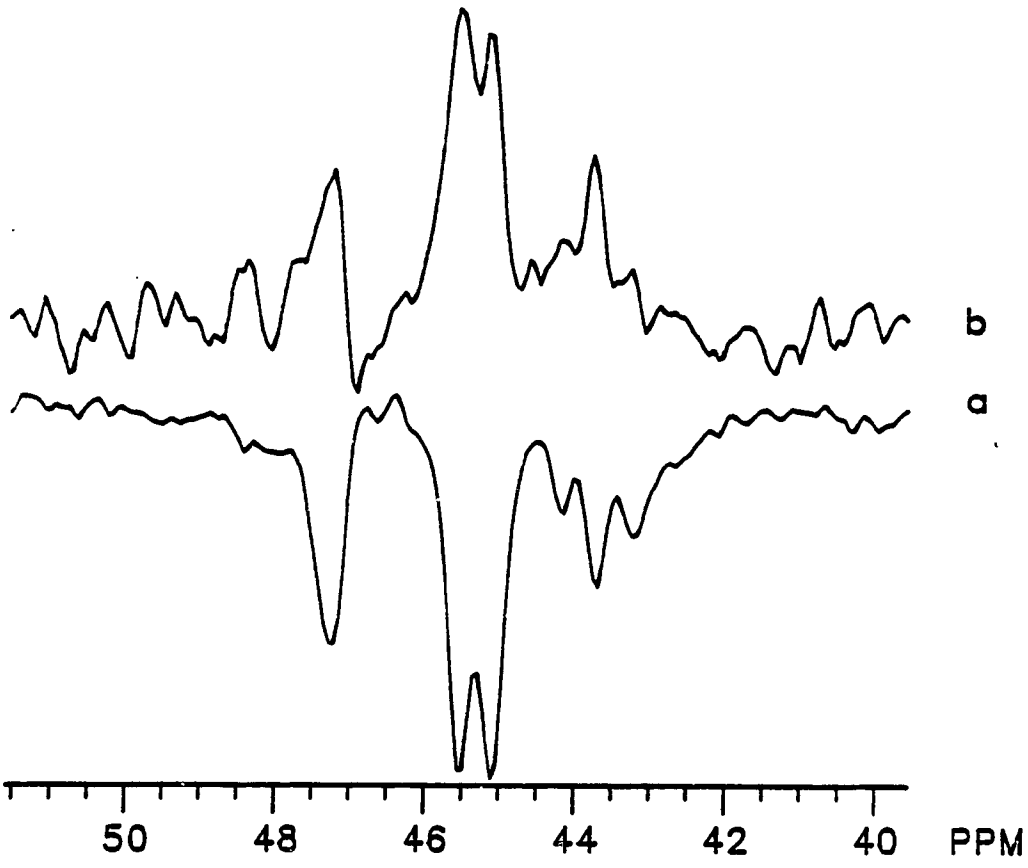
b
a
50
48
46
44
42
40
PPM

Appendix F

^{13}C and ^{15}N NMR spin lattic relaxation time (T_1) Study: T_1 was determined by the inversion-recovery method and was calculated by using a nonlinear three-parameter fitting procedure. This study was used to provide an essential parameter (delay time) for setting up quantitative NMR experiments. The results indicate that the T_1 values are independent of tacticity. Since the T_1 dominate mechanism is expected to be dipole-dipole relaxation of the directly attached protons, the T_1 value of the methine carbon is almost two times the T_1 value of the methylene carbon.

Figure 1: T_1 and T_2 as a function of correlation time for 75 MHz ^{13}C magnetic field strength. Isotropic rotation is assumed.

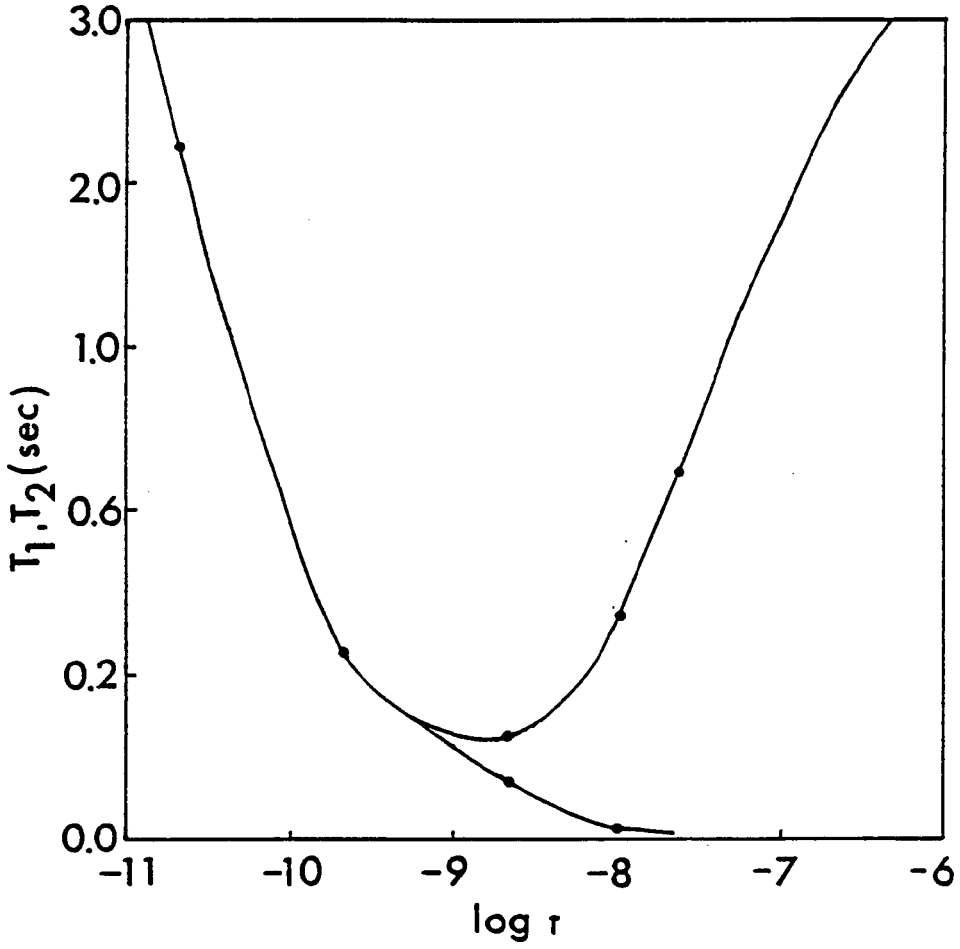
3.0
2.0
1.0
0.6
0.2
0.0
T_1, T_2 (sec)
-11
-10
-9
-8
-7
-6
log τ

Figure 2: T_1 measurements of PAA (MW = 1,000) for a 0.5 M solution in D_2O at pH = 12, 30°C for about 2200 acquisitions with a repetition rate of 3.5s and with delay values of (a) 0.01, (b) 0.03, (c) 0.2, (d) 0.6 and (e) 1.0 s, (CC07313.001-.006).

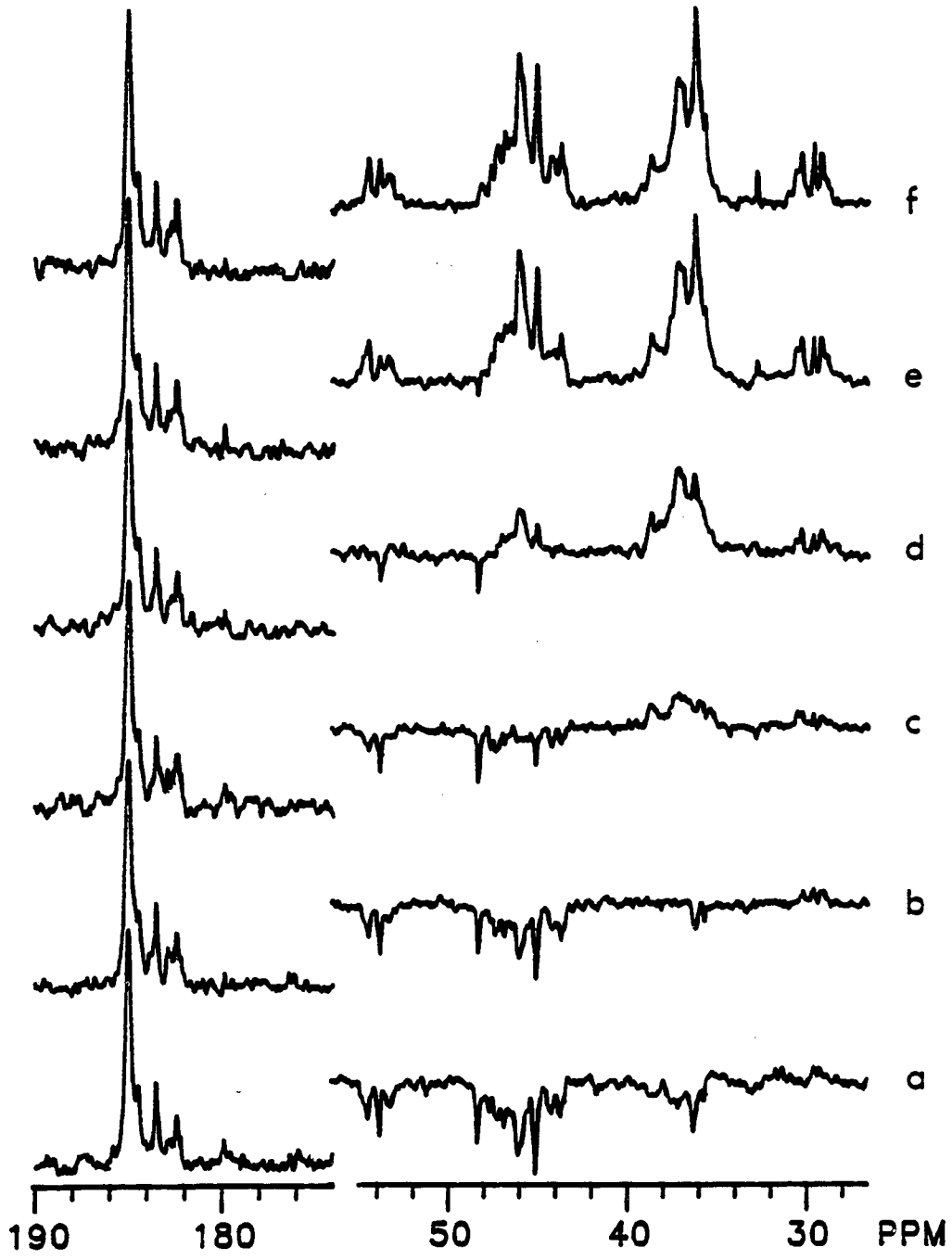
f
e
d
c
b
a
190
180
50
40
30
PPM

Figure 3: T_1 measurements of PAA (MW = 15,000) for a 0.5 M solution in D_2O at pH = 12, 75°C for about 2400 acquisitions with a repetition rate of 3.5 s and with delay values of (a) 0.025, (b) 0.08, (c) 0.2, (d) 1.0 and (e) 3.0s, (CC090C.001-.006).

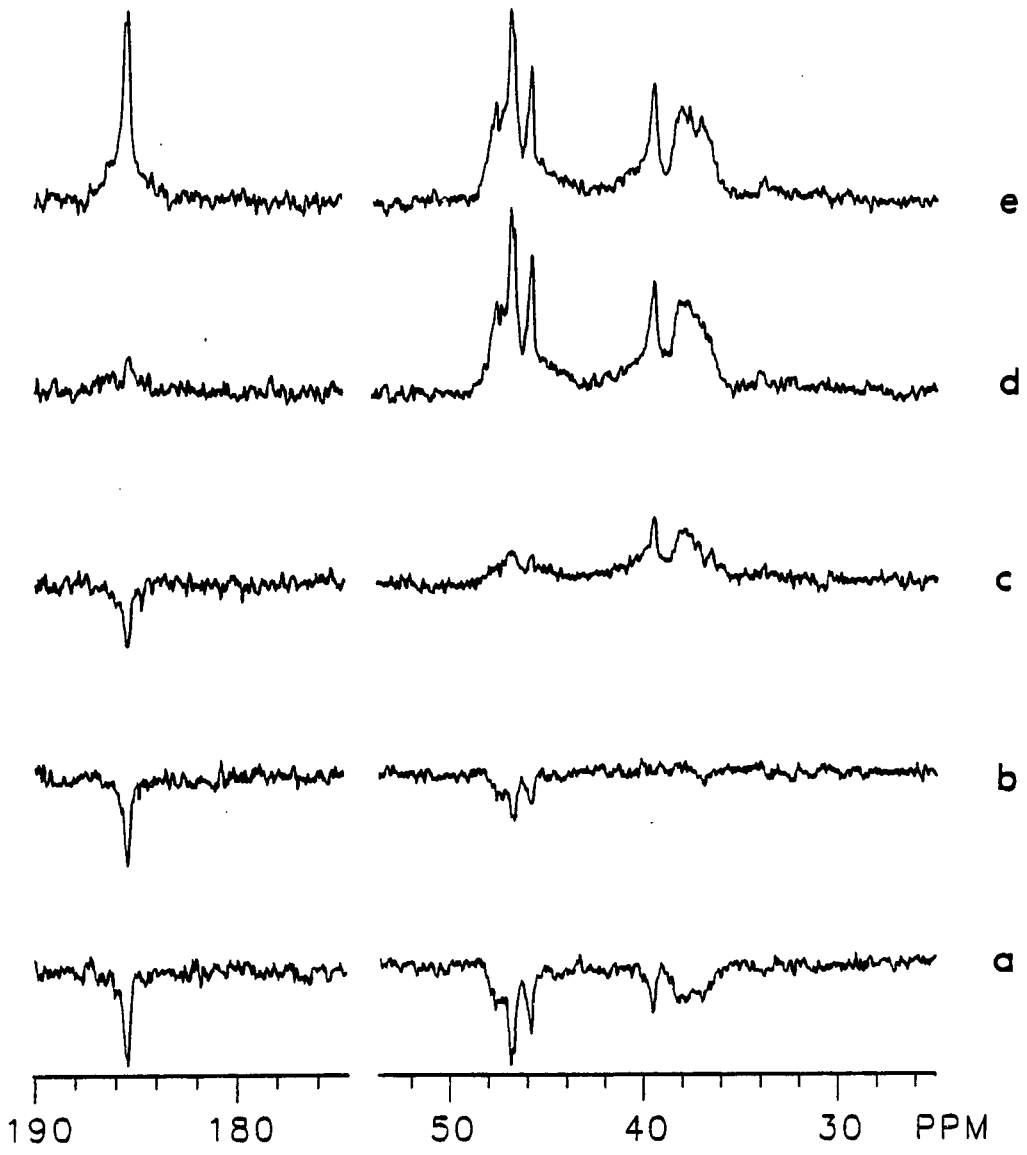
e
d
c
b
a
190
180
50
40
30
PPM

Figure 4: T_1 measurements of PAA (MW = 15,000) for a 0.5 M solution in 10% D_2O at pH = 2, 25°C for 2000 acquisitions with a repetition rate of 3.5 s and with delay values of (a) 0.01, (b) 0.07, (c) 0.2, (d) 0.9, (e) 2 and (f) 4 s, (CC097A.002-.007).

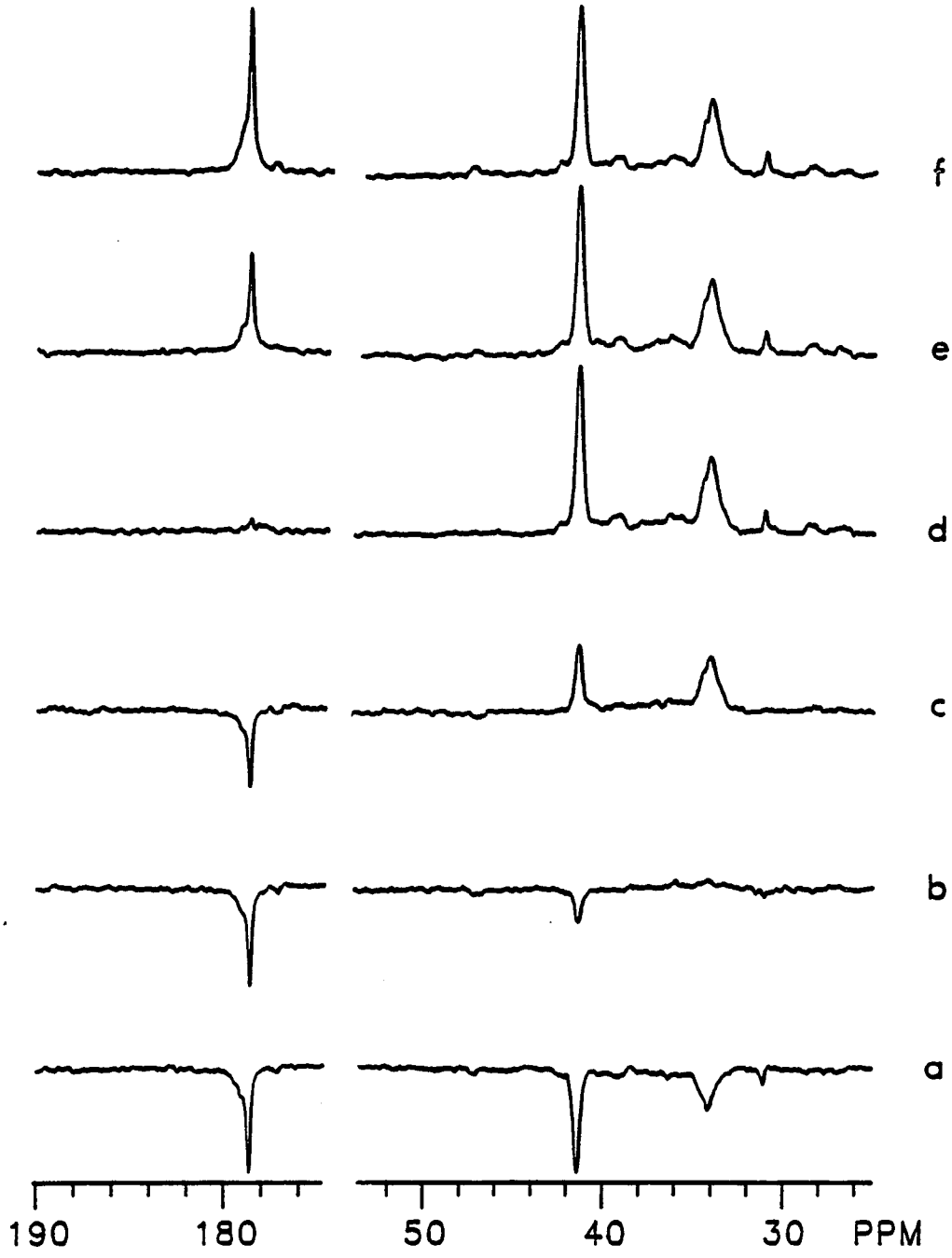
f
e
d
c
b
a
190
180
50
40
30
PPM

Figure 5: T_1 measurements of SP12 for a 0.5 M solution in D_2O at pH = 2, 25°C for 3200 acquisitions with a repetition rate of 3.5 s and with delay values of (a) 0.01, (b) 0.07, (c) 0.14, (d) 0.7, (e) 2.1 and (f) 4.2 s (CCB014.001-.006).

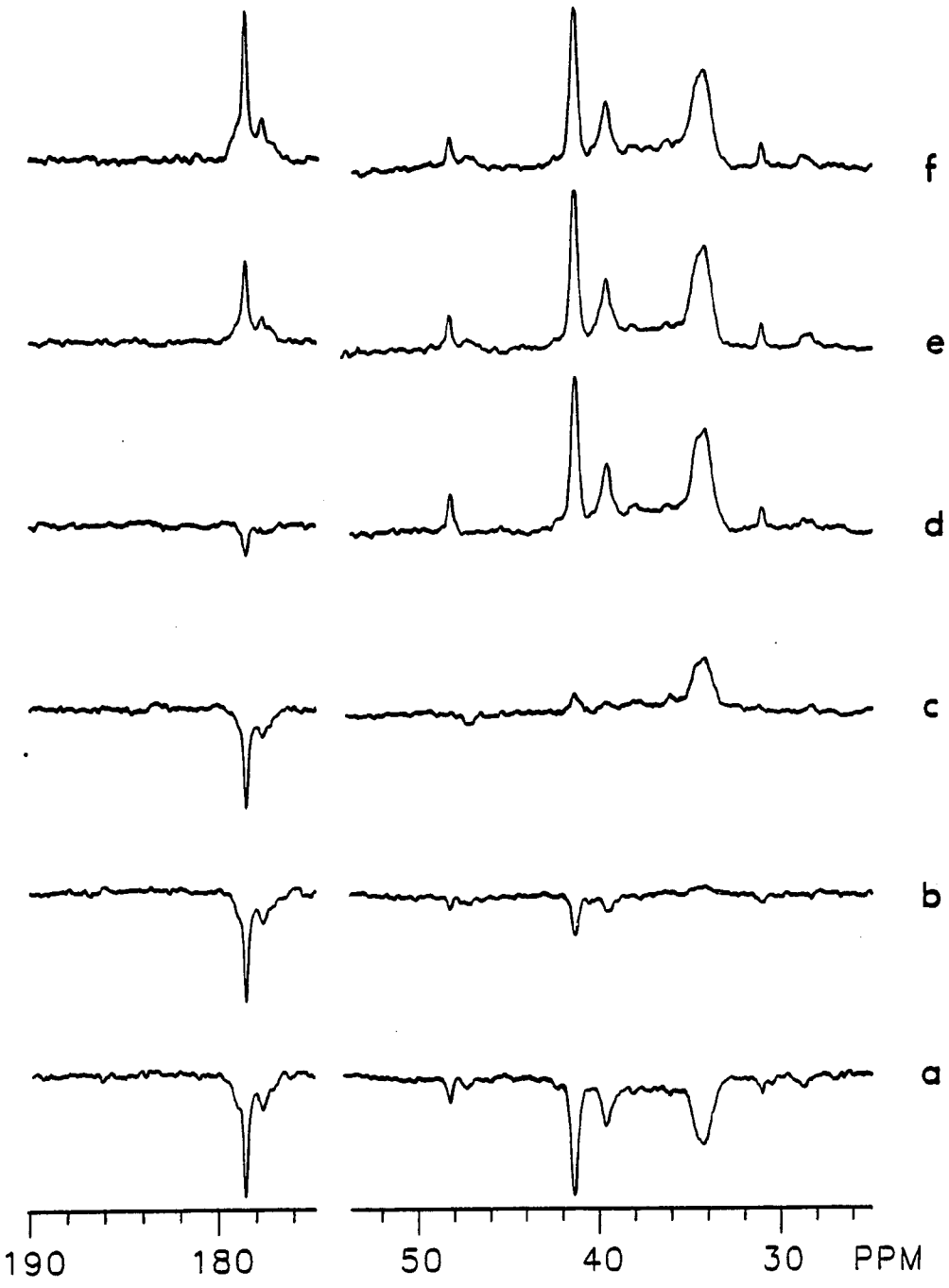
f
e
d
c
b
a
190
180
50
40
30
PPM

Figure 6: T_1 measurements of SP30 for a 0.5 M solution in D_2O at pH = 2. 25°C for 5800 acquisitions with a repetition rate of 3.5 s and with delay values of (a) 0.01, (b) 0.07, (c) 0.14, (d) 0.7, (e) 2.1 and (f) 4.2 s, (CCB020.001-.006).

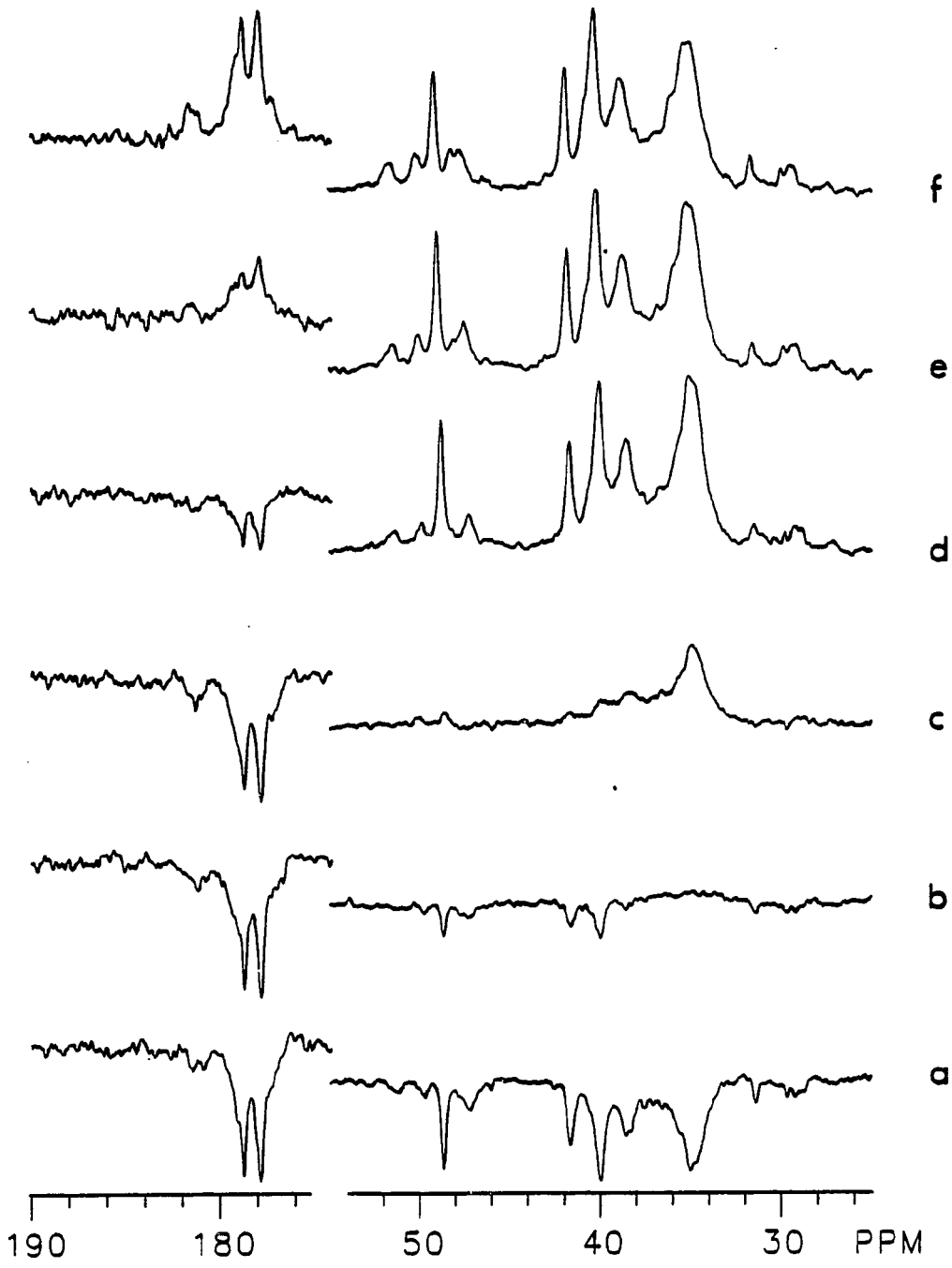
f
e
d
c
b
a
190
180
50
40
30
PPM

Figure 7: T_1 measurements of SP52 for a 0.5 M solution in D_2O at pH = 2, 25°C for 6800 acquisitions with a repetition rate of 3.5 s and with delay values of (a) 0.01, (b) 0.07, (c) 0.14, (b) 0.7, (e) 2.1 and (f) 4.2 s, (CCB021.001-.006).

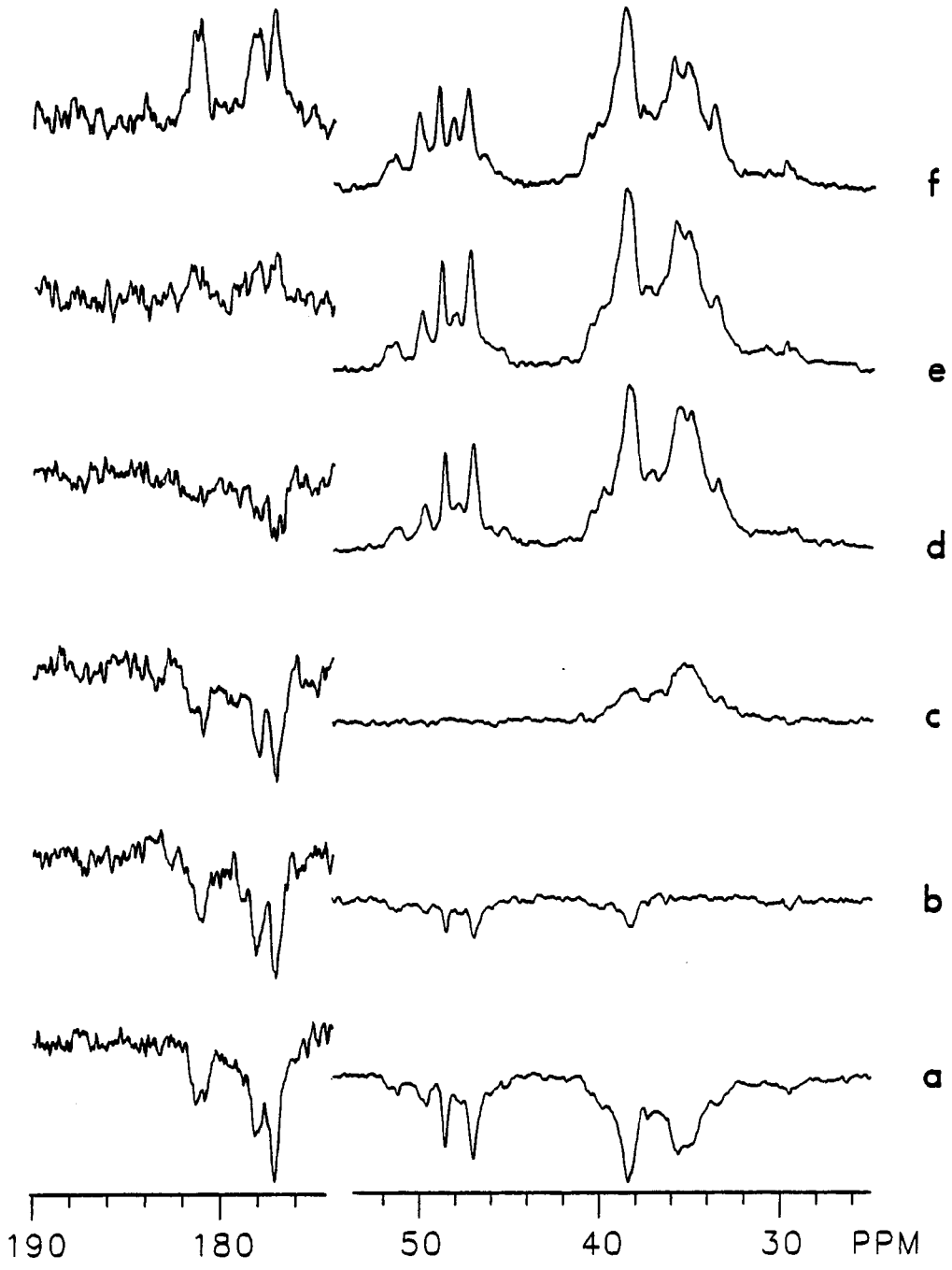
f
e
d
c
b
a
190
180
50
40
30
PPM

Figure 8: T_1 measurements of PVAm for a 0.5 M solution in 10% D_2O at pH = 2, 25°C for 2000 acquisitions with a repetition rate of 1.7 s and with delay values of (a) 0.01, (b) 0.05, (c) 0.1, (d) 0.3, (e) 0.9 and (f) 2.0 s, (CC098B.001-.006).

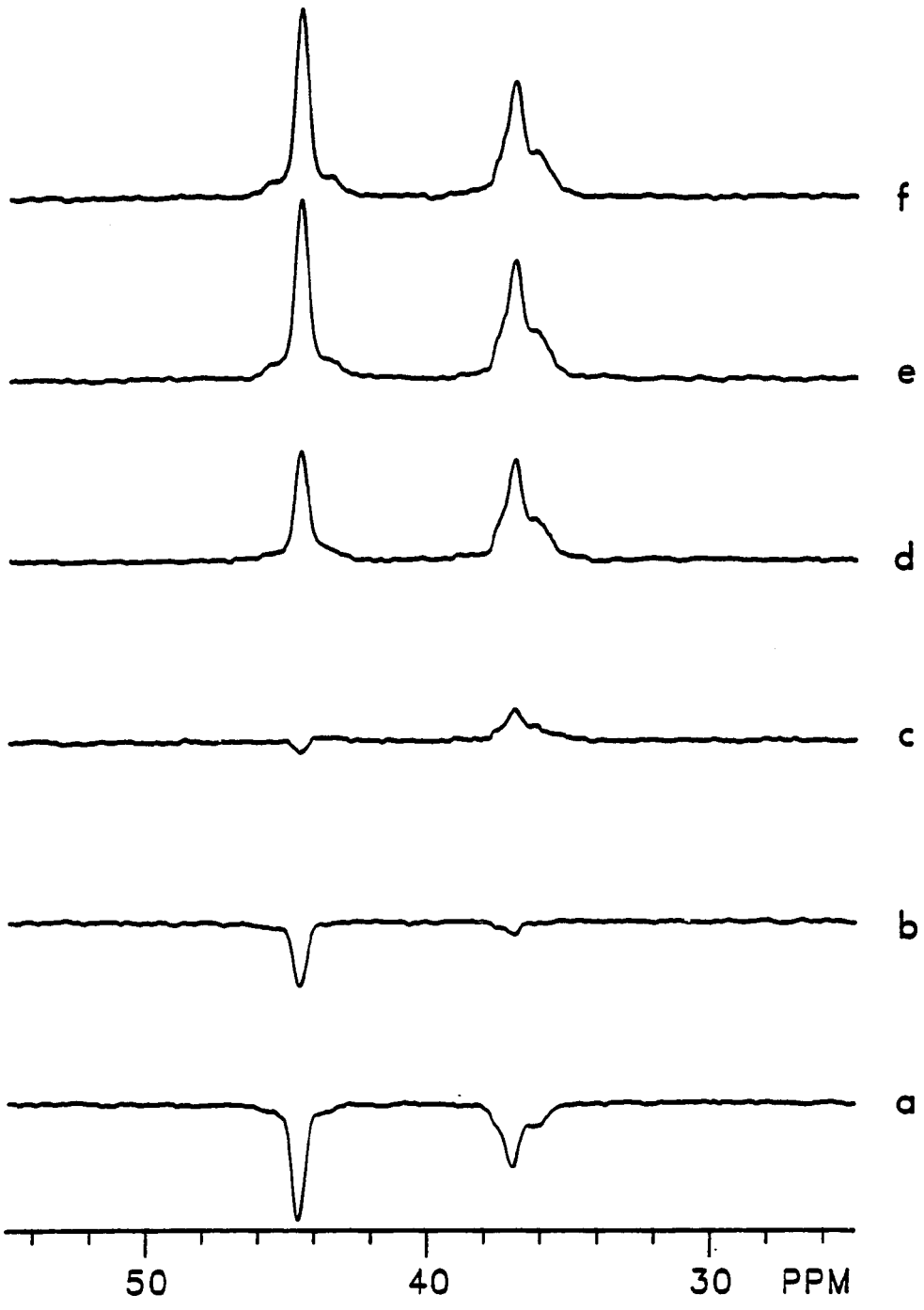
f
e
d
c
b
a
50
40
30
PPM

Figure 9: T_1 measurements of PVAm for a 0.5 M solution in 10% D_2O at pH = 2, 25°C for 2400 acquisitions with a repetition rate of 1.5 s and with delay values of (a) 0.01, (b) 0.05, (c) 0.1, (d) 0.2, (e) 0.5 and (f) 1.0 s, (CC098D.001-.006).

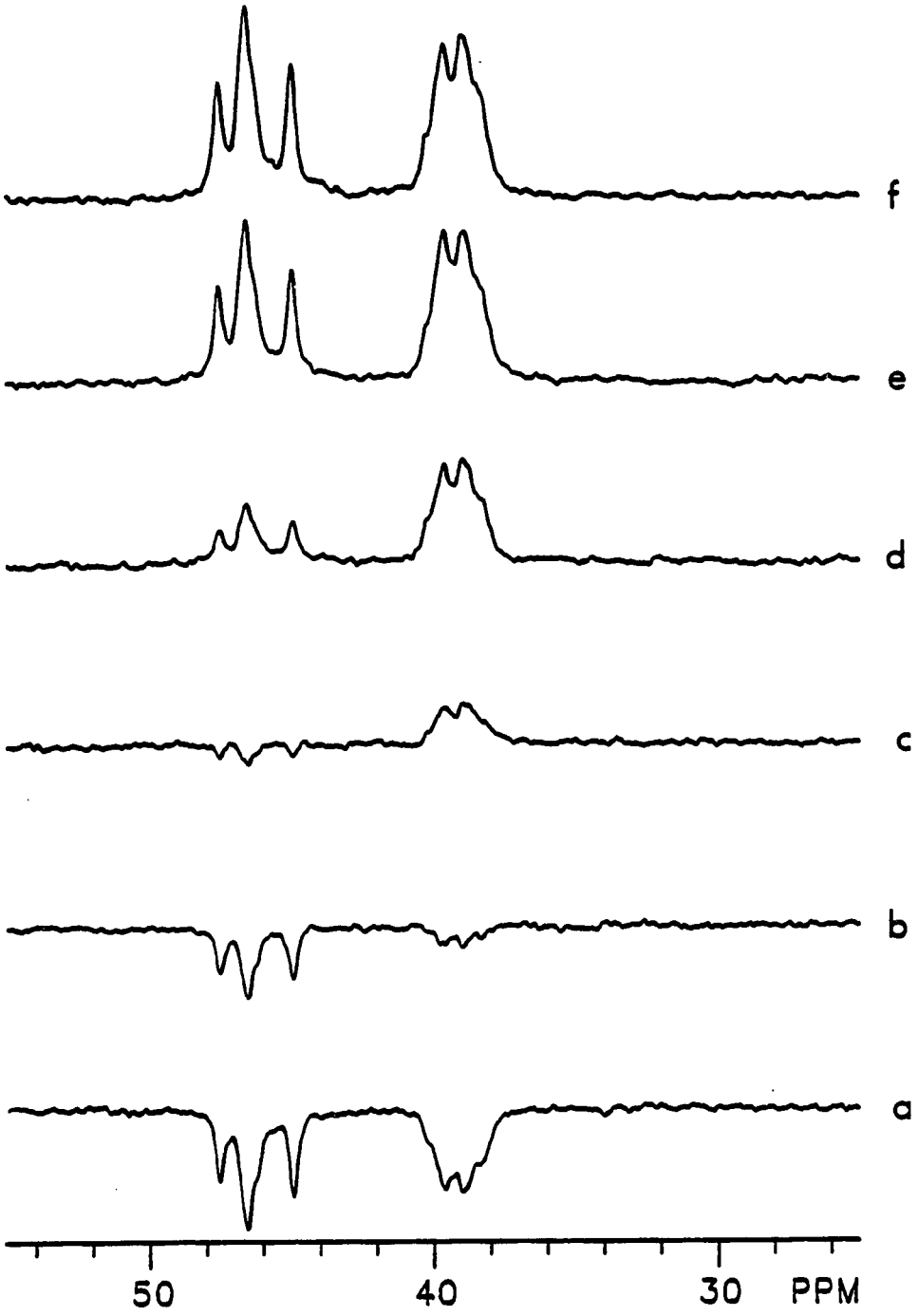
f
e
d
c
b
a
50
40
30
PPM

Figure 10: T_1 measuremnts of PVAm for a 0.5 M solution in 10% D_2O at pH = 2, 25°C for 2800 acquisitions wih a repetition rate of 1.5 s and with delay values of (a) 0.01, (b) 0.05, (c) 0.1, (d) 0.2, (e) 0.5 and (f) 1.4 s, (CC098G.001-.006).

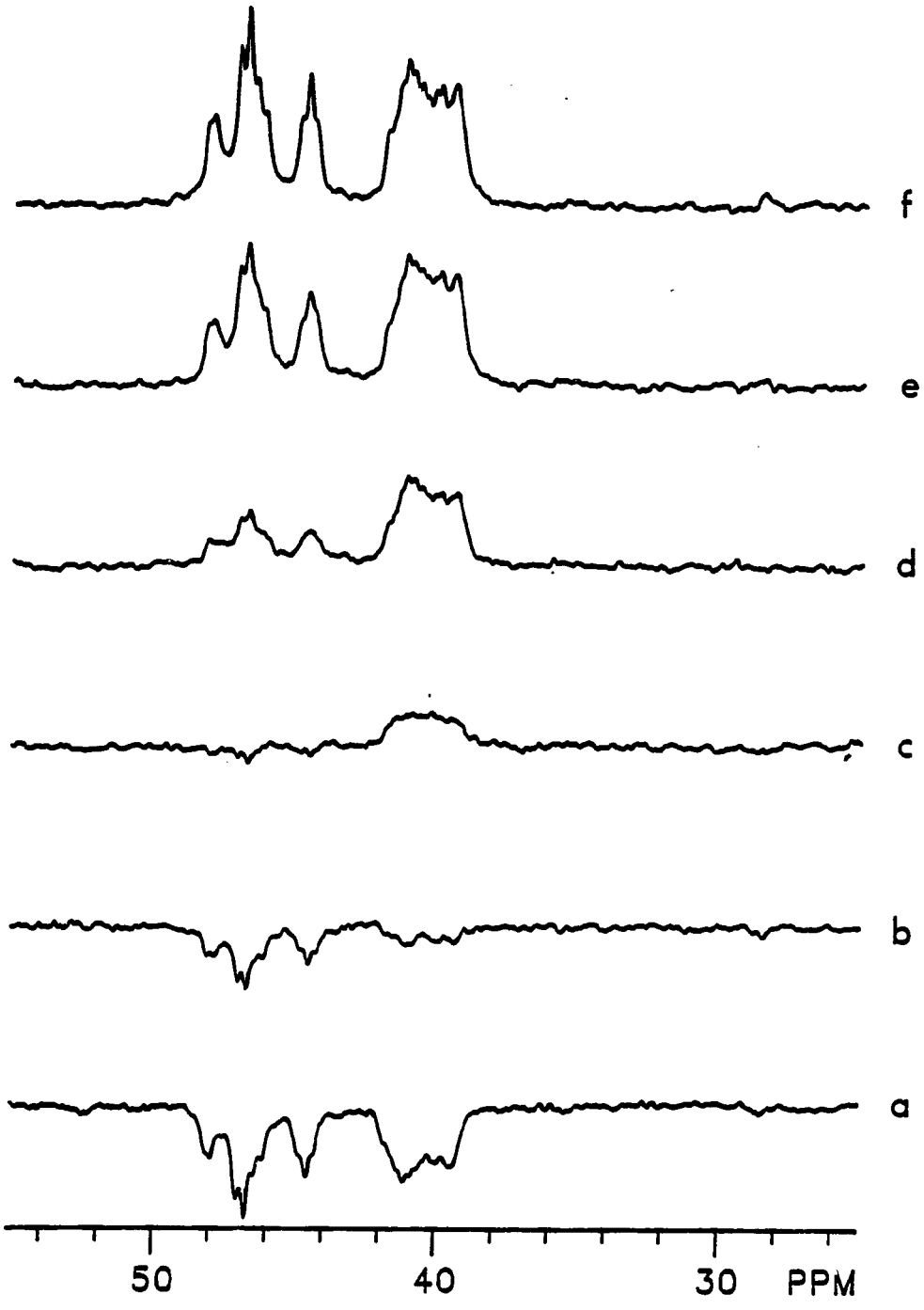
f
e
d
c
b
a
50
40
30
PPM

Figure 11: ^{15}N NMR T_1 measurements of PVAm for a 1.0 M soulution in 10% D_2O at pH = 10.5, 25°C for 6400 acquisitions with a repetition rate of 7.5 s and with delay values of (a) 0.01, (b) 0.2, (c) 0.7, (d) 2.0 and (e) 5.6 s, (CC034B.001-.005).

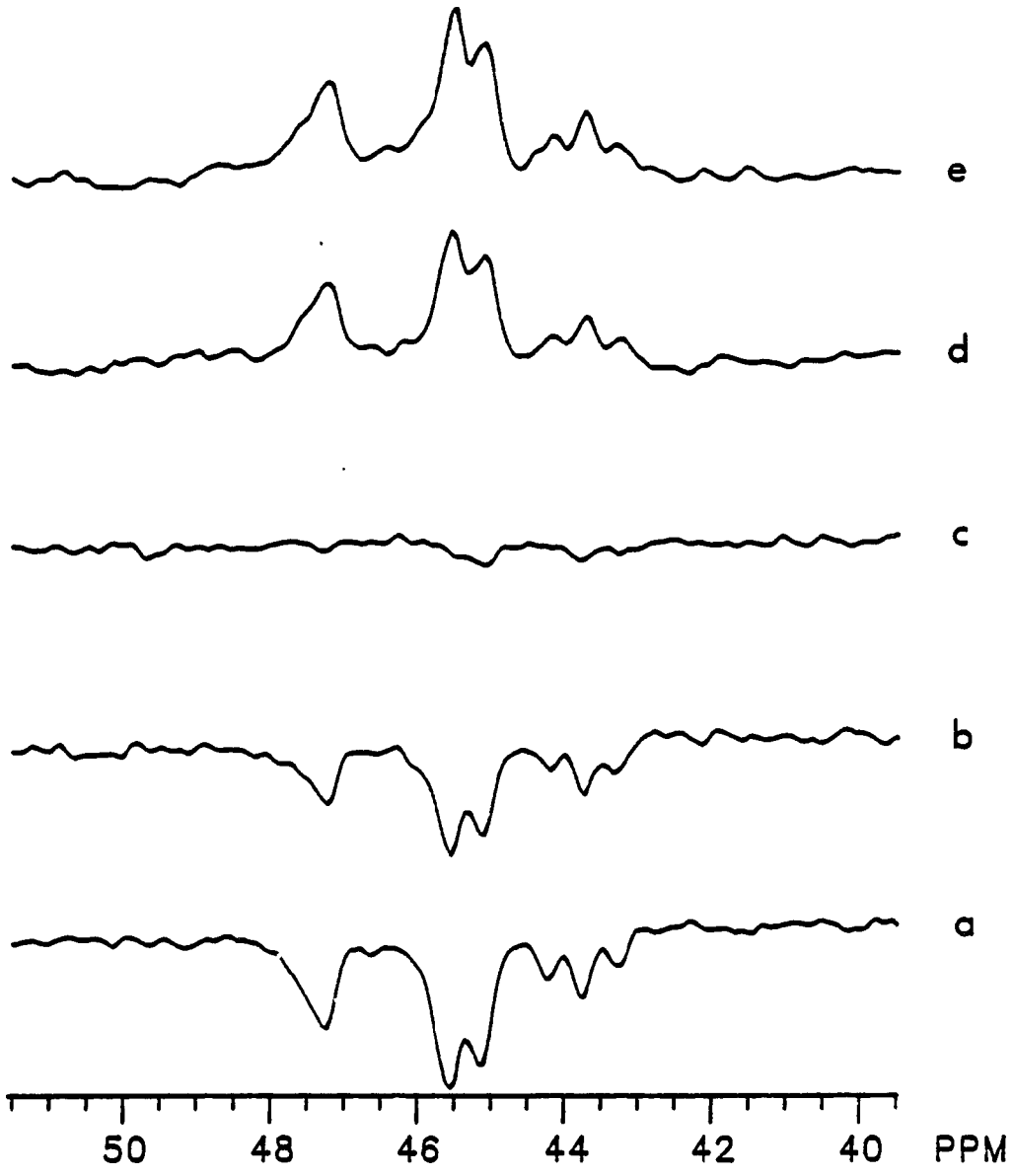
e
d
c
b
a
50
48
46
44
42
40
PPM

Appendix G

^{13}C NMR pH titration study of model compounds, m and r (DAP): In order to explore the acid-base behavior of polymers, the titration behavior of model compounds were examined. The detailed description of the titration of the model compounds is found in the Chapter IV.

Figure 1: Spectra of m DAP for 0.5 M solutions in 10% D_2O at 25°C for 100 acquisitions with a pulse angle of 62°C and a repetition rate of 3.5 s and with pH values of (a) 2.0, (b) 8.1, (c) 9.0 (d) 10.1 (e) 11.0 (f) 11.7, (g) 12.5 and (h) 13.1, (CCA08A.001-.012).

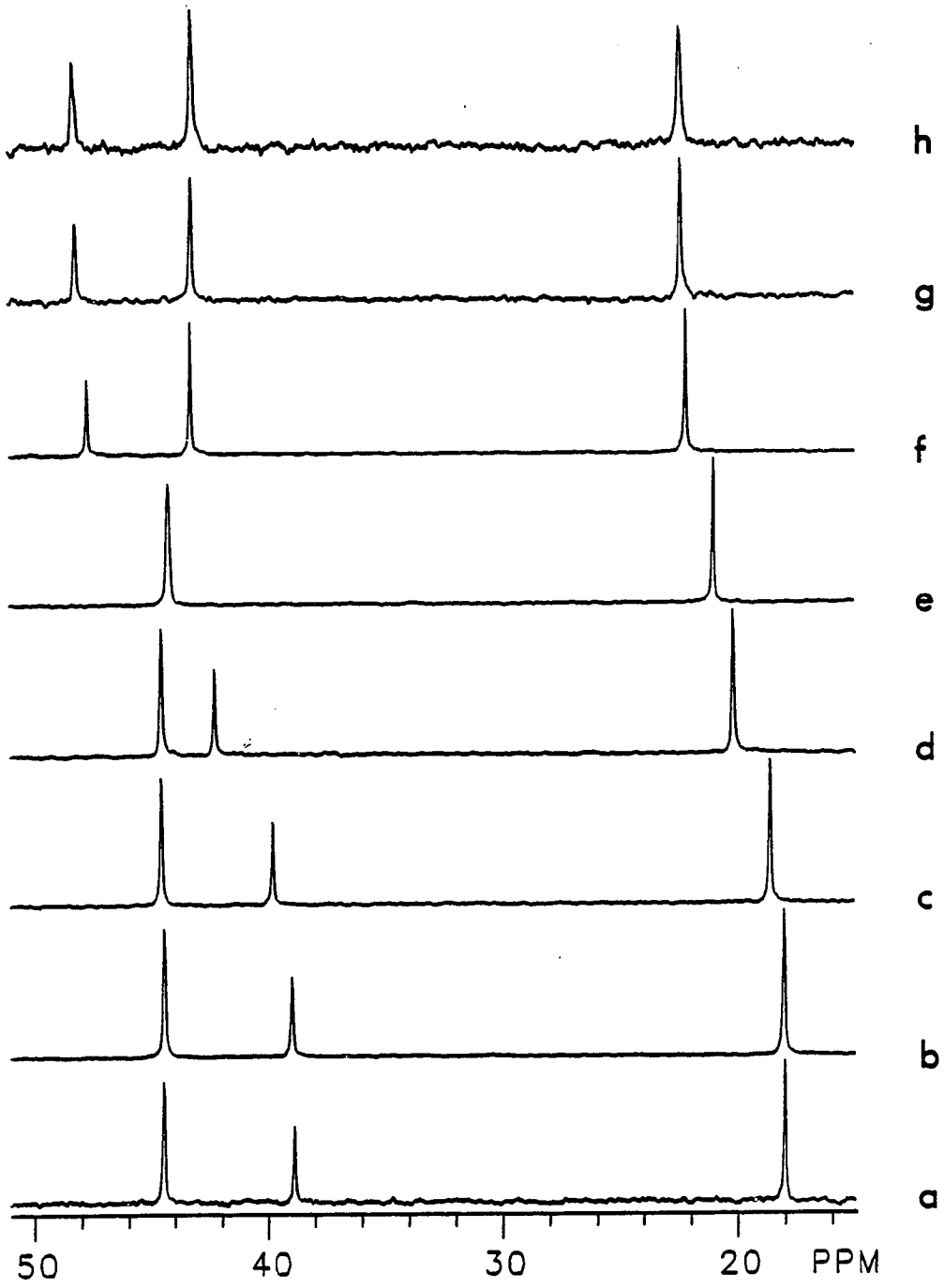
h
g
f
e
d
c
b
a
50
40
30
20
PPM

Figure 2: Spectra of r DAP for 0.5 M solutions in 10% D_2O at 25°C for 100 acquisitions with a pulse angle of 62°C and a repetition rate of 3.5 s and with pH values of (a) 2.0, (b) 8.1, (c) 9.0, (d) 10.1, (e) 11.0, (f) 11.7, (g) 12.5 and (h) 13.2, (CCA08B.001-.010).

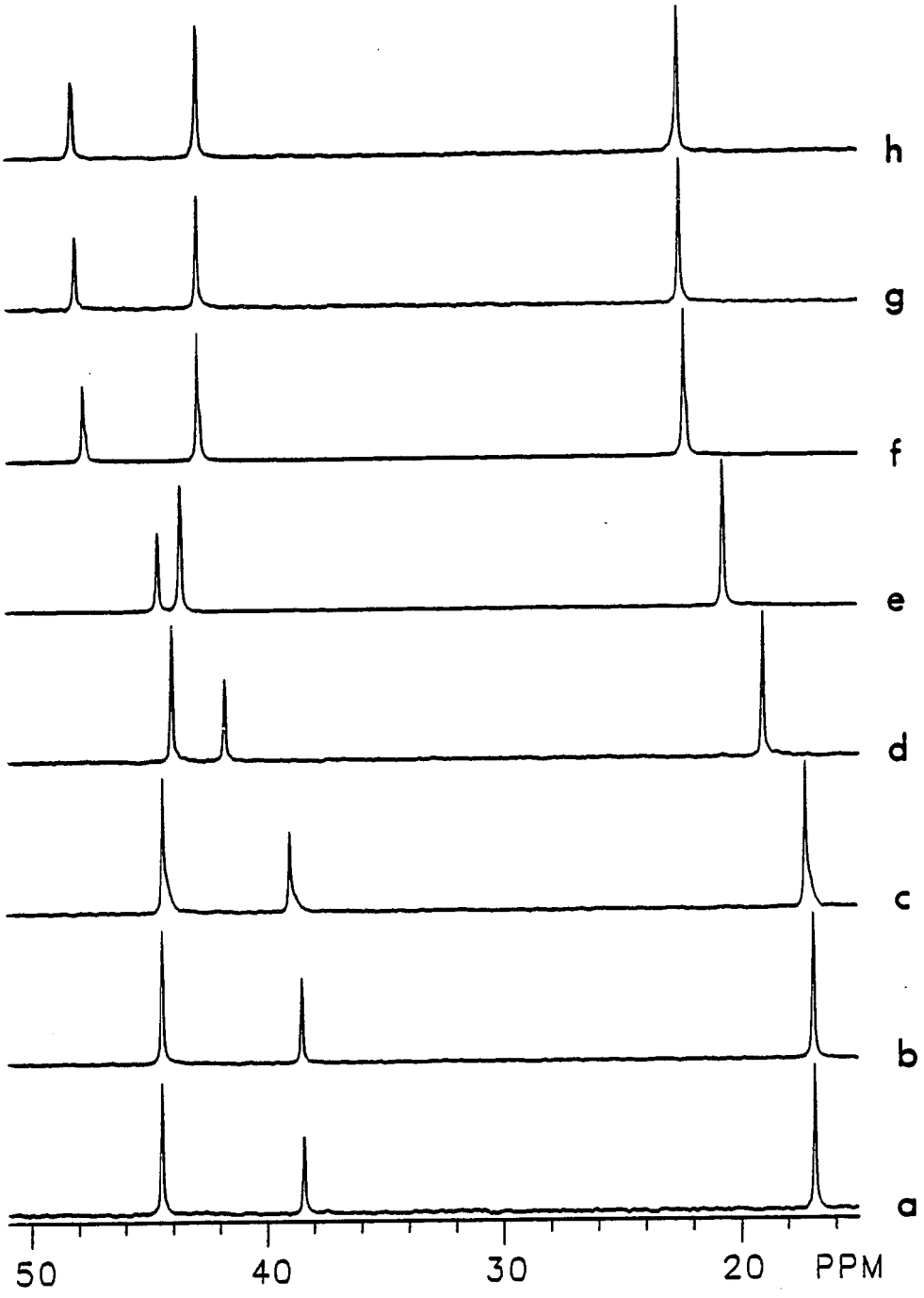
h
g
f
e
d
c
b
a
50
40
30
20
PPM

Appendix H

NMR pH titration study of polymers: The titration behavior of the polymers had been discussed in detail at Chapter I, IV and V. The ^{1}H NMR spectra were recorded for 0.05 M solutions at 25°C. The ^{13}C NMR spectra were recorded for 0.5 M solutions at 25°C.

Figure 1: ^{13}C NMR spectra of PAA (MW = 4,500) in H_2O for about 2000 acquisitions with a pulse angle of 62^{o} and a repetition rate of 3.5 s and with pH values of (a) 2.0, (b) 3.0, (c) 4.0, (d) 5.0, (e) 6.0 (f) 7.0, (g) 8.0 and (h) 10.0, (CC066A.001-.009).

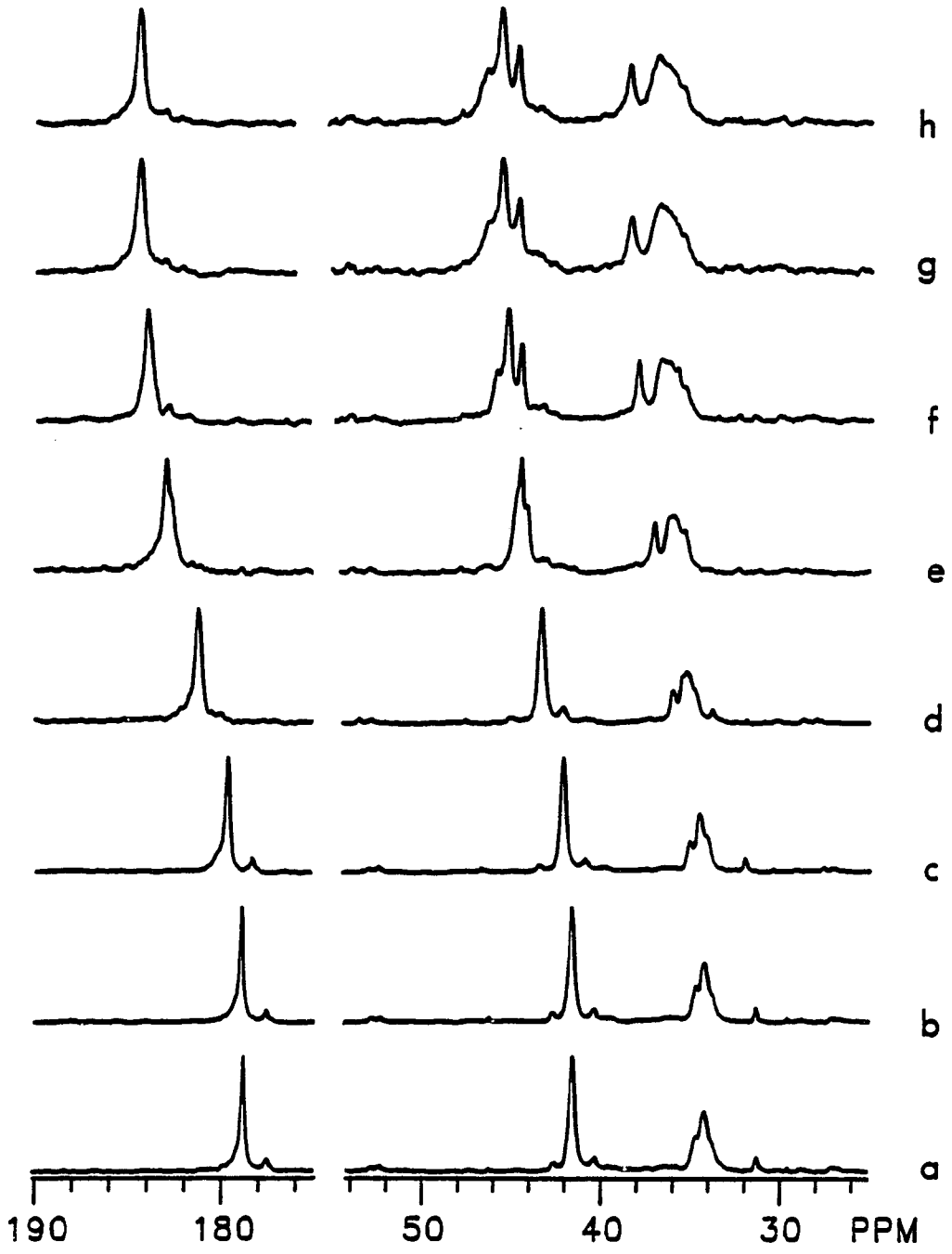
h
g
f
e
d
c
b
a
190
180
50
40
30
PPM

Figure 2: ^{13}C NMR spectra of PAA (MW = 15,000) in H_2O for about 2000 acquisitions with a pulse angle of 62^{o} and a repetition rate of 3.5 s and with pH values of (a) 1.4, (b) 3.0, (c) 4.0, (d) 5.0, (e) 6.0, (f) 7.0, (g) 8.0 and (h) 10.0, (CC065A.001-.012).

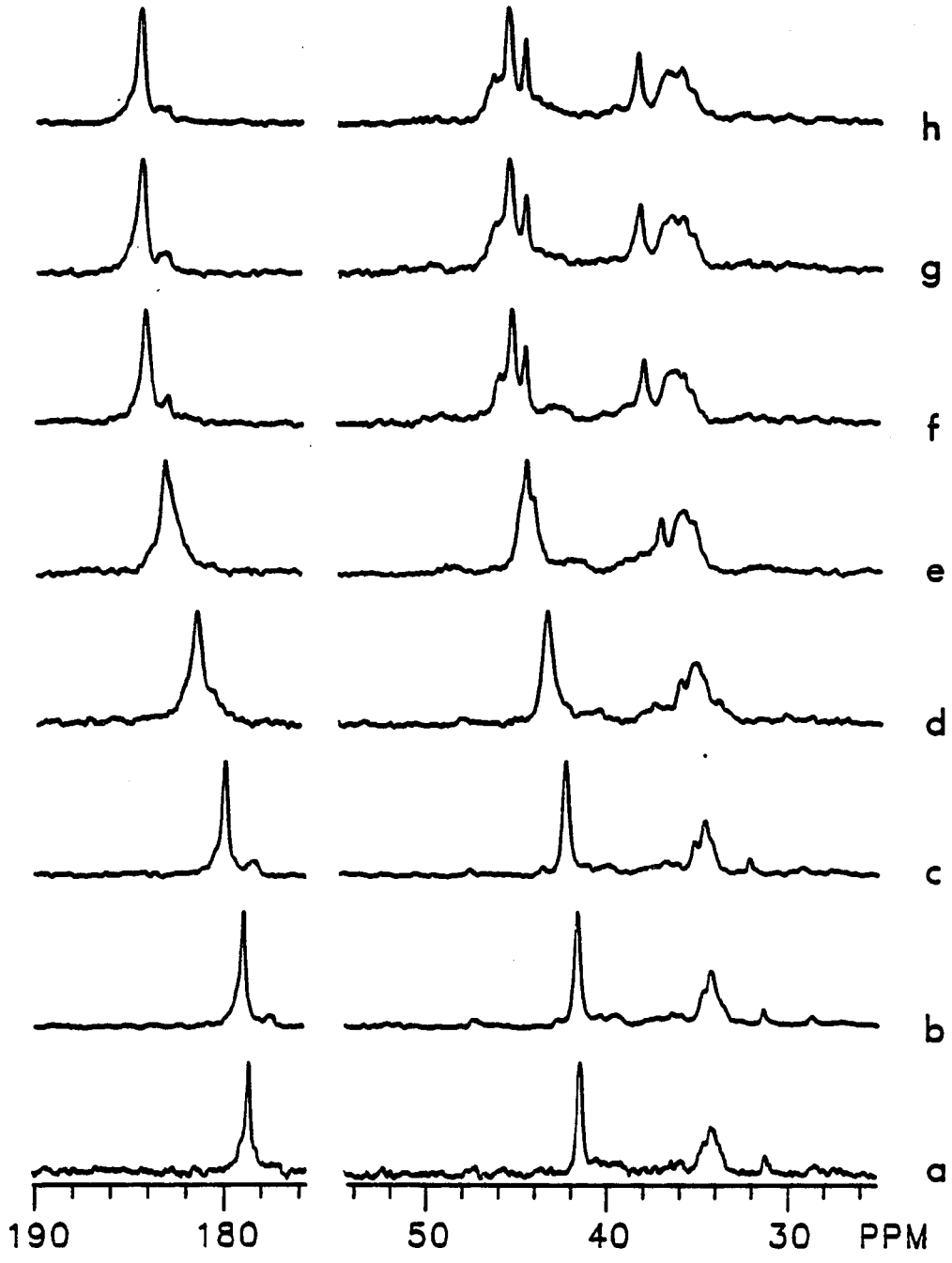
h
g
f
e
d
c
b
a
190
180
50
40
30
PPM

Figure 3: ^{13}C NMR spectra of SP12 in 10% D_2O for about 15,000 acquisitions with a pulse angle of 62° and a repetition rate of 1.5 s and with pH values of (a) 2.0, (b) 3.0, (c) 4.5, (d) 6.1, (e) 7.2, (f) 9.0, (g) 10.6 and (h) 12.1, (CC095B.001-.015).

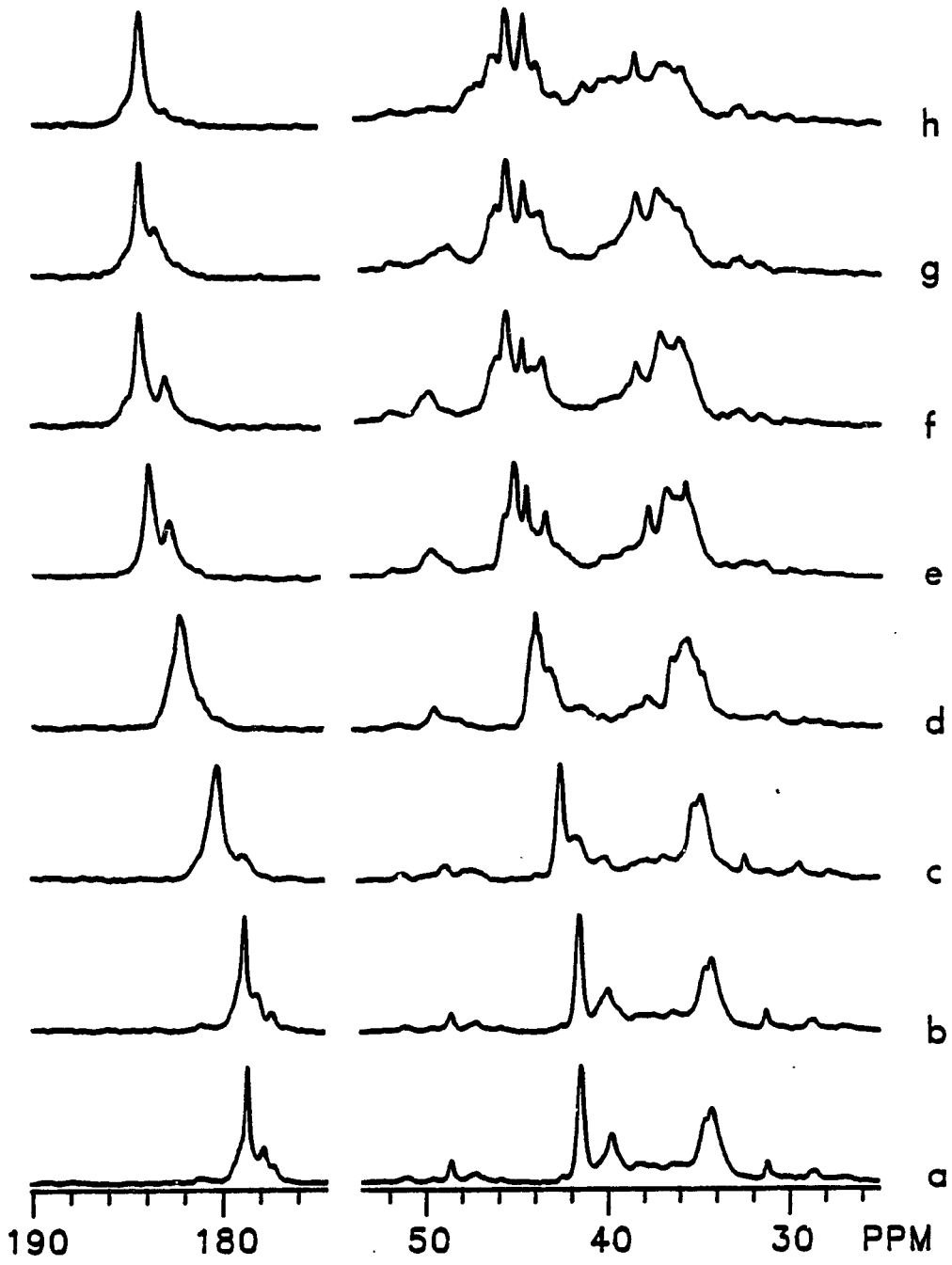
h
g
f
e
d
c
b
a
190
180
50
40
30
PPM

Figure 4: ^{13}C NMR spectra of SP30 in 10% D_2O for about 2500 acquisitions with a pulse angle of 62^{o} and a repetition rate of 3.5 s and with pH values of (a) 1.0, (b) 1.8, (c) 2.5, (d) 5.6 (e) 6.5, (f) 9.0, (g) 10.0 and (h) 12.0, (CC075A.001-.008).

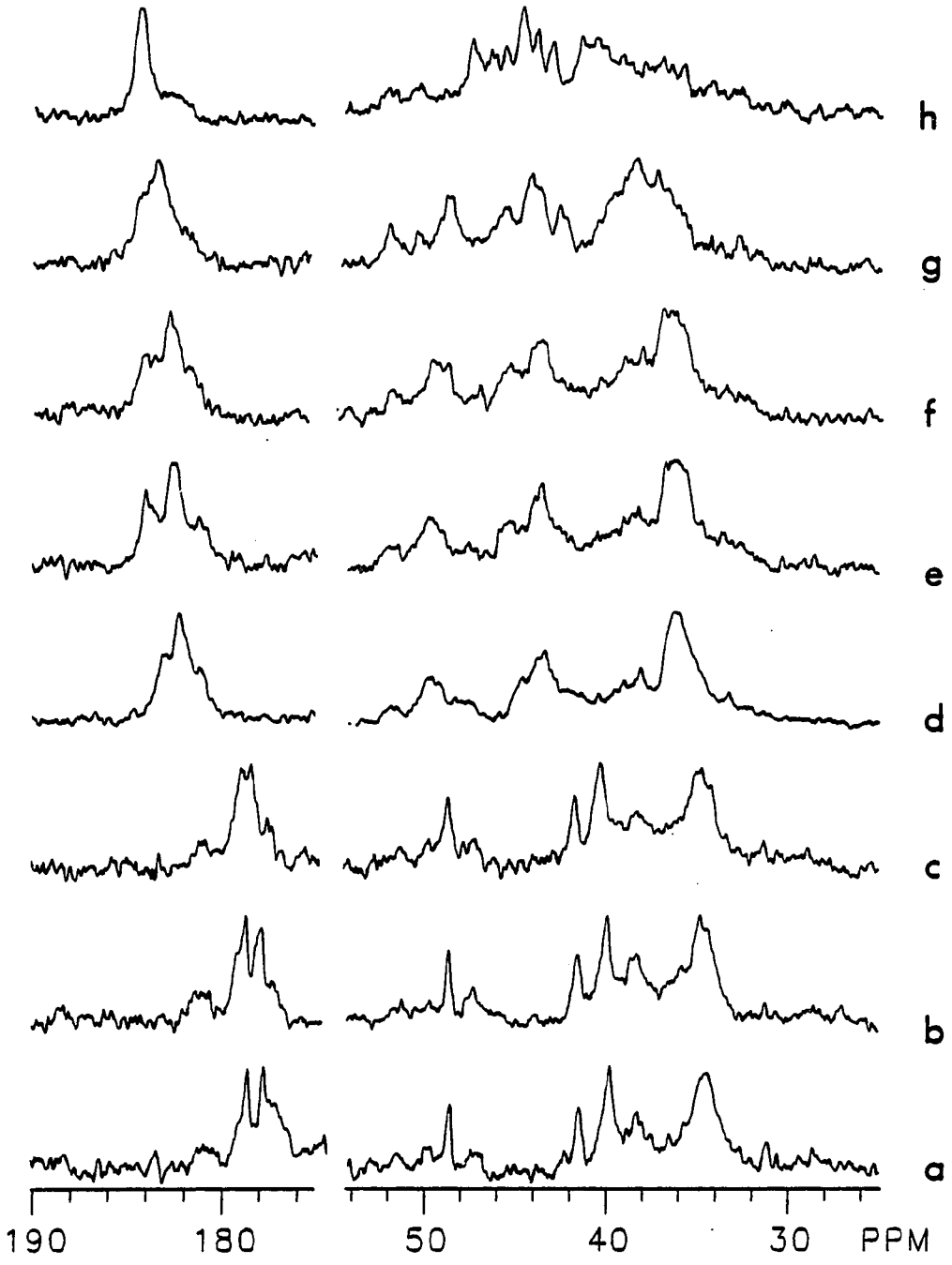
h
g
f
e
d
c
b
a
190
180
50
40
30
PPM

Figure 5: ^{13}C NMR spectra of SP52 in 10% D_2O for about 2500 acquisitions with a pulse angle of 62^{o} and a repetition rate of 3.5 s and with pH values of (a) 1.3, (b) 2.4, (c) 3.2, (d) 3.6, (e) 9.0, (f) 10.0, (g) 10.5 and (h) 12.0, (CC074A.001-.008).

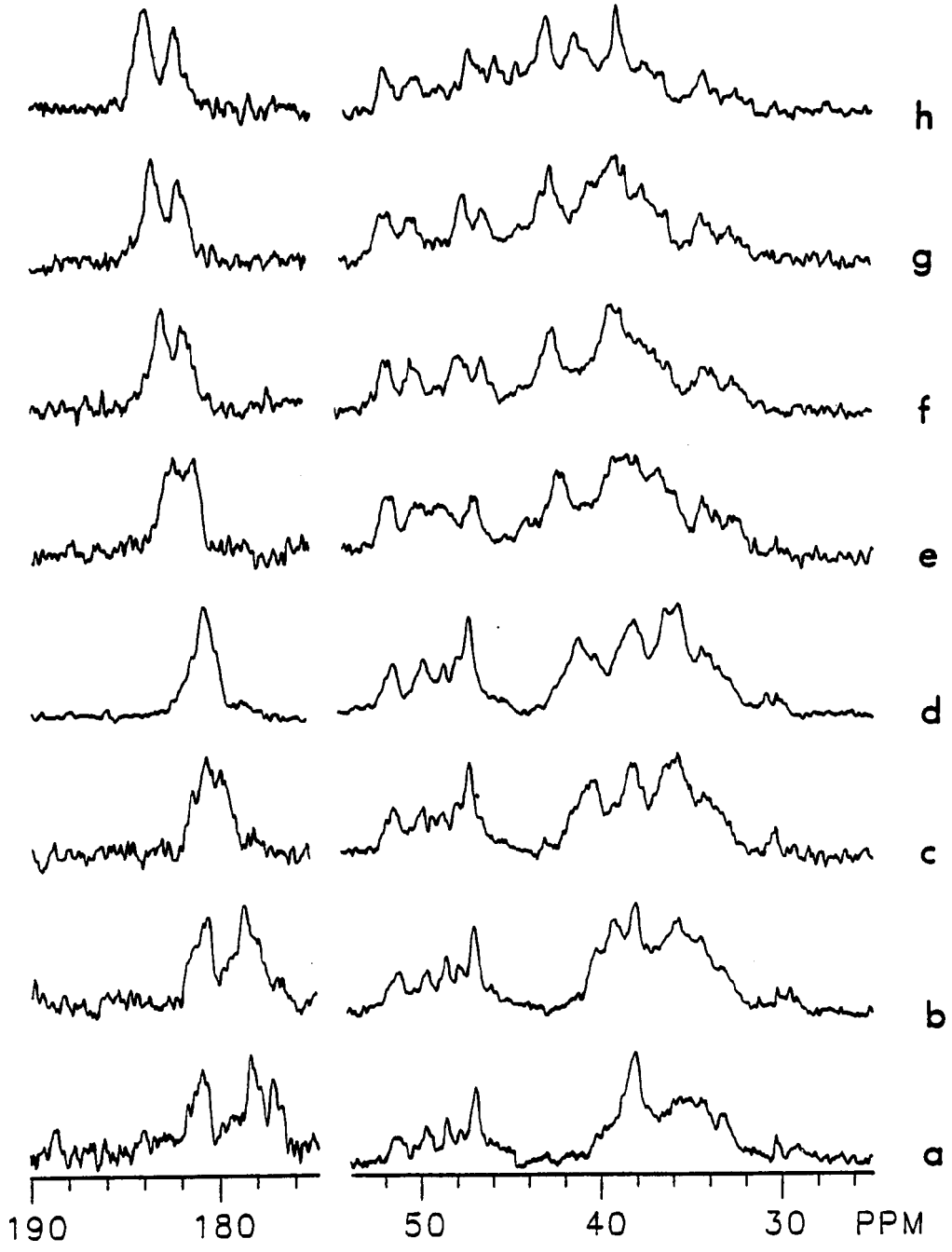
h
g
f
e
d
c
b
a
190
180
50
40
30
PPM

Figure 6: ^{13}C NMR spectra of PVAm in 10% D_2O for about 5000 acquisitions with a pulse angle of 62^{o} and a repetition rate of 1.5 s and with pH values of (a) 2.0, (b) 3.3, (c) 3.9, (d) 4.8, (e) 5.7, (f) 7.1, (g) 8.2 and (h) 9.8, (CC098A.001-.014).

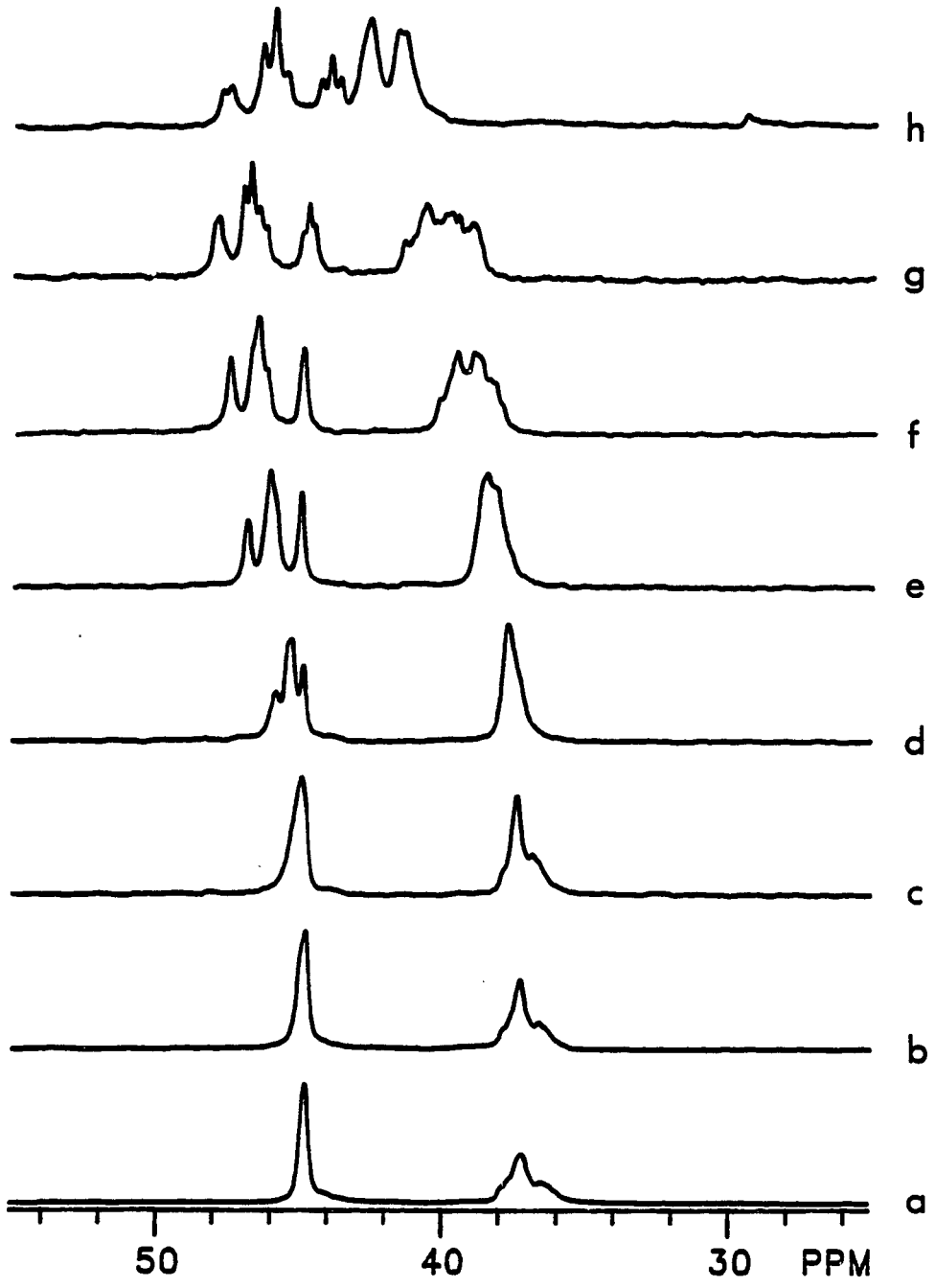
h
g
f
e
d
c
b
a
50
40
30
PPM

Figure 7: ^{13}C NMR spectra of PVAm in 10% D_2O for about 5000 acquisitions with a pulse angle of 62° and a repetition rate of 1.5 s and with pH values of (a) 9.8, (b) 10.3, (c) 10.7, (d) 11.3, (e) 11.8, (f) 12.3, (g) 12.8 and (h) 13.5, (CC098A.014-.021).

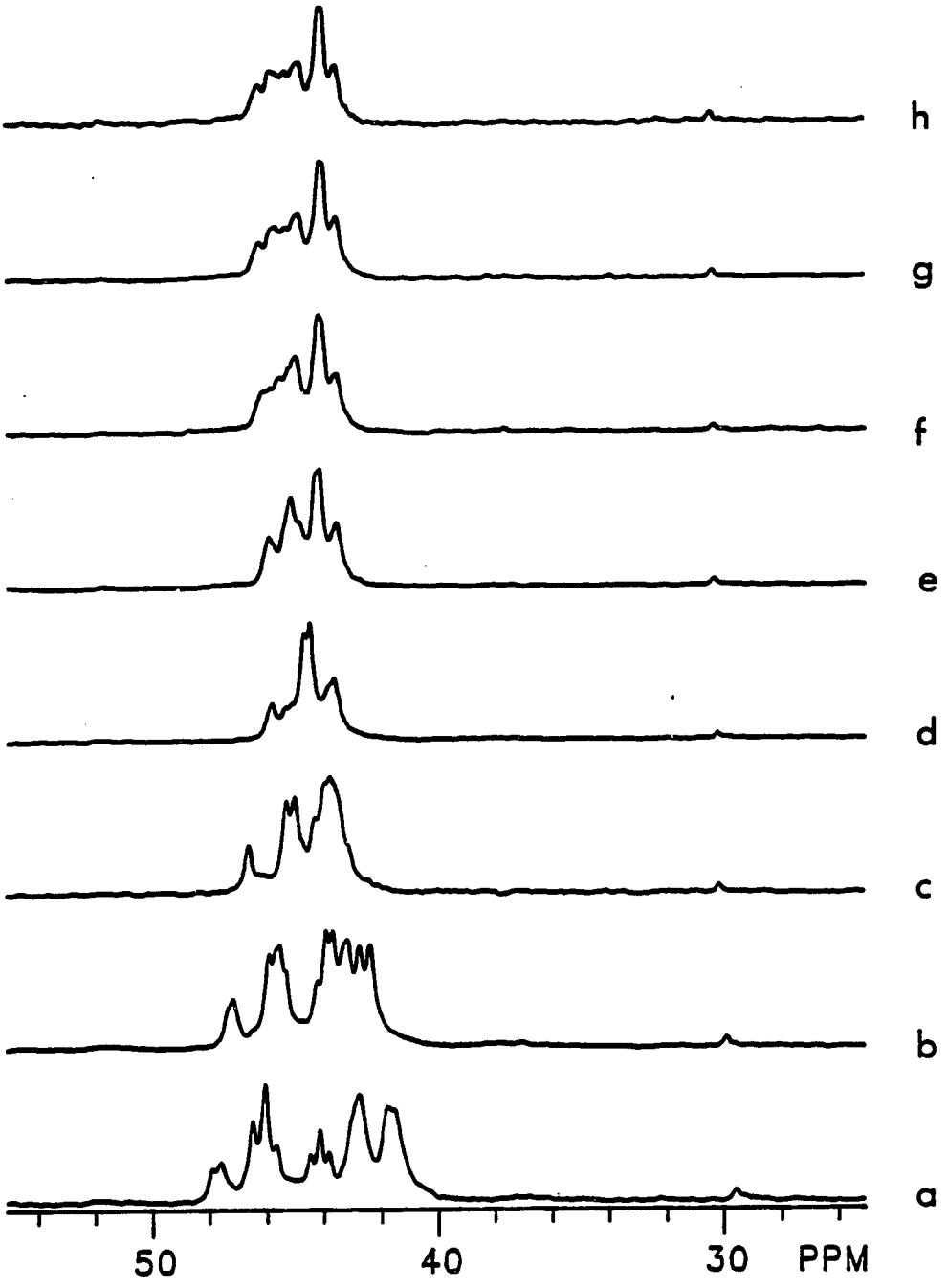
h
g
f
e
d
c
b
a
50
40
30
PPM

Figure 8: ^{1}H NMR spectra of PVAm in D_2O for about 100 acquisitions with a pulse angle of 75° and a repetition rate of 4.1 s and with pH values of (a) 1.3, (CC0010.006), (b) 9.6, (CC010.005) and (c) 13.2 (CCA015.001).

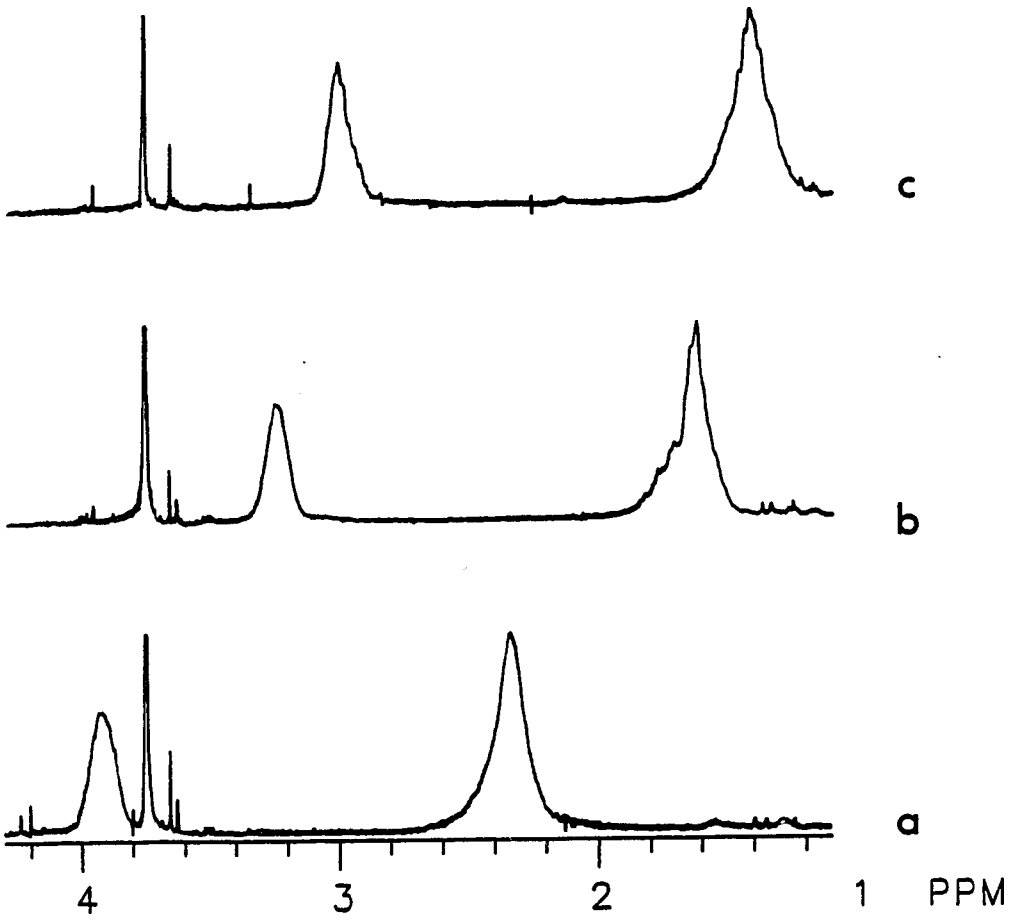
c
b
a
4
3
2
1
PPM

Appendix I

Two-dimensional heteronuclear NMR study of PVAm and its model compounds, m and r DAP: Since 2-D NMR experiments disperse the signals into two frequency domains, these experiments in principle separate peaks which are otherwise overlapping and in this case make configurational assignments of ^{13}C resonances based on the unique character the ^{1}H resonances of attached protons. ^{1}H- ^{13}C heteronuclear shift-correlated 2-D NMR experiments without broadband homonuclear decoupling (CSCM) and with broadband homonuclear decoupling (CSCMBB) were first employed in this study to determine the configuration of the vinyl polymers. These two experiments proved to be very useful for the dyad assignments of the methylene carbon of PVAm and further suggest that these techniques may be general ones for making dyad assignments in other vinyl polymers. The experimental conditions and parameters had been described in detail in Chapter II.

Figure 1: Contour plot for the CSCM experiment for a m:r =1:2 DAP at pH = 1.5 for 560 acquiditions per spectrum. The ^{1}H spectrum is above the ^{1}H axis. The ^{13}C spectrum from this experiment (a) and the proton decoupled ^{13}C NMR spectrum (b) are above the ^{13}C axis (T_1T_209.DAT).

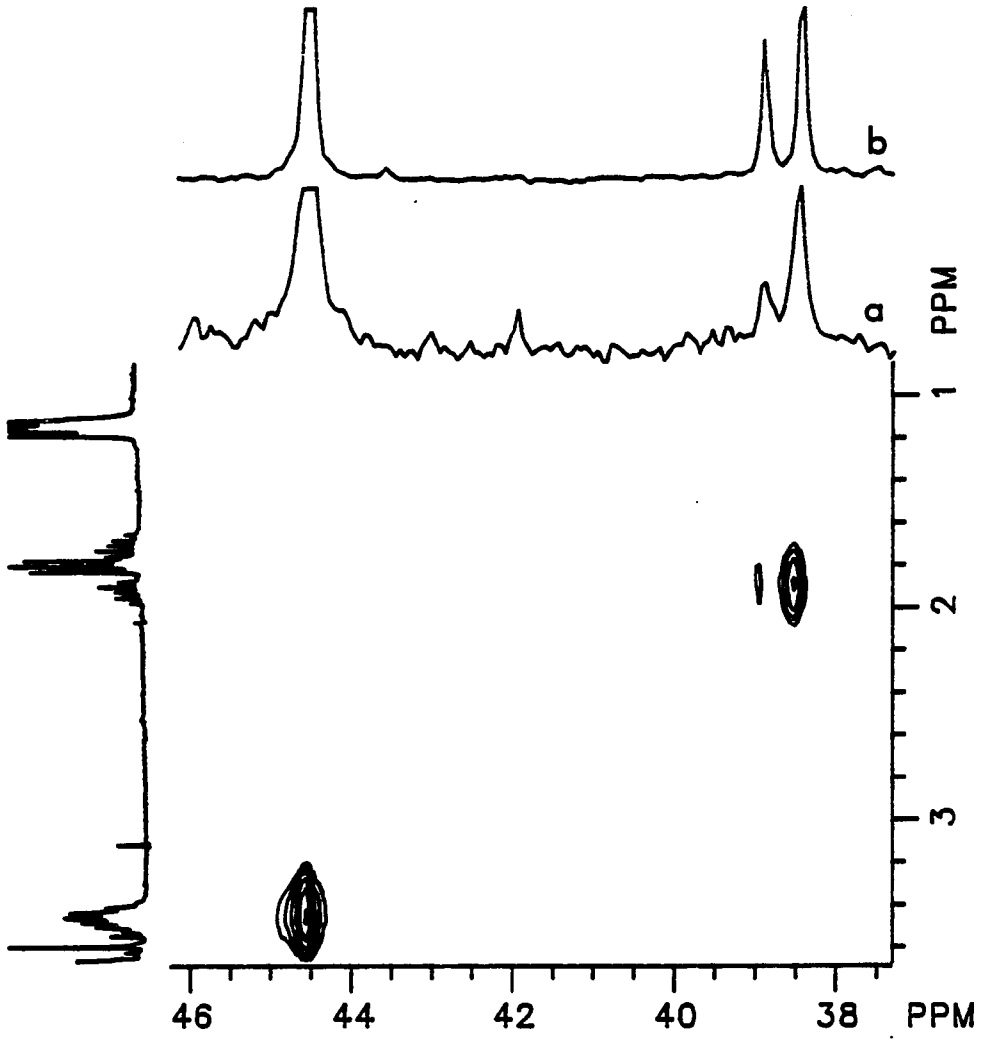
b
a
1
2
3
PPM
46
44
42
40
38
PPM

Figure 2: Contour plot for the CSCMBB experiment for a m:r = 1:2 mixture of DAP at pH = 1.5 for 512 acquisitions per spectrum. The ^{1}H spectrum is above the ^{1}H axis. The ^{13}C spectrum from this experiment (a) and the proton decoupled ^{13}C NMR spectrum (b) are above the ^{13}C axis ($T_1T_2$08.DAT).

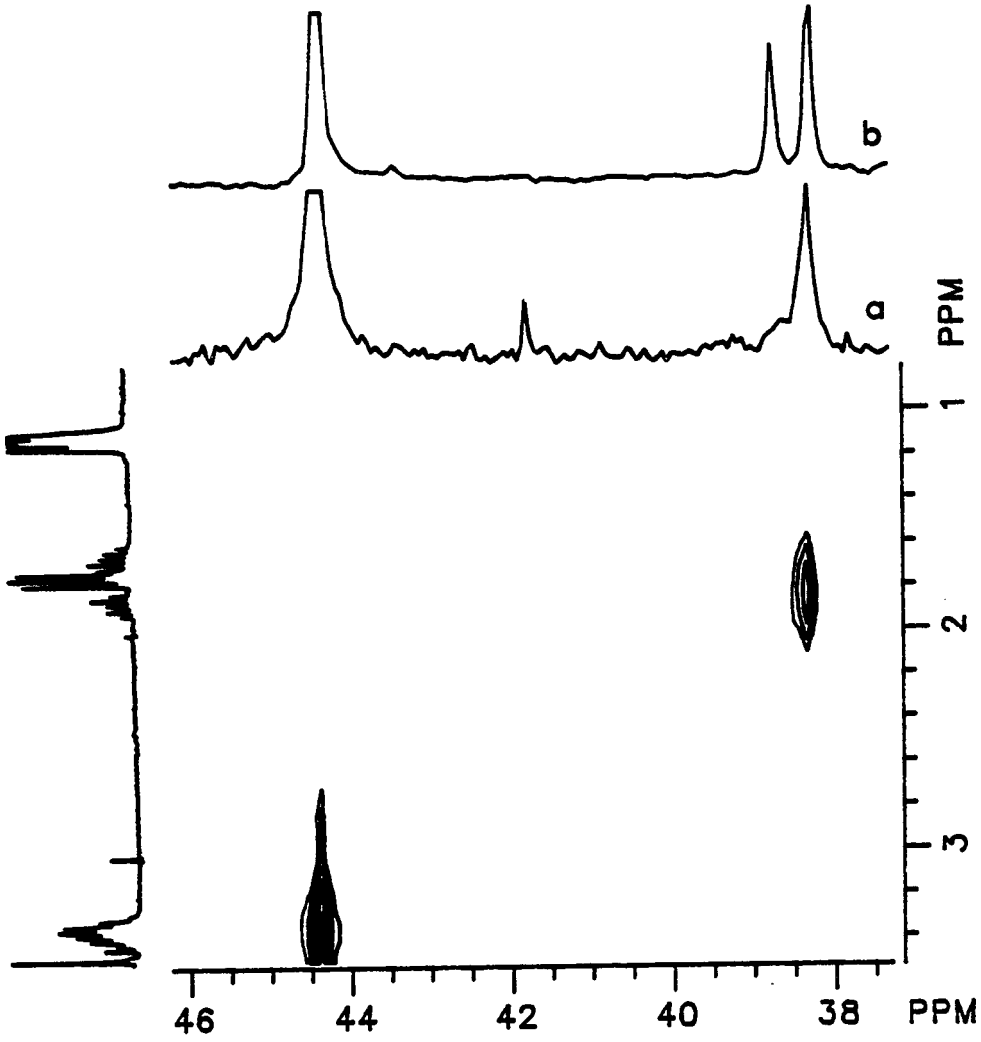
b
a
PPM
1
2
3
46
44
42
40
38
PPM

Figure 3: Cross sections parallel to the ^{1}H axis for the methylene protons of a m:r = 1:2 mixture of DAP at pH = 1.5. Spectra (a) and (b) correspond to the r and m of DAP from the CSCM experiment and spectra (c) and (d) correspond to the r and m isomers of DAP from CSCMBB experiment.

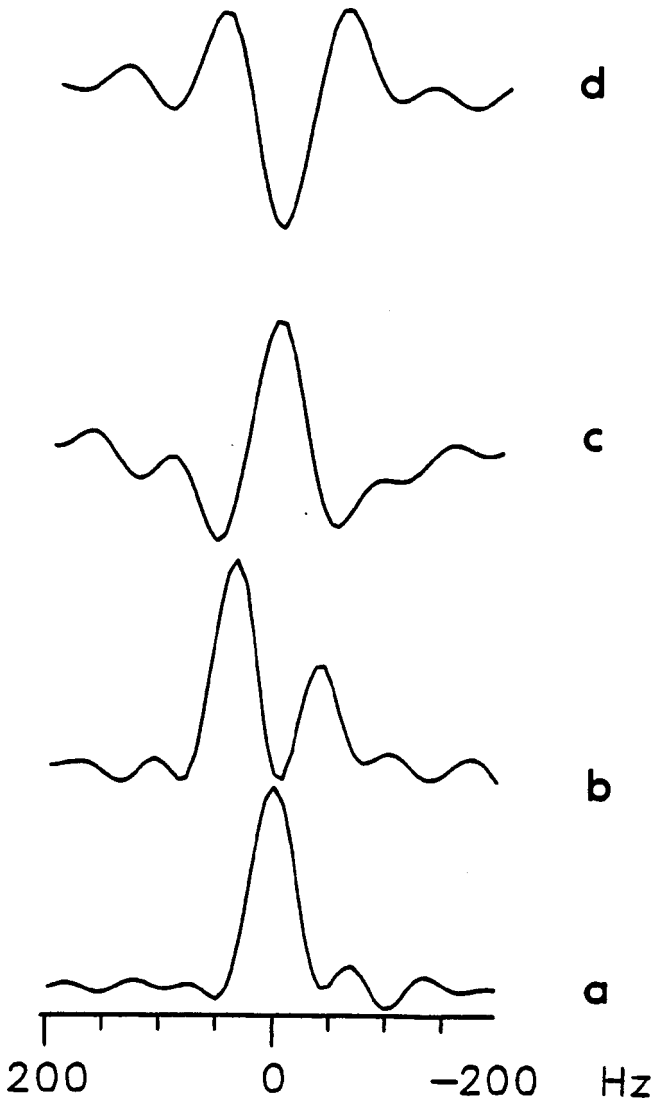
d
c
b
a
200
0
−200
Hz

Figure 4: Contour plot from the CSCMBB experiment with optimal methine carbon resonances for PVAm at pH = 6.5 for 1024 acquisitions per spectrum. The ^{1}H NMR spectrum is above the ^{1}H axis. The ^{13}C spectrum from this experiment (a) and the proton decoupled ^{13}C NMR spectrum (b) are above the ^{13}C axis (T_1T_201.DAT).

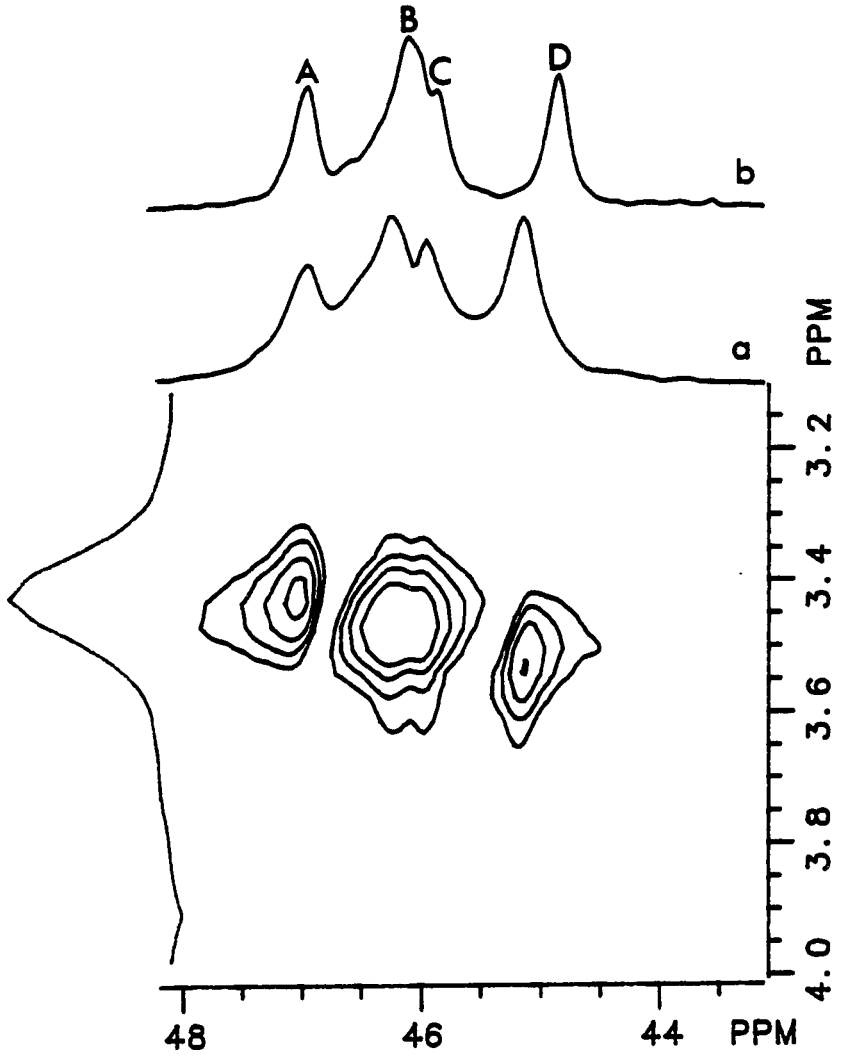
A
B
C
D
b
a
PPM
3.2
3.4
3.6
3.8
4.0
48
46
44
PPM

Figure 5: Cross sections parallel to the ^{1}H axis for the methine protons of PVAm at pH = 6.5. Spectra (a), (b), (c) and (d) correspond to the ^{13}C peaks a, b, c and d of Figure I4.

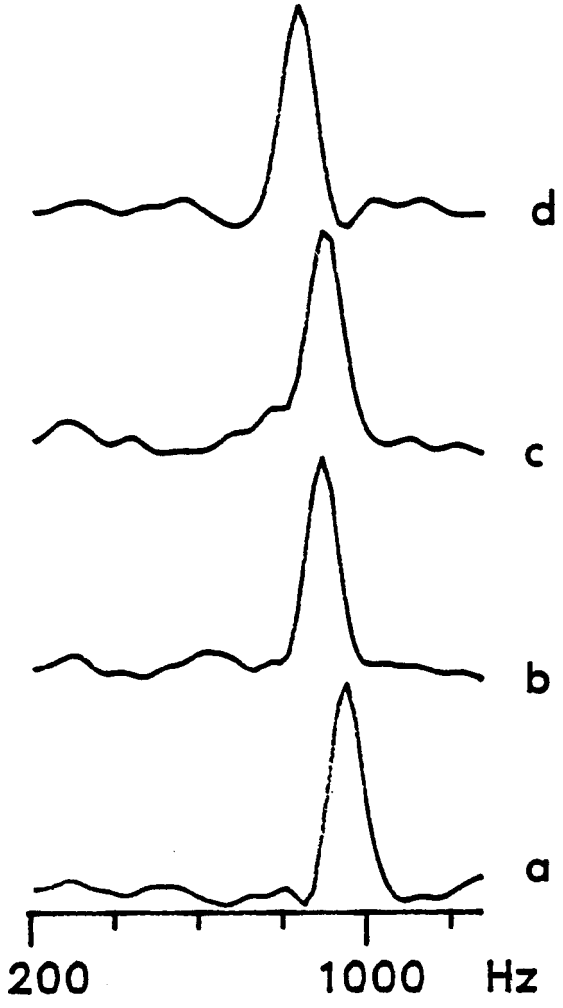
d
c
b
a
200
1000
Hz

Figure 6: Contour plot from the CSCMBB experiment with optimal methylene carbon resonances for PVAm at pH = 6.5 for 1024 acquisitions per spectrum. The ^{1}H spectrum is above the ^{1}H axis. The ^{13}C spectrum from this experiment (a) and the proton decoupled ^{13}C spectrum (b) are above the ^{13}C axis (T_1T_202.DAT).

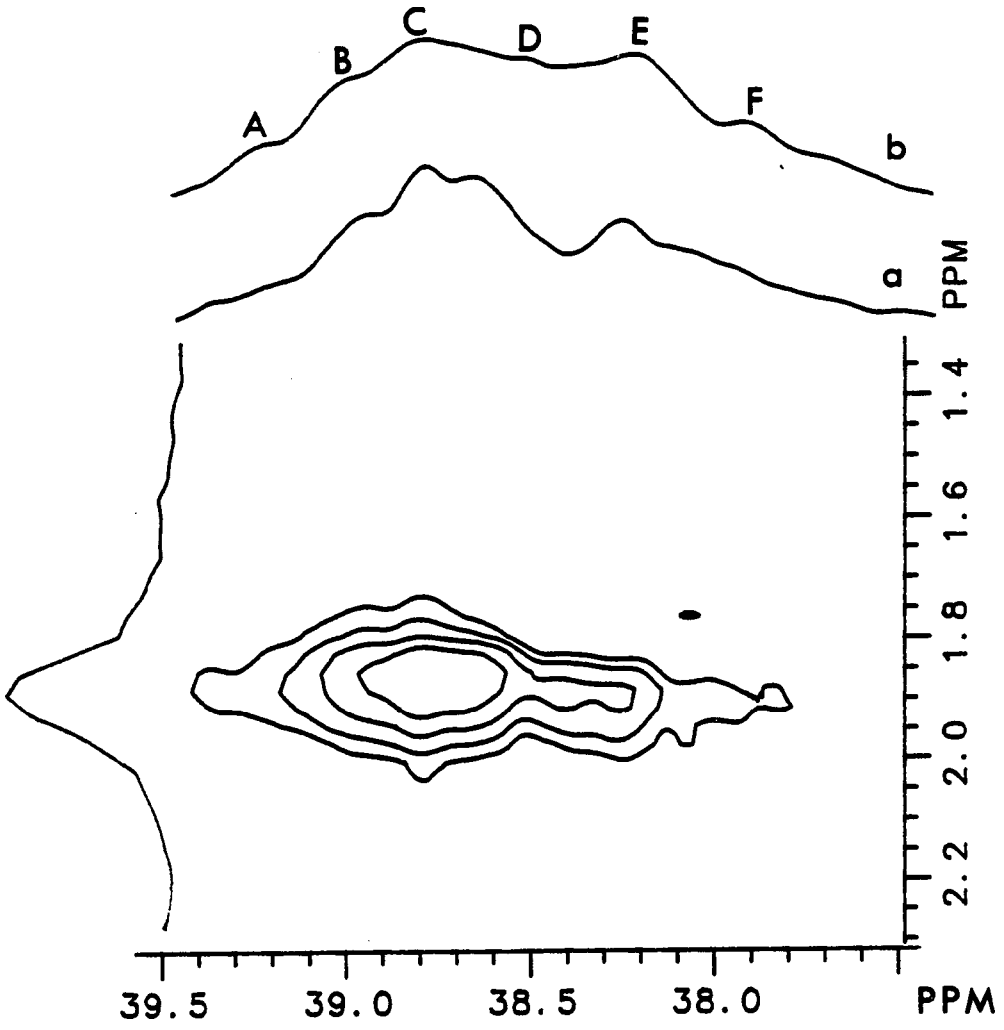
A
B
C
D
E
F
b
a
PPM
1.4
1.6
1.8
2.0
2.2
39.5
39.0
38.5
38.0
PPM

Figure 7: Cross sections parallel to the ^{1}H axis for the methylene protons of PVAm at pH = 6.5. Spectra (a), (b), (c), (d), (e) and (f) correspond to the ^{13}C peaks a, b, c, d, e and f of Figure I6.

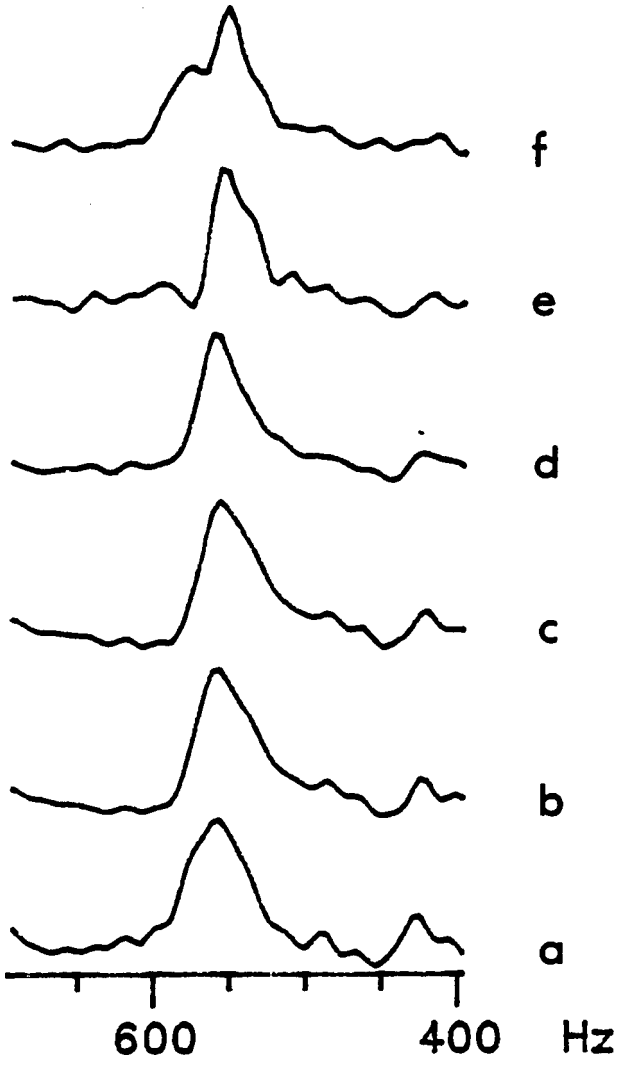
f
e
d
c
b
a
600
400
Hz

Figure 8: Contour plot form the CSCM experiment for a m:r = 1:2 mixture of DAP at pH = 8.8 for 512 acquisitions per spectrum. The ^{1}H spectrum is above the ^{1}H axis. The ^{13}C spectrum from this experiment (a) and the proton decoupled ^{13}C NMR spectrum (b) are above the ^{13}C axis (T_1T_207.DAT).

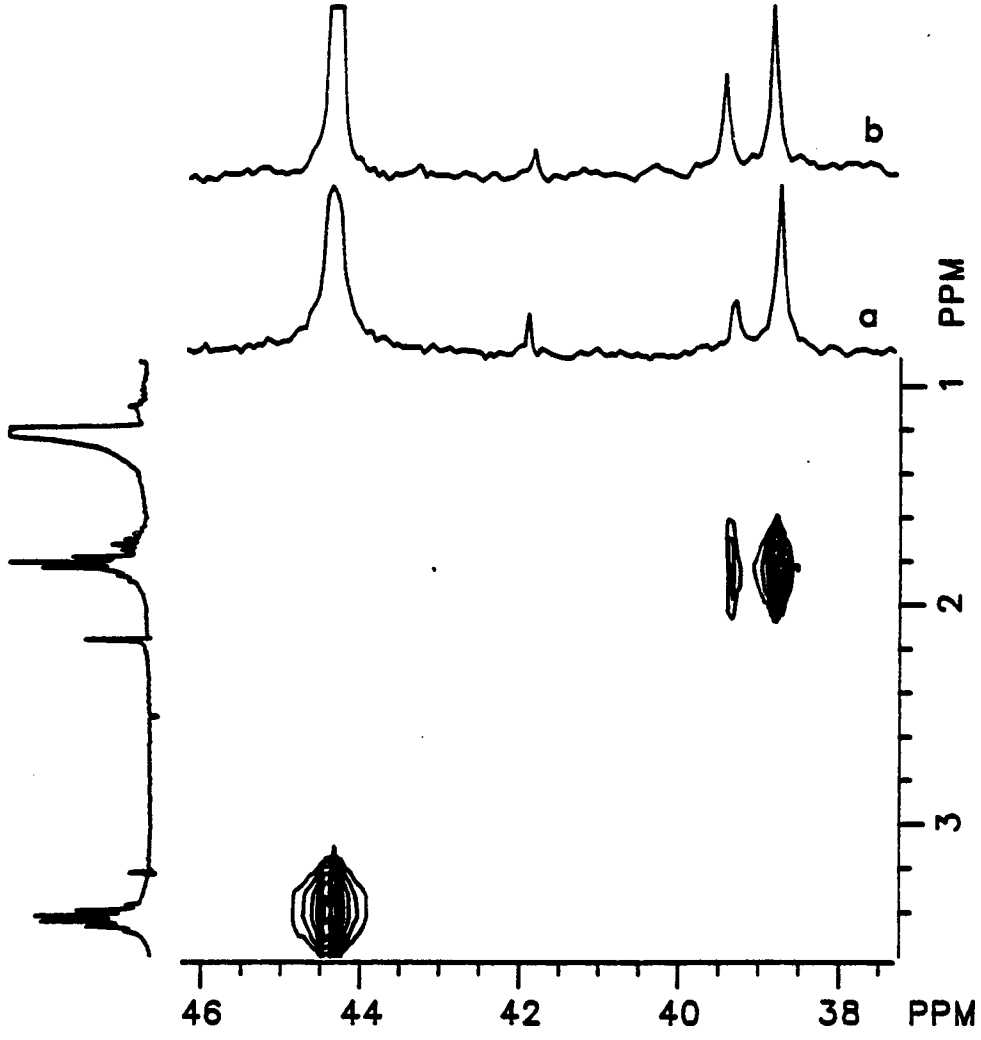
b
a
1
2
3
PPM
46
44
42
40
38
PPM

Figure 9: Contour plot from the CSCM experiment for PVAm at pH = 8.8 for 1400 acquisitions per spectrum. The ^{1}H spectrum is above the ^{1}H axis. The ^{13}C spectrum from this experiment (a) and the proton decoupled ^{13}C spectrum (b) are above the ^{13}C axis (CT_1T_2.DAT).

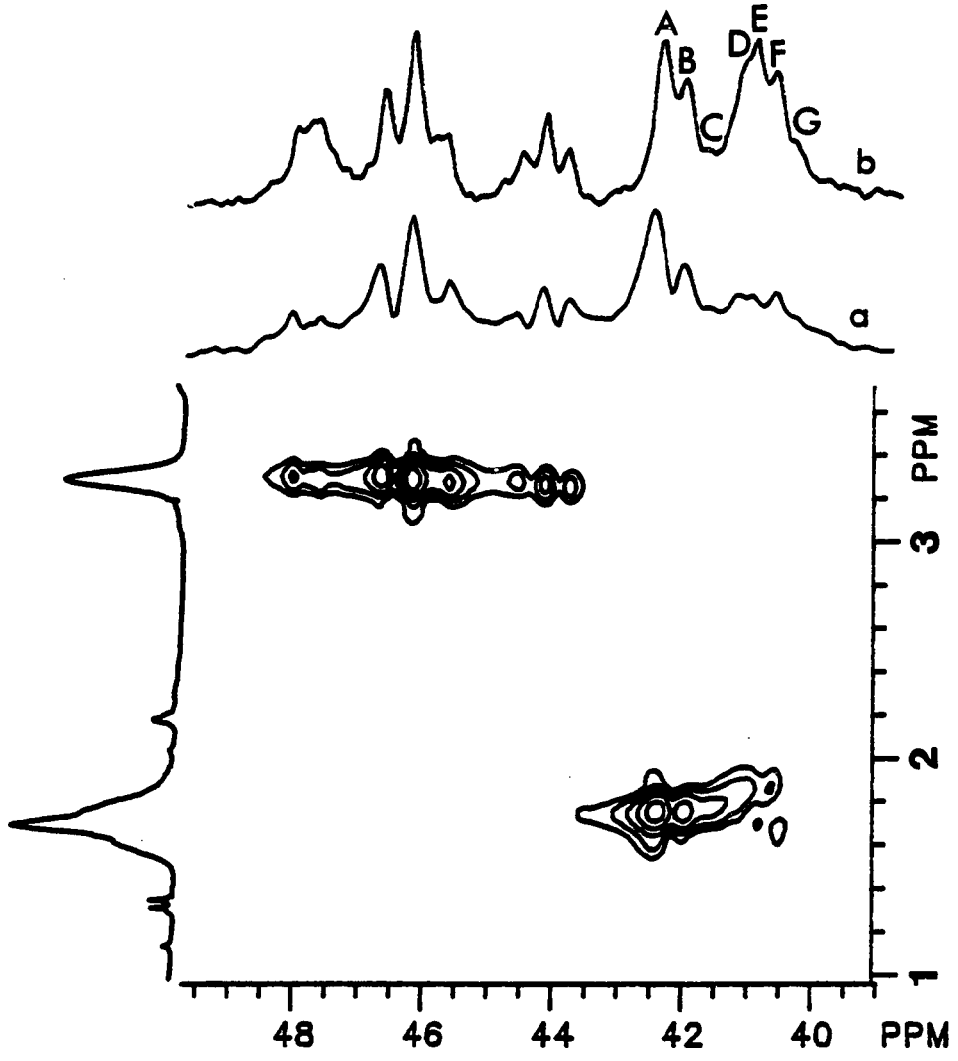
A
B
C
D
E
F
G
b
a
1
2
3
PPM
48
46
44
42
40
PPM

Figure 10: Cross sections parallel to the ^{1}H axis for the methylene protons of PVAm at pH = 8.8. Spectra (a), (b), (c), (d), (f) and (g) correspond to the ^{13}C peaks a, b, c, d, e, f and g of Figure I9.

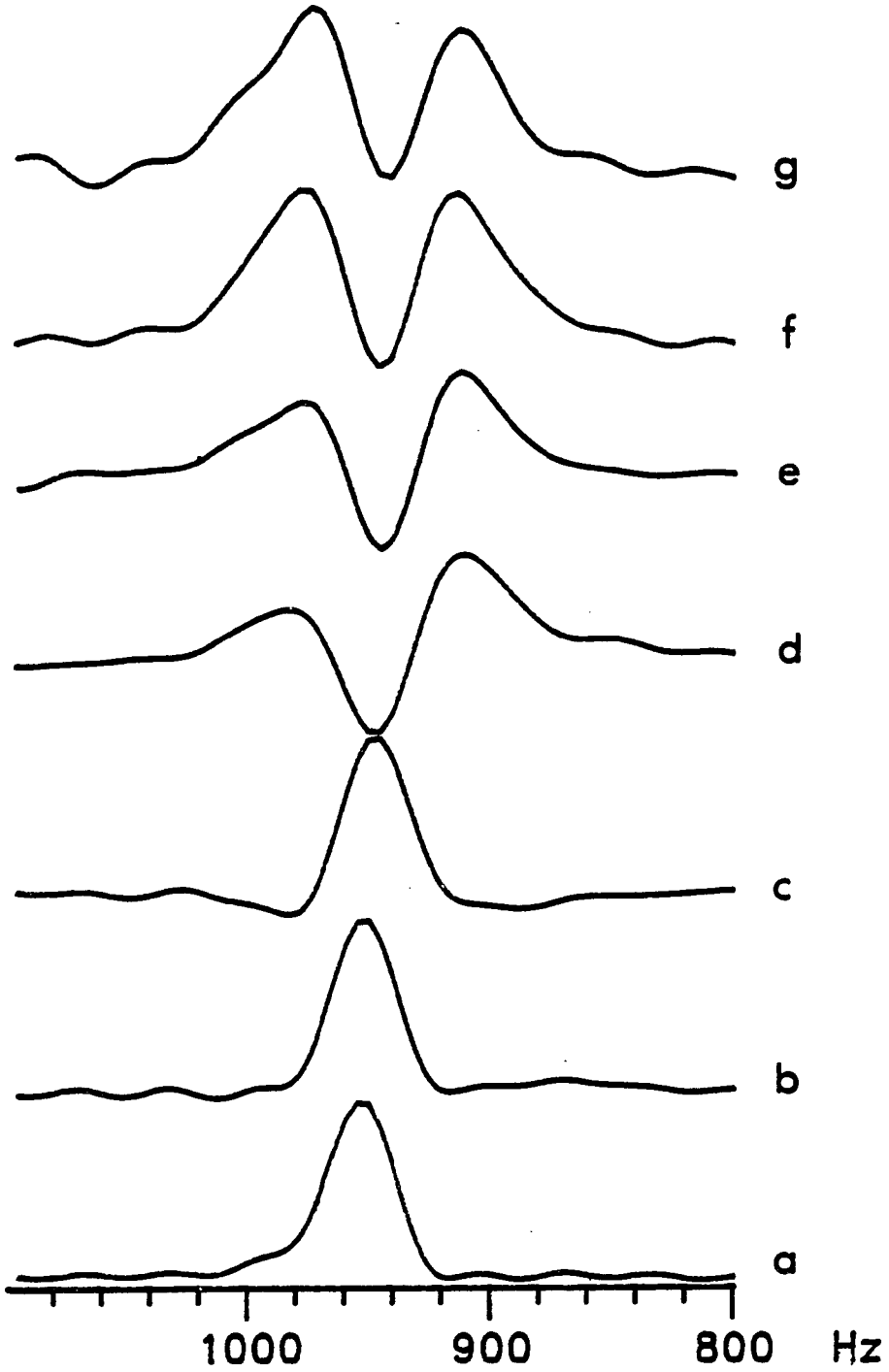
g
f
e
d
c
b
a
1000
900
800
Hz

Figure 11: Contour plot from the CSCMBB experiment for a m:r = 1:2 mixture of DAP at pH = 8.8 for 512 acquisitions per spectrum. The ^{1}H spectrum is above the ^{1}H axis. The ^{13}C spectrum from this experiment (a) and the proton decoupled ^{13}C spectrum (b) are above the ^{13}C axis ($T_1T_2$06.DAT).

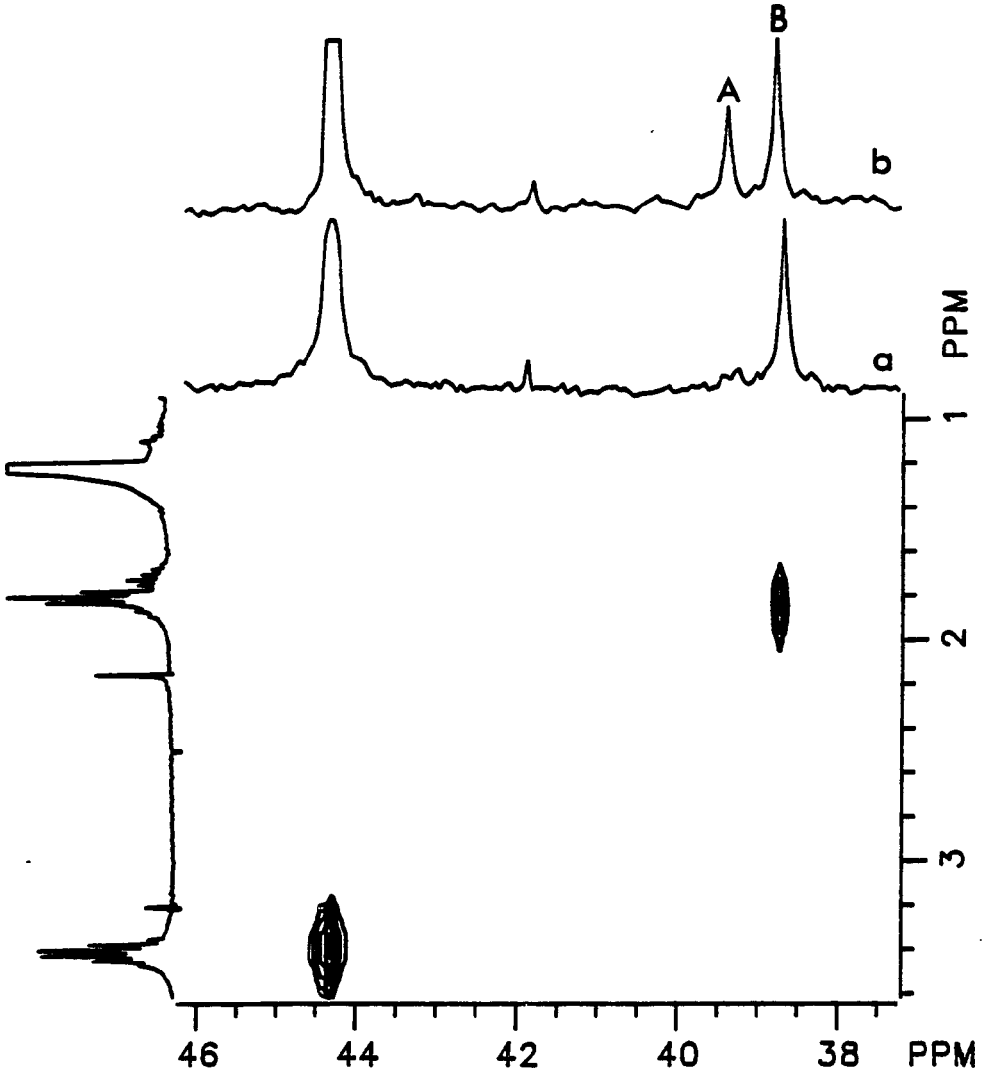
B
A
b
a
PPM
1
2
3
46
44
42
40
38
PPM

Figure 12: Contour plot form the CSCMBB experiment for PVAm at pH = 8.8 for 1680 acquisitions per spectrum. The ^{1}H spectrum is above the ^{1}H axis. The ^{13}C spectrum from this experiment (a) and the proton decoupled ^{13}C spectrum (b) are above the ^{13}C axis (D_1T_2.DAT).

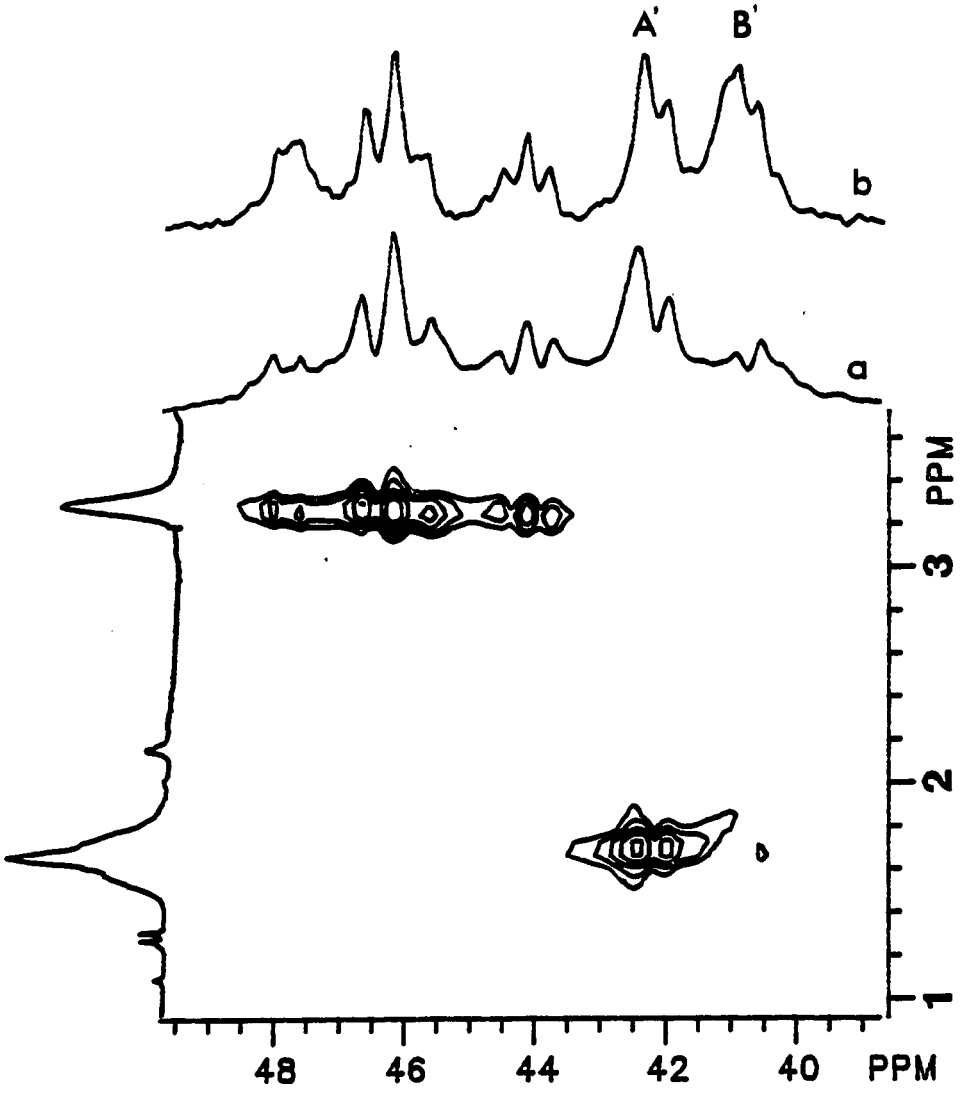
A'
B'
b
a
3 PPM
2
1
48
46
44
42
40
PPM

Figure 13: Cross sections parallel to the ^{1}H axis for the methylene protons of PVAmat pH = 8.8. Spectra (a) and (b) corresponds to the ^{13}C peaks A and B from Figure 11 and spectra (c) and (d) correspond to the ^{13}C peaks A' and B' from Figure I12.

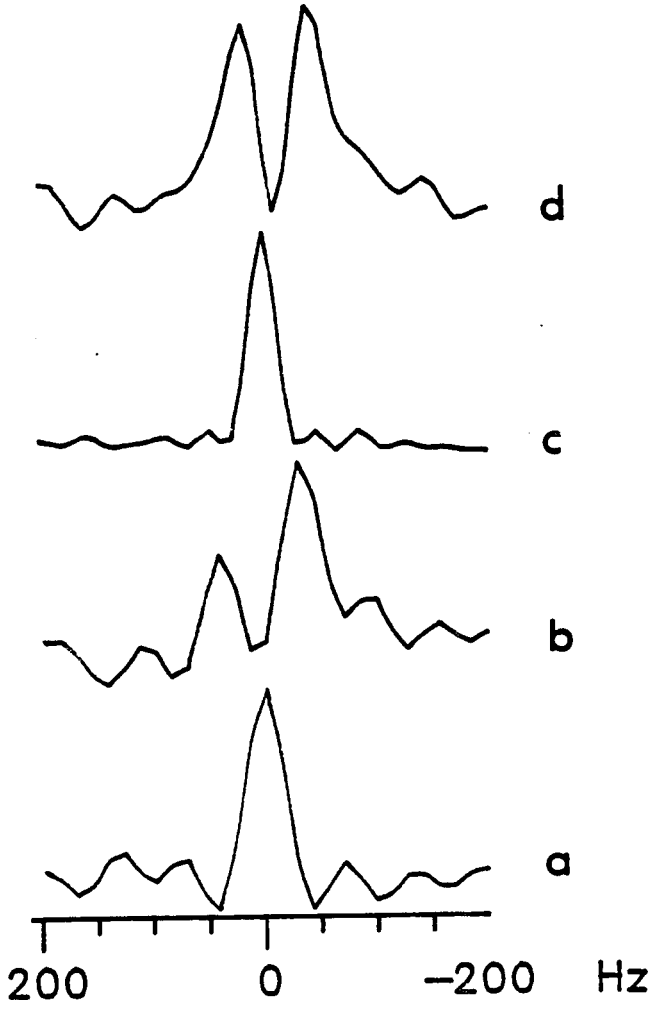
d
c
b
a
200
0
−200
Hz

GRADUATE SCHOOL
UNIVERSITY OF ALABAMA AT BIRMINGHAM
DISSERTATION APPROVAL FORM

Name of Candidate CHEN CHANG

Major Subject CHEMISTRY

Title of Dissertation DETERMINATION OF THE SEQUENCE DISTRIBUTION AND IONIZATION CONSTANT OF POLY(ACRYLIC ACID), POLY(VINYLAMINE) AND POLY(ACRYLIC ACID-CO-VINYLAMINE) BY NMR SPECTROSCOPY

Dissertation Committee:

Thomas H. Pinkerton, Chairman

Donald D. Muccio

Gerald S. Vigee

N. R. Thyagarajan

Director of Graduate Program

Dean, UAB Graduate School

Date November 8, 1985

PS-1428